

Portland State University

PDXScholar

Dissertations and Theses

Dissertations and Theses

5-29-1997

Syntheses and Characterizations of Unsymmetrical Porphyrins as Photosensitizers for a Solid-State Solar Cell

Yinping Zhao

Portland State University

Follow this and additional works at: https://pdxscholar.library.pdx.edu/open_access_etds

 Part of the [Chemistry Commons](#)

Let us know how access to this document benefits you.

Recommended Citation

Zhao, Yinping, "Syntheses and Characterizations of Unsymmetrical Porphyrins as Photosensitizers for a Solid-State Solar Cell" (1997). *Dissertations and Theses*. Paper 6287.


<https://doi.org/10.15760/etd.8147>

This Thesis is brought to you for free and open access. It has been accepted for inclusion in Dissertations and Theses by an authorized administrator of PDXScholar. Please contact us if we can make this document more accessible: pdxscholar@pdx.edu.

THESIS APPROVAL

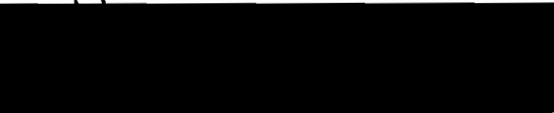
The abstract and thesis of Yinping Zhao for Master of Science degree in Chemistry were presented May 29, 1997 and accepted by the thesis committee and the department.

COMMITTEE APPROVALS:



Carl C. Wamser, Chair


David H. Peyton


Bryan Gilbert


Jonathan Abramson
Representative of the Office of Graduate Studies

DEPARTMENT APPROVAL:


David H. Peyton, Chair
Department of Chemistry

ACCEPTED FOR PORTLAND STATE UNIVERSITY BY THE LIBRARY

by  on Aug. 29, 1997

ABSTRACT

An abstract of the thesis of Yinping Zhao for the Master of Science in Chemistry presented May 29, 1997.

Title: Syntheses and Characterizations of Unsymmetrical Porphyrins as Photosensitizers for a Solid-state Solar Cell.

Solar light is the most important source of regenerative energy and represents mankind's only inexhaustible energy source. One of today's most promising tools to make use of solar energy is its direct conversion into electrical energy in a photovoltaic cell. The practical use of these solar cells depends on the price of the devices and therefore of the obtained energy. The conventional silicon cells, although efficient, are expensive for common consumer applications. The Grätzel cell is a photovoltaic system for harvesting the sun's energy that operates at about 10-15% overall efficiency, like a conventional solar cell, but does it at one-fifth the cost of conventional solar cells. However, the presence of the highly corrosive electrolyte, containing iodide and triiodide, hampers the incorporation of a highly conducting metallic grid and requires hermetic sealing of the module in order to prevent evaporation of the solvent as well as intrusion of water and

oxygen. Also the degradation of the photon energy is substantial in such a solar cell. Our goal is to replace the liquid-phase redox relay in such cells with a conductive polymer covalently bound to a porphyrin photosensitizer. Porphyrins with carboxylic acid functional groups as active sites for linkage of the porphyrin to TiO_2 and aminophenyl groups as sites for initiation of polyaniline growth or for anchoring a formed polyaniline chain are therefore the desired photosensitizers for our proposed solid-state solar cell.

An unsymmetrical porphyrin, 5,10,15-tri-[4-(carbomethoxy)phenyl]-20-[(4-acetamido)phenyl]porphyrin (TCM_3AAPP), with two different types of substituents around the porphyrin periphery, has been synthesized by a mixed aldehyde condensation with pyrrole in propionic acid. TCM_3AAPP was separated chromatographically from a mixture of six porphyrins formed by the reaction. The desired functional porphyrin 5,10,15-tri-(4-carboxyphenyl)-20-(4-aminophenyl)porphyrin (TC_3APP), which will be used as a photosensitizer on the proposed solid-state solar cell, was obtained by cleaving off protecting groups from TCM_3AAPP . Reaction conditions for synthesis of the parent porphyrin have been optimized by HPLC analysis. The desired porphyrin TC_3APP has been identified by NMR and mass spectra and characterized by UV-visible and fluorescence spectra. Attempted synthetic methods for TCPP-TAPP dyad are also presented in this thesis.

SYNTHESES AND CHARACTERIZATIONS OF UNSYMMETRICAL
PORPHYRINS AS PHOTSENSITIZERS FOR A
SOLID-STATE SOLAR CELL

by

YINPING ZHAO

A thesis submitted in partial fulfillment of the
requirements for the degree of

MASTER OF SCIENCE

in

CHEMISTRY

Portland State University

1997

ACKNOWLEDGMENTS

I extend my greatest appreciation and gratitude to my advisor, Dr. Carl Wamser, for always taking time out to offer suggestions and advice, for his endless patience and support throughout the process of completing this study. It was an honor to work with someone possessing such incredible knowledge. Special thanks go to Dr. David Peyton for teaching and helping me obtain NMR spectra and Dr. Bryant Gilbert for taking time to give me some very valuable suggestions about synthesis and HPLC analysis.

I would also like to take this opportunity to thank our research group (Dr. Peter Pessiki, Suman Cherian, Judith Lebzelter, Tristan Jenkins, James Weinkauff and Chang-Hwa Ryu) for their help and making me feel at home and I am grateful to my friend, Jane Kelley, for her kindness, friendship and support, especially when time was rough.

This sincere word of thanks goes to my husband, Tingmin, for the words of encouragement and endless support. Without his love I never could have accomplished what I have. A special thank goes to my wonderful daughter, Sara. I wish you enjoy all those weekends and nights you shared with me in my Lab, and hope I have instilled in you the importance of education, and the desire to reach for the stars. Finally, my love and appreciation go to my parents and my sisters for their love, endless support and warm wishes.

TABLE OF CONTENTS

	PAGE
ACKNOWLEDGMENTS	i
LIST OF FIGURES	v
CHAPTER	
I. INTRODUCTION	1
Solar energy cells	1
The Grätzel cell	2
Mechanism of dye-sensitized semiconductor cell	6
Solid-state solar cell	9
II. EXPERIMENTAL	18
Introduction	18
Materials	20
Instrumentation	21
Attempted Syntheses of the TCPP-TAPP Dyad	22
General approach	22
Synthesis of TCM ₃ CPP from TCPP	25
Synthesis of TCM ₃ CPP from pyrrole and mixed	

substituted benzaldehydes.	27
Synthesis of TCM ₃ CPP from TCM ₄ PP	30
Coupling TCM ₃ CPP with TAPP	31
Synthesis of TC ₃ APP	32
General approach	32
Synthesis of TCM ₃ AAPP from pyrrole and mixed substituted benzaldehydes	33
Synthesis of TCM ₃ AAPP from thermodynamic equilibrium method	35
Synthesis of TC ₃ APP from hydrolysis of TCM ₃ AAPP.	36
III. RESULTS AND DISCUSSION.	38
Chromatography.	38
Column chromatography	38
HPLC analysis	40
Spectroscopy.	42
NMR spectroscopy	42
Mass spectrometry	44
Ultraviolet/Visible spectroscopy.	45
Fluorescence spectroscopy.	57

Fluorescence life times	65
Conclusion	69
REFERENCES	71
APPENDIX	77

LIST OF FIGURES

FIGURE	PAGE
1. Grätzel cell	3
2. Energy level diagram for a typical dye-sensitized TiO ₂ solar cell	6
3. Energy level diagram for the proposed TiO ₂ /TCPP/PAni solar cell	10
4. Structure of TCPP-TAPP dyad	16
5. Structure and abbreviations for the porphyrins referred to in this work.	17
6. Energy levels of TCPP, TAPP, TiO ₂ and PAni.	20
7. Absorption spectra of successive acid-titration additions of TCPP.	50
8. Absorption spectra of successive acid-titration additions of TC ₃ APP	51
9. Resonance forms for the dication of TC ₃ APP	54
10. Absorption spectra of successive base-titration	

	additions of TCPP	55
11.	Absorption spectra of successive base-titration	
	additions of TC ₃ APP	56
12.	Emission spectra of TCPP and TCPP(2+) excited at 435 nm.	60
13.	Emission spectra of TC ₃ APP and TC ₃ APP(2+)	
	excited at 420 nm	61
14.	Emission spectra of TC ₃ APP(2+) and TC ₃ APP(3+)	
	excited at 435 nm	62
15.	Emission spectra of TCPP and TCPP(6-) excited at 429 nm	63
16.	Emission spectra of TC ₃ APP and TC ₃ APP(5-)	
	excited at 429 nm	64
17.	500 MHz ¹ H NMR spectrum of TCM ₄ PP	78
18.	500 MHz ¹ H NMR spectrum (7-9 ppm) of TCM ₄ PP.	79
19.	500 MHz ¹ H NMR spectrum of TCM ₃ AAPP.	80
20.	500 MHz ¹ H NMR spectrum (7-9 ppm) of TCM ₃ AAPP.	81
21.	500 MHz ¹ H NMR spectrum of TCM ₃ CPP.	82
22.	500 MHz ¹ H NMR spectrum (7-9 ppm) of TCM ₃ CPP	83
23.	500 MHz ¹ H NMR spectrum of TC ₃ APP	84
24.	500 MHz ¹ H NMR spectrum (7-9 ppm) of TC ₃ APP	85
25.	Mass spectra of TCM ₃ AAPP	86
26.	Mass spectra of TC ₃ APP	87

27.	Absorption spectrum of TCM ₄ PP in DCM	88
28.	Absorption spectrum of TCM ₃ CPP in DCM	89
29.	Absorption spectrum of TCM ₃ AAPP in DCM	90
30.	Absorption spectrum of TAPP in DMSO	91
31.	Absorption spectrum of TCPP in DMSO	92
32.	Absorption spectrum of TC ₃ APP in DMSO	93
33.	Excitation and emission spectra of TCM ₄ PP in DCM	94
34.	Excitation and emission spectra of TCM ₃ CPP in DCM	95
35.	Excitation and emission spectra of TCM ₃ AAPP in DCM	96
36.	Excitation and emission spectra of TAPP in DMSO	97
37.	Excitation and emission spectra of TCPP in DMSO	98
38.	Excitation and emission spectra of TC ₃ APP in DMSO	99
39.	Excitation and emission spectra of TCPP(2+) in DMSO	100
40.	Excitation and emission spectra of TC ₃ APP(2+) in DMSO	101
41.	Excitation and emission spectra of TC ₃ APP(3+) in DMSO	102
42.	Excitation and emission spectra of TCPP(6-) in DMSO	103
43.	Excitation and emission spectra of TC ₃ APP(5-) in DMSO	104
44.	HPLC report of analysis of crude product (5:1)	105
45.	HPLC report of analysis of crude product (3:1)	106
46.	HPLC report of analysis of crude product (2:1)	107

CHAPTER I

INTRODUCTION

Solar energy cells:

Solar light is the most important source of regenerative energy (and also the source of waterpower, wind and biomass) and represents mankind's only inexhaustible energy source. The annual energy input of solar irradiation on Earth (5% UV, 43% visible, 52% IR) exceeds the world's yearly energy consumption by several thousand times. For the conversion of solar energy, fundamentally new developments are important. One of today's most promising tools to make use of solar energy is its direct conversion into electrical energy in a photovoltaic cell.

The practical use of these solar cells depends on the costs of the devices and therefore of the obtained energy. For years, the technology to convert sunlight directly into electricity was available only for the space program. The crystalline silicon cells used in this process, although efficient (typically, single crystalline silicon, 22%; polycrystalline silicon, 15%; amorphous silicon, 11%),¹ are too expensive for common consumer applications. A second generation of solar cells, made of very thin films of light-capturing molecular or polymeric organic compounds, did reduce the cost some, but overall energy conversion efficiency

(typically 0.5%)¹ is too low to be attractive for applications other than small consumer products.

Green leaves are nature's solar cells. They convert and store solar energy efficiently through the process of photosynthesis. Unlike in conventional solar cells, in leaves the functions of light absorption and charge transport are separated. In the green leaf, light is absorbed by chlorophyll molecules. The functions of charge separation and charge transport are performed by a series of mediators placed across the photosynthetic membrane. This process has been working successfully for almost three billion years. A new type of low-cost solar cell, based on dye-sensitized nanocrystalline titanium dioxide, has been developed in Switzerland by Michael Grätzel and his co-workers. It operates on principles similar to those used by green leaves. These cells are considerably cheaper and hold the promise of clean, plentiful solar energy.

The Grätzel Cell:

The Grätzel cell is a photovoltaic system for harvesting the sun's energy which closely parallels the way plants do it, and does it at one-fifth the cost of conventional solar cells.² In the simplest version³ the dye sensitized solar cell consists of two glass plates with a transparent conducting coating such as SnO₂ (Figure 1). One side, the photoelectrode, is coated with a porous layer of a wide band gap semiconductor, usually TiO₂, which is sensitized for visible light by an

adsorbed dye. Another conducting glass electrode is coated with a catalytic amount of platinum and serves as the counter electrode. The space between the two electrodes is filled with an electrolyte containing a redox couple, such as iodide (I^-)/triiodide(I_3^-).

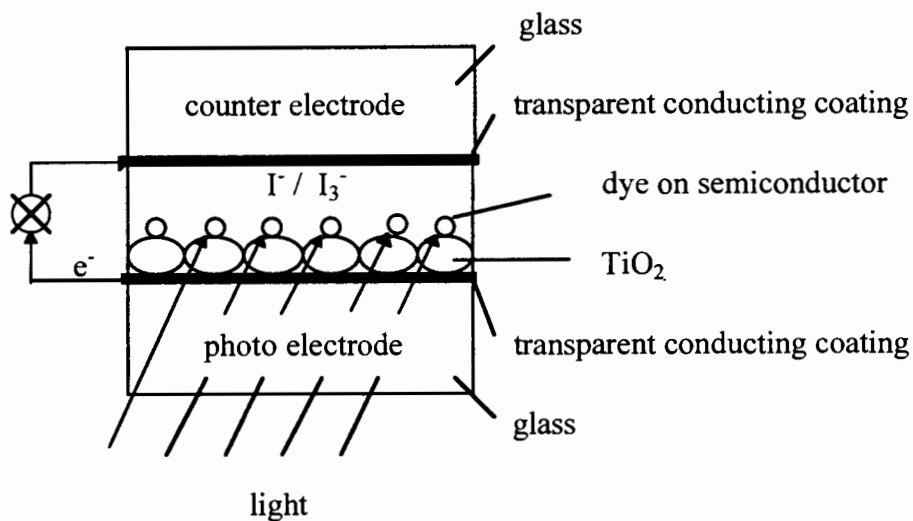


Figure 1. Grätzel cell

The dye molecules are adsorbed as a monolayer on the TiO₂ particles. Since a single dye monolayer absorbs less than 1% of the incident light, the surface area of the photoelectrode has to be enlarged by a factor of about 1000. This is achieved by using nanocrystalline TiO₂ particles with a diameter around 20 nm. For strong adsorption on the TiO₂ surface, the dye, most often a ruthenium complex, is functionalized with attachment groups, e.g., carboxyl or phosphonate groups.

After absorption of a photon, the dye molecule becomes electronically excited. The excited state then injects an electron into the TiO_2 particle, to which it is attached. The electron is conducted by the TiO_2 particles, which are sintered together at their contact points, until it reaches the conducting SnO_2 back contact. The oxidized dye resulting from the photoinduced electron transfer is reduced by iodide (I^-) in the electrolyte, which fills the pores of the photoelectrode. The produced triiodide (I_3^-) diffuses to the counterelectrode, where it is reduced back to iodide by an electron arriving from the external circuit. The nanostructured TiO_2 films modified with ruthenium polypyridyl complex exhibit incident photon-to-current efficiency (IPCE) of nearly 90% under optimized light-harvesting conditions³ and over 10% photoconversion efficiency,⁴ which is comparable to that of amorphous silicon-based photovoltaic cells and over twice the efficiency of natural photosynthesis. However, such design is not suitable for practical solar cells of large surface area, since the distance between photo- and counterelectrode soon becomes too large ($>20 \mu\text{m}$) due to the limited flatness of the separate substrates, causing additional ohmic losses and even diffusion limitation of the photocurrent in the electrolyte layer. Moreover the sheet resistivity of the SnO_2 coating limits the width of the cell to less than 1 cm. The incorporation of a highly conducting metallic grid, as proven from silicon cell technology, is hampered by the presence of the highly corrosive electrolyte, containing iodide and triiodide, that attacks most metals, such as silver, aluminum, copper, nickel and even gold.

In the newest version⁵ of Grätzel cell, each solar cell element consists of three porous layers on a transparent conducting substrate, namely a photoelectrode of dye sensitized nanocrystalline TiO₂ (anatase), a spacer of electrically insulating, light-reflecting particles of TiO₂ (rutile), and a counterelectrode of graphite powder and carbon black. The pores of these layers are filled with redox electrolyte containing iodide for hole transport between photo- and counterelectrode. The monolithic series connection on the transparent conducting substrate, e.g., SnO₂ coated glass, is achieved by simple overlap of each carbon counterelectrode with the back contact of the adjacent photoelectrode. A small module comprised six series-connected elements of 4.7 * 0.7 cm² each gave an efficiency of 5.29% ($V_{\max} = 3.90$ V, $I_{\max} = 28.55$ mA, fill factor = 61.4%) at 1000 W/m² with respect to the total surface area of 21.06 cm² (5.65% with respect to the active surface). Such new design of the dye-sensitized solar cell reduces significantly the materials costs of the solar cell, since only a single transparent conducting substrate is required. The electrolyte is fixed by capillary forces in the porous matrix and does not constitute an additional, free flow layer. Also there are some other advantages over the old design.⁵ Such modules may be produced in a continuous non-vacuum process by simple printing techniques. However, the leakage problem associated with liquid electrolytes are still remaining.

Mechanism of Dye-Sensitized Semiconductor Cell:

A simple energy level diagram for a typical dye-sensitized TiO₂ solar cell is illustrated in Figure 2. Three important processes control the efficiency of incident photon-to-charge-carrier generation. They include (i) the primary photochemical event of charge injection from excited sensitizer into semiconductor nanocrystallites, (ii) charge transport across the nanocrystalline film and (iii) regeneration of sensitizer with a suitable redox couple.

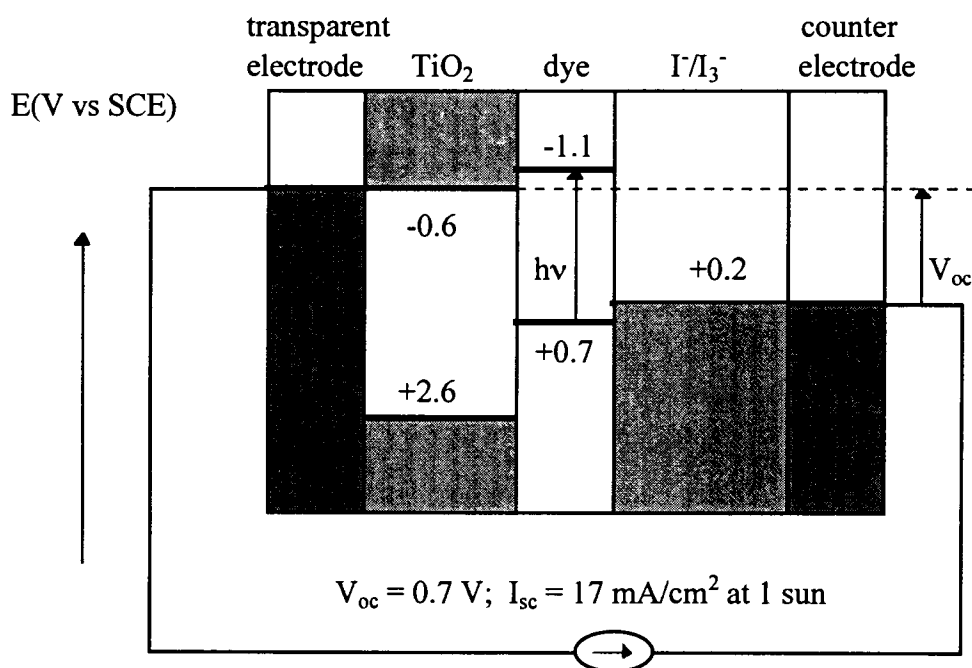


Figure 2. Energy level diagram for a typical dye-sensitized TiO₂ solar cell

The energy difference between the conduction band of the semiconductor and the oxidation potential of the excited sensitizer is the major driving force for the excited state charge transfer. The charge injection from singlet excited sensitizer into the conduction band of a large bandgap semiconductor is usually considered to be an ultrafast process. Charge injection process in the case of organic dyes such as anthracene carboxylate,⁶ squaraines⁷ and cresyl violet^{8,9} has been shown to occur within 20 ps. In contrast, relatively smaller charge injection rate constants (10^8 - 10^9 s⁻¹) have been reported by several research groups investigating the photophysical behavior of ruthenium complexes adsorbed on various semiconductor surfaces.^{4,10,11,12} Since the excited state of ruthenium complex involves metal to ligand charge transfer state, the implication is that such an electronic configuration of excited state plays an important role in controlling the electron injection rates.⁴

Back electron transfer between the injected charge and the sensitizing dye is a process that results in recombination losses.^{13,14} To achieve long term stability the forward reaction steps must be 10^6 times faster than irreversible degradation steps. Quick regeneration with a redox couple, such as I_3^-/I^- , is an essential step for the stability of the photochemical solar cells. The reverse electron transfer is usually monitored from the recovery of the sensitizer or from the decay of oxidized sensitizer. The reverse electron transfer is often a multiexponential process with a range of rate constants and suggests inhomogeneity of trap and/or

surface sites that control the heterogeneous electron transfer. In the case of Ru(II) polypyridyl complex/TiO₂ system, a Grätzel cell, the reverse electron transfer rate constant is 3-6 orders of magnitude lower than the rate constant of the charge injection process. The slow back electron transfer is particularly remarkable since the forward electron transfer (charge injection) is not as fast as in organic dye systems and contrasts with relatively fast reverse electron transfer observed in organic dye systems. This is apparently a unique characteristic of metal-oxide semiconductor/ Ru(II) polypyridyl complex systems that permits efficient operation of the photochemical solar cell.⁴

The high porosity and strong surface bonding property of nanostructured semiconductor films facilitate surface modification with organic dyes or organometallic complexes. The use of a single monolayer of dye also assures that every dye is in direct contact with the semiconductor electrode, which helps optimize the yield of photoinduced electron transfer. Extensive efforts have been made in various laboratories to modify the semiconductor surface with various sensitizing dyes, such as chlorophylls a and b,^{15,16} squaraines¹⁷ and oxazine.¹⁸ These dyes are directly adsorbed on the semiconductor surface either by electrostatic interaction or by charge transfer interaction. Functional groups such as carboxylates and phosphonates are useful for binding the dyes to oxide surface. Ruthenium(II) polypyridyl complexes have so far been proved to be most efficient in sensitizing nanocrystalline TiO₂ semiconductor films, as discussed in

the previous section. TCPP (meso-tetrakis(4-carboxyphenyl)porphyrin) as a photosensitizer has been studied by another graduate student (Suman Cherian) in our research group. The action spectra, light harvesting efficiencies and the electron injection efficiencies have been studied. The overall energy conversion efficiency has so far been found to be approximately 5% under best conditions, which is comparable to that of Grätzel cell sensitized by ruthenium complex.

Solid-state solar cell:

Although the photocurrent yield (I_{sc} = short-circuit photocurrent) is nearly perfect in terms of electrons per absorbed photon in the Grätzel cell, the degradation of the photon energy is substantial. A photopotential (V_{oc} = open-circuit photopotential) typically around 0.7 V is obtained, though the original photon energy, which must exceed the band gap of the dye, is about 1.8 V (Figure 2). Thus optimization of the photopotential is a clear remaining need for cells of this type. Also, the presence of the highly corrosive electrolyte, containing iodide and triiodide, hampers the incorporation of a highly conducting metallic grid and requires hermetic sealing of the module in order to prevent evaporation of the solvent as well as intrusion of water and oxygen.

Therefore, one goal of our research group is to replace the liquid-phase redox relay in such cells (typically I^-/I_3^-) with a conductive polymer, such as polyaniline (PAni), covalently bound to a porphyrin photosensitizer. Advantages

of such a solid-state solar cell are that (i) the band gap energy could be substantially less degraded with an appropriate choice of photosensitizer and conductive polymer, and (ii) the cell could be a completely solid-state cell without the attendant disadvantages of the liquid redox system. This approach effectively amounts to an interpenetrating network of two conductive materials, colloidal TiO_2 as an n-type semiconductor (electron transfer agent), and a conductive polymer as a p-type semiconductor (hole transfer agent), with the high-surface-area porphyrin/ TiO_2 interface as the charge separation zone. A simple energy level diagram for the proposed TiO_2 /TCPP/PAni solar cell is illustrated in Figure 3. The theoretical maximum of open-circuit photopotential (V_{oc}) is 1.4 V.

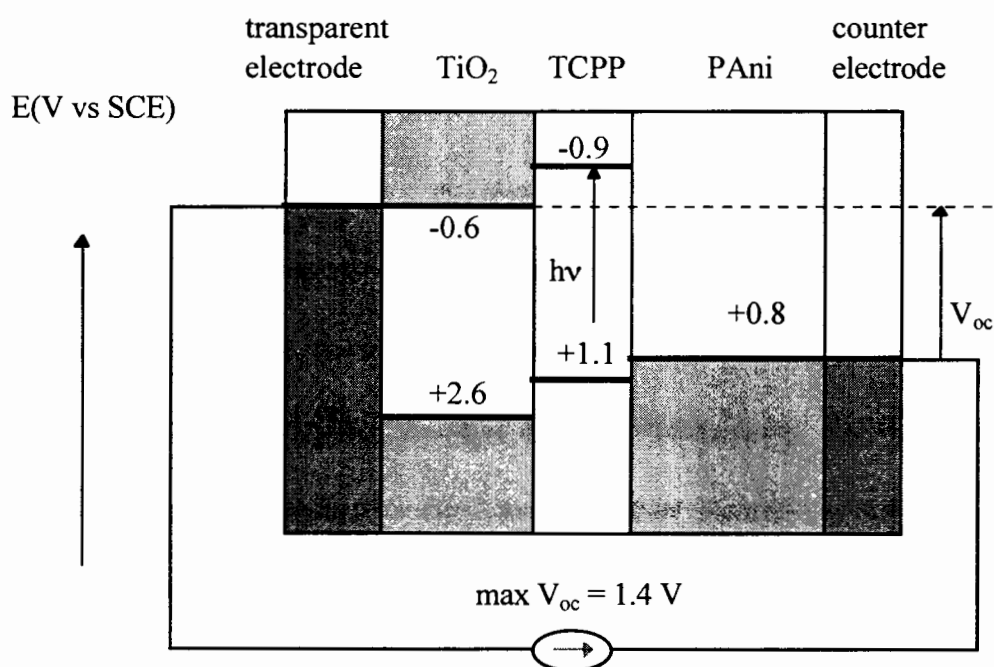


Figure. 3. Energy level diagram for the proposed TiO_2 /TCPP/PAni solar cell

The design criteria for the individual components in our solid-state solar cell will now be discussed in more detail.

1. The photoelectrode

The TiO_2 electrode consists of a wide band gap, porous semiconductor of high surface area, which is sensitized for the visible spectrum by a dye adsorbed on its surface, and has been primarily developed in the Grätzel group in Switzerland. Titanium dioxide (TiO_2) offers some unique properties⁵ making it the preferred semiconductor for dye sensitized solar cell. Its conduction band edge lies slightly below the excited state energy level of many dyes, which is one condition for efficient electron injection. The high dielectric constant of TiO_2 ($\epsilon = 80$ for anatase) provides good electrostatic shielding of the injected electron from the oxidized dye molecule attached to the TiO_2 surface, thus preventing recombination before reduction of the dye by the redox electrolyte. The related high refractive index of TiO_2 ($n = 2.5$ for anatase) results in efficient diffuse scattering of the light inside the porous photoelectrode, which significantly enhances the light absorption. Last, but not least, TiO_2 is a cheap, easily available, photostable and non toxic compound, that is already widely employed as white pigment in paints and toothpaste. Therefore TiO_2 and its standard well-documented preparation method for solar cells will be taken to be the photoelectrode of choice for this work.

2. Conductive polymer

A conductive polymer will serve as the redox relay (*i.e.*, electron transfer to photosensitizer) in a solid-state solar cell. Polymers have been used in photovoltaic cells just recently, in a phase-separated bicontinuous network of interpenetrating donor and acceptor materials (a fullerene derivative and a p-type conductive polymer),^{19,20} or in a polymer blend of donor and acceptor conductive polymer,²¹ and in a dye-sensitized TiO₂ solar cell with a p-type semiconductor (CuSCN) as the hole conductor.²² In first two cases, the photocurrent efficiencies were very low (< 10% in the absence of an external bias potential). Although greater efficiency (>70%) was obtained in the last case, it is due to a rapid photoinduced hole transfer instead of the more typical rapid photoinduced electron transfer observed at TiO₂. However, the combination of conductive polymer with the dye-sensitized high-surface-area TiO₂ electrode offers the opportunity to optimize absorption, electron transfer, and hole transfer.

Optimization of photopotential of a solar cell requires that the conductive polymer must have appropriate energy levels. In particular, the oxidation potential of valence band should be just above that of photosensitizer, but the conduction band should be relatively high to avoid any significant competitive light absorption. In order to assure rapid and efficient hole transfer (*i.e.*, electron transfer to the oxidized photosensitizer), the conductive polymer must also be strongly coupled electronically to the photosensitizer. Although a physical

connection may offer acceptable levels of conductivity for most electronic applications, covalent connection with photosensitizer through a direct conjugative linkage may be the best way for solar energy system. In addition, the conductive polymer must maintain a high level of conductivity during the operation of the cell.

Polyaniline (PAni) is generally considered to be the most stable and versatile of the common conductive polymers. It has an unique and useful property that allows it to be doped into its conducting state by oxidation and/or protonation. Conditions for the copolymerization of aniline with porphyrin derivatives, in particular tetra(4-aminophenyl)porphyrin (TAPP), which, like aniline, can be oxidatively electropolymerized into conductive polymer, have been investigated by Matthew J. Shiveley (an undergraduate student) in our research group. We therefore will take PAni and various derivatives^{23,24, 25} to be the solid-state conductive polymer of choice.

3. Photosensitizer

A photosensitizer is used to extend the optical response of semiconductors which do not absorb light of the desired wavelength. Dye sensitization occurs when a photoexcited dye at the surface of a semiconductor injects an electron into the conduction band of the semiconductor substrate. Criteria for an effective photosensitizer include (i) a UV-visible spectrum that leads to absorption of a high fraction of the solar spectrum, (ii) a closely matched

redox energy level to the energy level of semiconductor and conductive polymer, (iii) a rapid and efficient photoinduced electron injection into the TiO₂ and hole injection into the conductive polymer, (iv) general long-term photostability, thermal stability, and compatibility with the other components of the integrated system.

Porphyrin derivatives have wide range of UV-visible spectra, characterized with a strong Soret band around 420 nm and four Q bands in the range from 500 nm to 700 nm. Porphyrin derivatives also have suitable redox potentials. It was found that functional groups that lead to good adsorption and sensitization on TiO₂ surface are carboxylic acid^{26, 27} and phosphonates.^{28,29} An FTIR study of benzoic acid adsorbed on TiO₂ suggested that the nature of the linkage to the surface involved coordination of both oxygen atoms of the carboxyl group to a single surface titanium atom.³⁰ As noted earlier, TCPP (tetra(4-carboxyphenyl)-porphyrin) by itself can act as a photosensitizer for TiO₂ electrode, and resulting photocurrents and photovoltages are comparable to those reported for Grätzel cell. Also, TAPP (tetra(4-aminophenyl)porphyrin) can be polymerized, either with itself or with aniline, to form a conductive polymer. Therefore, porphyrins with carboxylic acid functional groups as active sites for linkage of the porphyrin to TiO₂ and aminophenyl groups as sites for initiation of PANi growth or for anchoring a formed PANi chain are desired photosensitizers for our proposed solid-state solar cell. Porphyrins with these functionalities could be a TCPP-

TAPP dyad linked via a single amide bond or a single porphyrin that contains both carboxyl and amino groups on the same macrocycle, such as, tri-(4-carboxyphenyl)-mono-(4-aminophenyl)porphyrin (TC₃APP). The research presented in this thesis describes synthetic method and characterizations of TC₃APP and attempted synthetic method of TCPP-TAPP dyad.

The structure of TCPP-TAPP is shown in Figure 4. The structures of the various porphyrins referred to this study, and their corresponding abbreviations, are shown in Figure 5.

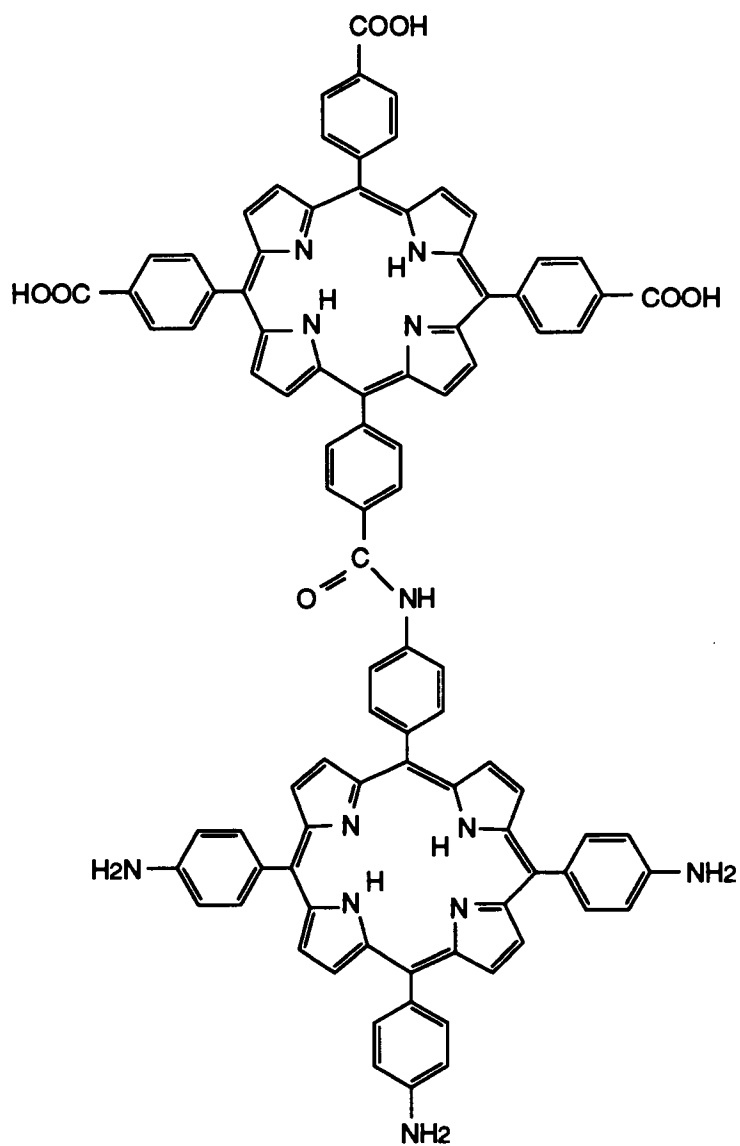
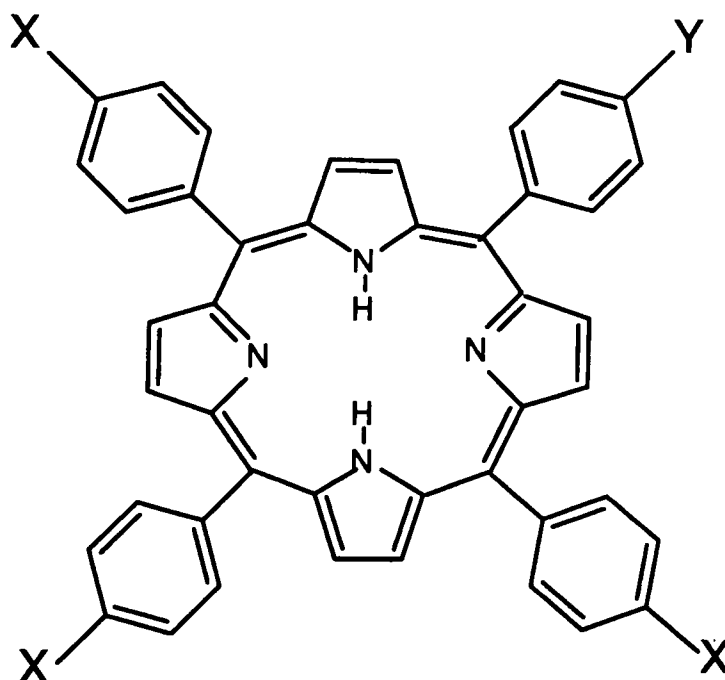


Figure 4. Structure of TCPP-TAPP dyad



TAPP: $X = Y = \text{NH}_2$;

TCPP: $X = Y = \text{COOH}$

TCM₄PP: $X = Y = \text{COOCH}_3$;

TCCPP: $X = Y = \text{COCl}$

TCM₃CPP: $X = \text{COOCH}_3$, $Y = \text{COOH}$

TCM₃AAPP: $X = \text{COOCH}_3$, $Y = \text{NHCOCH}_3$

TC₃APP: $X = \text{COOH}$, $Y = \text{NH}_2$

Figure 5. Structure and abbreviations for the porphyrins referred to in this work

CHAPTER II
EXPERIMENTAL
INTRODUCTION

The goal of this research project was to synthesize and characterize porphyrins containing carboxylic acid and aminophenyl groups, such as TC₃APP (Figure 5) or TCPP-TAPP dyad (Figure 4), as photosensitizers for the proposed solid-state solar cell. Studies of surface coverage of TCPP on colloidal TiO₂ electrode suggest that the molecules are not lying flat, but are oriented with the plane of the macrocycle more or less perpendicular to the surface, i.e., the porphyrin is anchored with only one or two carboxyl groups.³¹ The best combination of carboxyl groups for use on TiO₂ electrode is unclear, but at least two adjacent carboxyl groups seem to be necessary for good binding to TiO₂. At least one aminophenyl group is assumed to be necessary for attachment to PANi. Both TC₃APP and TCPP-TAPP dyad offer the requisite carboxyl groups and aminophenyl groups for attachment to TiO₂ and PANi. The redox potentials of TCPP and TAPP have been measured with cyclic voltammetry methods³² by a former graduate student in our research group. They are shown in Figure 6. Presumably, the redox potential of TC₃APP will be between that of TCPP and

TAPP, which matches the energy levels of TiO_2 and conductive polymer, since TC_3APP will have three quarters properties of TCPP and one quarter properties of TAPP. It has been proved that TCPP is a good photosensitizer on TiO_2 electrode.³¹ Preliminary study of TCPP and TAPP copolymerization also indicated that the energy levels are favorable for charge transfer from TAPP to TCPP³² and that polymeric porphyrin films made from TCPP and TAPP shows directional charge transfer.^{33,34} Thus in the case of TCPP-TAPP dyad as the photosensitizer, TAPP will serve as an electron donor and TCPP will serve as an electron acceptor, followed by electron transfer to semiconductor. Although TCPP-TAPP dyad could offer three sites for multiple connection to the conductive polymer network instead of only one site on TC_3APP , the advantage of TC_3APP over TCPP-TAPP dyad would be the shorter distance and presumed closer coupling (i.e., electron transfer and hole transfer) between the TiO_2 and conductive polymer, without the necessity for a porphyrin-to-porphyrin electron transfer. Thus we expect that the TC_3APP and TCPP-TAPP dyad will be promising for the desired purposes. TC_3APP has been successfully synthesized during this research project. A synthesis of TCPP-TAPP dyad also has been attempted.

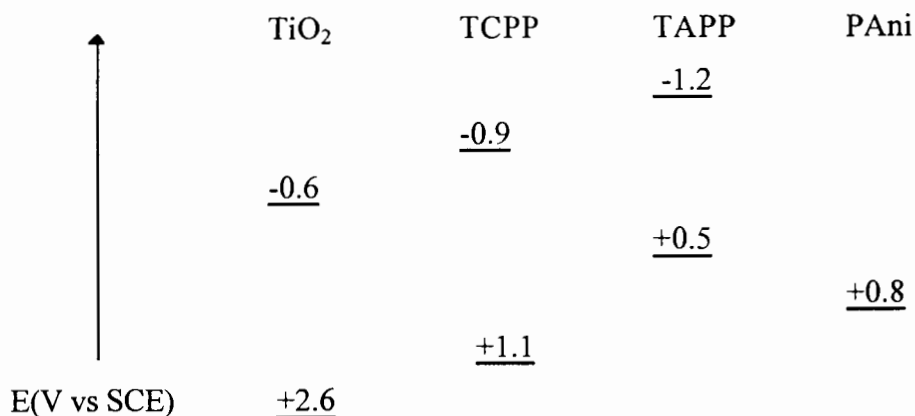


Figure 6. Energy levels of TCPP, TAPP, TiO₂ and PAni.

Materials:

All solvents, chloroform, dichloromethane (DCM), ethyl acetate, dimethyl sulfoxide and methanol, were HPLC grade from Aldrich and used as received. Trifluoroacetic acid and pyrrole were also from Aldrich. Methanesulfonic acid and trifluoromethanesulfonic acid were from Avocado Research Chemicals Ltd. Concentrated HCl was from J.T. Baker Inc. Sodium methoxide was from Mallinckrodt Chemical Works. Chloroform-*d* was from Aldrich and was stored under nitrogen. Dimethyl sulfoxide-*d*₆ was from Cambridge Isotope Laboratories.

Thin layer chromatography was carried out on Whatman PE SIL G/UV silica gel coated plastic plates. Column chromatography was performed using silica gel, on Merck grade 60, 70-230 mesh, from Aldrich.

Instrumentation:

UV-visible absorption spectra were acquired on a Shimadzu UV-260 spectrophotometer using a 2 mm slit width, 1 cm quartz cells, and an appropriate reference solution, which usually was the same solvent used to prepare the sample solution. The software used was Shimadzu Spectroscopy Interface Software, v. 3.1. All UV-visible spectra presented in this thesis were printed with Igor Pro, v. 2.02.

Fluorescence excitation and emission spectra were performed on a Spex Fluorolog Model 112 spectrofluorometer using a 150 W xenon lamp as light source. Slit widths were 1.25 mm for the excitation spectrometer and 2.5 mm for the emission spectrometer, except where noted. The concentration of sample was generally 0.1 μM and samples were placed in a 1 cm quartz cell. Right angle detection was used in all experiments. The software used with this instrument was DataMax for Windows, v. 2.0. All excitation and emission spectra presented in this thesis were printed with Igor Pro, v. 2.02.

The fluorescence lifetimes were measured by phase modulation method on a SPEX Fluorolog Tau-2 instrument at the University of Texas in the laboratories of Professor Stephen Webber. The conditions of measurements are as follows: the excitation wavelength was 420 nm, a glycogen/water colloid solution was taken as a zero lifetime standard, a filter cut-off at 550 nm was inserted between the sample cell and the photomultiplier, and the modulation frequency ranged from 10

to 100 MHz. The data of phase shift and demodulation at all frequencies were employed to analyze the fluorescence lifetime of the samples.

All reported ^1H NMR spectra were obtained on a Nicolet NT-500 MHz Spectrometer modified with a Tecmag Libra interface to a Macintosh IIfx computer. Chemical shifts are reported versus Me_4Si as an internal standard. The software used was MacNMR Tecmag, TX, v. 5.3. A pulse width of $8\ \mu\text{s}$ was used, and the data was acquired over a total of 12000 Hz in 16384 data points with a recycle delay of 3.4 s.

HPLC analyses were performed on a silica gel column (Si 80-125-C5) from Rainin Instrument Co. with two pumps, pressure monitor, and a DYNAMAX Model UV-1 absorbance detector. The column was 25 cm in length. All organic solvents were 50% water saturated. To prepare 1000 mL 50 % water-saturated solvent, 500 mL of solvent with 20 mL deionized water was stirred for 4 hours to prepare a 100% water-saturated solution, which was then mixed with an equal volume of anhydrous solvent.

ATTEMPTED SYNTHESIS OF THE TCPP-TAPP DYAD

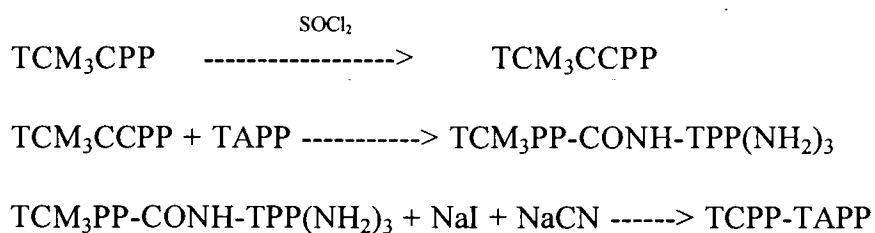
General Approach

The synthetic goal of this part of the project was to couple TAPP and TCPP via a single amide bond as shown in Figure 4. Most amide syntheses

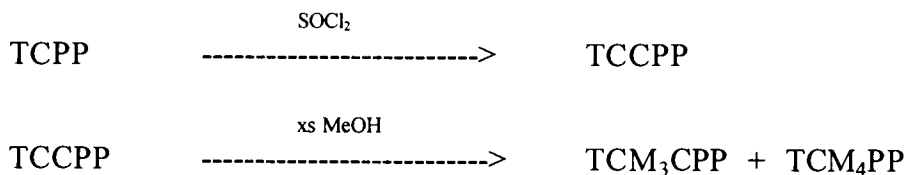
proceed via activation of the carboxyl group with a suitable coupling agent, followed by nucleophilic attack of the amine at the carbonyl carbon. Much work has been done on this project by a former graduate student (Dale A. Braden) in our research group. It was found that the amino group on TAPP is a very weak nucleophilic agent, possibly resulting from the lone pair electrons of amino group conjugated with the porphyrin macrocycle. Thus the synthetic strategy employed in this research project is that the carboxylic acid of a TCPP derivative (TCM_3CPP) was activated with thionyl chloride and then allowed to react with excess of TAPP, followed by deprotection of the ester groups (Scheme 1). Initially, TCM_3CPP was synthesized from TCPP by activating all carboxyl groups with thionyl chloride to acid chloride, followed by esterification in excess methanol (Scheme 2). The crude product is a mixture of various esterified porphyrins (i.e., mono-, di-, tri- and tetra-methyl esters of TCPP), predominately TCM_4PP and TCM_3CPP . Since the yield of TCM_3CPP was very low and there was so much trouble to remove the produced HCl, a more efficient and economical method was investigated. Hence TCM_3CPP was prepared directly from cyclization of pyrrole with mixtures of substituted benzaldehyde (Scheme 3) by a standard method for preparing tetraphenylporphyrins with mixed substituents.^{35,36,37} I also attempted to synthesize TCM_3CPP from TCM_4PP by cleaving off one ester group since TCM_4PP is easier to synthesize by the standard method and also commercially available. This was tried with a mild and non-

hydrolytic method³⁸ using NaI and NaCN in hot DMF. The yield of TCM₃CPP was just 10% even after 60 hours. TCM₃CPP was then activated with thionyl chloride to the acid chloride and coupled to TAPP. Purification of the produced dimer on silica gel column was unsuccessful. Gel filtration may be a better method. The subsequent deprotection of ester groups would appear to be feasible since an ester group is usually easier to cleave off than an amide group. These reactions are summarized in Scheme 1-3.

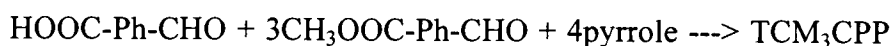
Scheme 1.



Scheme 2.



Scheme 3.



Synthesis of TCM₃CPP from TCPP

To synthesize the TCPP-TAPP dyad, the first step was to block three of the carboxyl groups of TCPP by methylation, thus limiting reactivity to the one remaining site, and facilitating chromatography of the product since porphyrins with carboxylic acid substituents are difficult to wash out from a silica gel column. The protection was done by activating all carboxylic acid groups with thionyl chloride, followed by esterification in excess methanol (see Scheme 2).

TCPP was refluxed in excess thionyl chloride for 2.5 hours. The excess thionyl chloride was removed by rotoevaporation and the green (protonated) product was placed in a vacuum oven at 80 °C overnight. The TCCPP was purple, which is normal porphyrin color.

TCCPP was then dissolved in DCM and excess methanol was added. The reaction mixture was stirred overnight and then solvents were removed by rotoevaporation. TLC analysis of the crude products in 1:1 (v/v) of DCM and ethyl acetate showed three spots, which means at least three different esterified porphyrins were produced. The product mixture was green, so that the porphyrins were likely protonated. This conclusion was confirmed by two Q bands instead of four Q bands appearing in UV-visible spectrum of this crude product. The green crude product was applied to a silica gel column. The silica gel column was prepared according to Dale Braden's suggestion by deactivating it with acetone and 15% water before using it.³⁹ Only the first band eluted, the rest

remained on the top of the column and could not be washed out even by using ethyl acetate alone. So the experiment was repeated and the product mixture was placed in vacuum oven at 80 °C and vacuum line (in Prof. Gary Gard's Lab) overnight. Although the crude product still looked a little bit green, we decided to separate it again. Three purple bands were collected by using a mixed solvent of DCM and ethyl acetate on a silica gel column. The solvent system was started with 3:1 (v/v) of DCM and ethyl acetate, followed by increasing the ratio of ethyl acetate in the solvent mixture until only ethyl acetate remained. A green band still remained on the top of column at the end of the run, which means that we might lose some protonated porphyrins on the column.

The UV-visible spectra of these three isolated products were very similar to TCPP. The NMR spectra of the first two bands indicated that they were TCM_4PP and TCM_3CPP . The NMR spectrum of the third band was really complicated and hard to say what it is. It might be the cis- and trans-diesterified TCPP, or a mixture of them.

In conclusion, the acid chloride of TCPP appear to be very reactive and moisture sensitive. So the methylation product was a mixture of various esterified TCPP since some acid chloride groups were hydrolyzed at some point. Trace HCl in the product mixture could cause purification problem due to the strong absorption of protonated porphyrines on silica gel column. The yield of

TCM₃CPP was very low. Also, the total porphyrin recovery is very low since some material was lost during column chromatographic separation.

Synthesis of TCM₃CPP from pyrrole and mixed substituted benzaldehydes.

The standard Rothmund and Adler-Longo method was used to synthesize porphyrins since this method is amenable to large-scale syntheses.³⁵ The introduction of two different types of substituents around the porphyrin periphery can be achieved in an expedient manner by a mixed aldehyde condensation.³⁷ Usually, a mixed aldehyde condensation of aldehyde of A and B with pyrrole affords a mixture of six porphyrins and tar. The desired A₃B-porphyrin is separated chromatographically. In the synthesis of our desired A₃B-porphyrin, aldehyde of B provides the reactive para-substituent and aldehyde of A serves to complete the construction of the porphyrin. The eventually desired feature of aldehyde A is that the produced porphyrin contains some para carboxylic acid group, which helps to chemisorb on TiO₂ surface. Since three of those carboxylic acid groups need to be masked in order to limit the following coupling reactivity to only one site, methyl 4-formylbenzoate was used as aldehyde A because of ready availability and high yield in the porphyrin-forming reaction. The desired feature of aldehyde B is that produced porphyrin contains a para carboxylic acid group for further dimerization in this case. The produced

porphyrin were further coupled to TAPP and deprotected to achieve desired features. The overall experiment is shown in Scheme 3.

To obtain high yield of TCM₃CPP, the synthetic conditions have been investigated. The mixed substituent benzaldehydes were dissolved in propionic acid. The solution was gently heated to 90 °C until the solution was clear. Pyrrole was then added to the reaction mixture. After refluxing for 40 minutes, the solution was cooled to room temperature and placed in an ice bath for a short time, followed by the suction filtration. The filter cake was washed thoroughly with methanol and the resulting crystals were air dried. The filter cake usually was bright purple crystals, but sometimes black precipitates. The black impurities are believed to be polypyrromethane. The trick of this reaction is the timing of filtration. If one waits too long, then often tar comes out of solution, which is to be avoided. If one does not wait long enough, few crystals will be obtained. Slowly cooling the reaction mixture to room temperature with vigorous stirring helps to obtain purple crystals.

Since longer reaction time in propionic acid does not appreciably improve the yield, but actually decreases the purity of the products,³⁹ the best refluxing time was determined to be 40 mins. The yield of mixed porphyrins was analyzed by absorption spectroscopy. The yield of total porphyrins is proportional to the intensity of the Soret band (419 nm in CH₂Cl₂).³⁹ So the intensity of Soret band

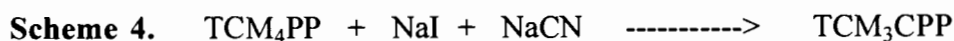
vs refluxing time was plotted. The intensity of absorption was increased with time and leveled off after 35 mins.

It was found that the yield of A₃B-porphyrin was affected by the mole ratio of the different functional benzaldehydes. An initial experiment of 3:1 mole ratio of A- to B-benzaldehyde condensation indicated the yield of A₄-porphyrin (TCM₄PP) was much higher than A₃B-porphyrin (TCM₃CPP), which means that ester aldehyde(A) is easier to form porphyrin than acid aldehyde(B). Initially, I thought that decreasing the mole ratios of A- to B-benzaldehyde may increase the yield of A₃B-porphyrin. However, the yield of mixed porphyrins was extremely low. The reason for this low yield may be that TCM₃CPP cannot be crystallized out as easy as TCM₄PP because of its higher polarity due to the carboxylic acid substituent on porphyrin. This would be a problem since the reaction was carried out in a very polar solvent, propionic acid. Increasing mole ratios of A- to B-benzaldehyde increased the total yield of porphyrins and also A₃B-porphyrin. It appears that 5:1 mole ratio of A- to B-benzaldehyde mole ratio is the best combination. The explanation could be that increasing mole ratio of A to B-benzaldehyde gives B-aldehyde more chance to form A₃B-porphyrin. However, the increased yield of A₃B-porphyrin due to increasing the mole ratio of A- to B-benzaldehyde may also suggest that cocrystallization plays an important role in this case since the structures of A₃B- and A₄-porphyrins are so similar. Thus increasing mole ratio of A- to B-benzaldehyde actually increased the yield of A₄-

porphyrin. The increased yield of A₃B-porphyrin probably resulted from cocrystallization of A₃B-porphyrin with A₄-porphyrin.

Synthesis of TCM₃CPP from TCM₄PP

Since TCM₄PP is easier to synthesize from standard method and also commercially available, it was attempted to synthesize TCM₃CPP from TCM₄PP with a mild and non-hydrolytic method³⁸ by using NaI and NaCN in DMF and refluxing at 140 °C. Also, this reaction was proposed to be the final step to cleave off all the ester protecting groups. Thus the reaction conditions and efficiency were of interest. The overall experiment is as follows:



The mole ratio of TCM₄PP to NaI and NaCN was 1:5:1. The concentration of TCM₄PP was 0.02 M. All chemicals were dried in vacuum oven overnight. The reactant mixture was refluxed under N₂. TLC was used to monitor the reaction. The crude product was a mixture of porphyrins. When the mixture was cooled to room temperature, the solvent was removed by rotoevaporation. The desired TCM₃CPP was further purified chromatographically on a silica gel column. The yield of TCM₃CPP was just 10%, with the rest unreacted TCM₄PP even after refluxed 60 hours. Increasing the mole ratio of TCM₄PP to NaI and NaCN to 1:5:2 did not seem to increase the yield of TCM₃CPP. The reason probably is that the concentration of TCM₄PP was too low because of the

solubility limitation of porphyrins. Higher concentration of NaI and a lewis acid as catalyst may increase the rate. Me_3SiI may be a better nucleophilic reagent.

Coupling TCM_3CPP with TAPP

TCM_3CPP was initially converted to acid chloride by activating the carboxylic acid with thionyl chloride in toluene. Excess thionyl chloride was added and reaction was monitored by TLC. After stirring for one hour at room temperature, no TCM_3CPP was shown on TLC plate. The reaction solvents were removed by rotoevaporation. The product looked green, so it was placed in vacuum oven at $80\text{ }^\circ\text{C}$ overnight. TCM_3CCPP was then coupled to TAPP in chloroform. Pyridine was used as the catalyst. After stirring at room temperature for one hour, the reaction was stopped and solvents were removed by rotoevaporation. TLC analysis in 1:4 (v/v) methanol and chloroform showed five spots, which were identified by comparing with standard compounds on same TLC plate. The first and biggest spot might be mono-(carboethoxyphenyl)-tri-(carbomethoxyphenyl)porphyrin since the R_f value was almost the same as TCM_4PP , which might result from TCM_3CCPP reacting with the trace ethanol in chloroform. The second spot was TCM_3CPP because of the same R_f value, which might result from hydrolysis of TCM_3CCPP at some point. The third spot was unreacted TAPP. The fourth little spot might be the dyad we wanted and the last black tiny spot might be some impurities. Further purification on silica gel column

was unsuccessful since it was so hard to wash out and the amount of dyad was too little, thus most was lost on column. Gel filtration may be a better method to purify dyad, which has been successfully used to purify TCPP and TAPP pentamer by another graduate student (Tristan J. Jenkins) in our research group. Chloroform should not be used as reaction solvent since it usually contains ethanol as the stabilizer. More caution should be paid in order to improve the yield since acid chloride was very sensitive to moisture.

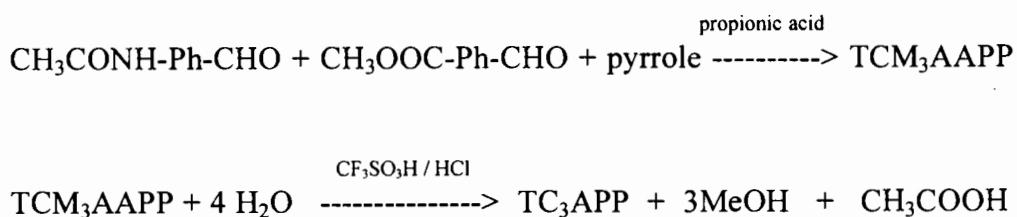
SYNTHESIS OF TC₃APP

General approach

The synthetic goal of this part of the project was to make a single porphyrin with carboxylic acid functional groups and aminophenyl groups on the same macrocycle as a photosensitizer for our proposed solid-state solar cell, since the TCPP-TAPP dyad was so difficult to make (see above). TC₃APP was the first case that came to our mind since we already had some experience with making A₃B-porphyrin directly from the cyclization of pyrrole with mixed substituted benzaldehydes. However, the porphyrin with carboxylic acid and amino groups cannot be directly synthesized by the standard method since neither the carboxy nor amino derivatives undergo cyclization to porphyrins very well.^{36,37} The parent porphyrin prepared was TCM₃AAPP, which has the carboxylic acid and amino

groups protected as esters and amide. Methyl 4-formylbenzoate and 4-acetamidobenzaldehyde were used as the ester and amide substituted benzaldehydes because of their ready availability and high yield in the porphyrin-forming reaction. The desired TC₃APP was obtained from further hydrolysis of TCM₃AAPP (scheme 5).

Scheme 5.



Synthesis of TCM₃AAPP from pyrrole and mixed substituted benzaldehydes

TCM₃AAPP was synthesized from the standard Rothmund and Adler-Longo method as described in synthesis of TCM₃CPP section. The crude product was a mixture of six porphyrins and tar. TCM₃AAPP was separated chromatographically. The black precipitate was the major problem, which usually took two or more flash chromatographic procedures to get pure TCM₃AAPP, especially when the mole ratio of ester benzaldehyde to amide benzaldehyde in the reactant mixture was lower than 3:1.

It was found that the total porphyrin yield was around 18%, which is very close to the literature value for synthesis of similar porphyrins,^{35,36} and not affected by changing mole ratio of mixed benzaldehydes, though the yield of

TCM₃AAPP (A₃B-porphyrin) was affected as we expected. In mixed aldehyde condensation, the yield of the A₃B-porphyrin usually is a function of the yields of the respective A₄- and B₄-porphyrins.³⁷ The yields of various porphyrins in crude products were analyzed by HPLC on a silica gel column with 3:2 (v/v) of ethyl acetate and DCM (Table 1). It is more likely that decreasing mole ratio of A- to B-benzaldehyde will increase the yield of A₃B-porphyrin. However, decreasing mole ratio of A- to B-benzaldehyde often result in black precipitates, which could cause further purification problem. Thus in terms of practical approach, 3:1 mole ratio of A- to B-benzaldehyde seemed to be the best combination.

Table 1. % yield of various porphyrins in the crude product

A:B mole ratio	2:1	3:1	4:1*	5:1
A ₄ -porphyrin yield (%)	36	50	64	66
A ₃ B-porphyrin yield (%)	45	41	33	29
A ₂ B ₂ -porphyrin yield (%)	15	8		3
Total porphyrin yield (%)	19	20	17	18

*These data were calculated from actual yield since no sample was available for HPLC analysis.

In conclusion, the batch to batch reproducibility of this reaction was poor and the high level of tar produced presented a purification problem. Results are summarized in Table 1.

Synthesis of TCM₃AAPP from thermodynamic equilibrium method

The room-temperature condensation followed by 2,3-dichloro-5,6-dicyano-1,4-benzoquinone (DDQ) oxidation is another method currently used to synthesize porphyrins with some sensitive substituents and usually give higher yield than Rothmund and Adler-Longo method.^{36,37,41,42} In order to get higher yield and alleviate the purification problem from the black precipitate, the synthesis TCM₃AAPP was tried by this method too.

The reaction was performed in a 250 mL, three-necked, round bottomed flask fitted with a septum port, a reflux condenser, and a gas inlet port. The reaction was carried out under nitrogen. The flask was charged with 100 mL of DCM and mixed aldehydes. When the solution was clear, pyrrole was added. The initial concentration of aldehydes and pyrrole were 10 mM. After a few minutes, BF₃ in MeOH was added into solution. The solution color changed from faint yellow to orange. The solution was stirred at room temperature for 90 mins. Then powdered DDQ was added into solution. The color changed to black immediately. The solution was continuously stirred one more hour. Then solvent was removed by rotary evaporation.

The crude product was totally black and TLC analysis of crude product showed that it did contain two main porphyrins (A₄- and A₃B-porphyrins), but it also showed more spots than the sample from Rothmund and Adler-Longo

method, which made it more difficult to separate TCM₃AAPP from the mixed porphyrins. The reaction also has to be carried out in very low concentration, such as 0.01 M, which means it would not be suitable for large-scale syntheses.

Synthesis of TC₃AAPP from hydrolysis of TCM₃AAPP

Hydrolysis of TCM₃AAPP was initially carried out with 1:1 (v/v) of concentrated HCl and TFA (trifluoroacetic acid) in a 80-90 °C oil bath. TLC was used to monitor the reaction. NMR spectra of the product indicated that ester groups were removed but the amide group was not completely removed even after refluxing for 48 hours. The increasing amount of HCl in the reactant mixture did not help and sometimes resulted in a solubility problem. Therefore a stronger acid, trifluoromethanesulfonic acid (TFMSA), was used instead of TFA.

A sample of TCM₃AAPP (34 mg) was dissolved in 5 mL trifluoromethanesulfonic acid. Then 10 mL conc. HCl was added yielding a fuming solution. The reaction mixture was placed in an oil bath at 80-90 °C and stirred magnetically for 48 hours. The green solution was allowed to cool to room temperature. Then it was carefully poured into a 6 M NaOH solution to neutralize acid and dilute the solution. The pH was adjusted to 5, followed by liquid-liquid extraction with ethyl acetate. Sometimes the pH needed to be adjusted to basic with NaOH first and then adjusted back to 5-6 with concentrated

HCl. Otherwise, the porphyrin could not be extracted into organic layer and the reason is not known. In order to remove all the organic or inorganic impurities, the organic layer was washed with water, NaCl-saturated solution and the porphyrin was extracted back into aqueous solution with 0.1 M NaOH solution. Then the separated aqueous solution was washed with ethyl acetate, followed by adjusting pH to 5-6 and extracting the porphyrin back into ethyl acetate. This organic layer was dried with Na_2SO_4 for a couple of days. The final product was isolated by rotoevaporation to dryness, or by crystallizing out by addition of n-heptane in ethyl acetate. The NMR spectrum of TC_3APP in DMSO clearly indicated that all ester and amide groups were completely removed. The yield of this reaction was about 80%.

CHAPTER III

RESULTS AND DISCUSSIONS

CHROMATOGRAPHY

Column chromatography:

Flash column chromatography was used to separate A₃B-porphyrins from mixed porphyrins instead of the classic column chromatography. Flash column chromatography saved substantial time during packing column and eluting the desired compound, and prevented the tailing problem from the classic column chromatography, especially when the quantities of sample being separated exceeded 1g.

Pretreatment of silica gel with water was claimed to be necessary to separate TCM₃CPP from the porphyrin mixture with dichloromethane and ethyl acetate as solvent system by a former graduate student (Dale A. Braden). What I found was that either chloroform or DCM with methanol as the polar medium was suitable and that the water pretreatment was not necessary. The reason pretreatment may help in some cases is that porphyrins with carboxylic group usually tend to strongly adsorb on the silica gel because of the hydrogen bonding. Using a solvent with hydroxyl group, such as methanol, will solve this problem

because the porphyrin with carboxylic acid groups is more soluble in methanol than in ethyl acetate due to the hydrogen bonding.

The successful solvent system for purifying TCM₃CPP on a silica gel column was a chlorinated hydrocarbon (either chloroform or DCM) as the non-polar medium and methanol as the polar medium. One may start with chloroform (or 2.5% (v/v) MeOH in DCM), which will elute out TCM₄PP, then increase polarity of solvent by using 3% (v/v) methanol in chloroform (or 6% (v/v) methanol in DCM). The second band is the desired TCM₃CPP. There is not much difference in polarity between chloroform and DCM, but the difference during eluting out porphyrin is because chloroform is usually stabilized with ethanol. The crude product usually contained some insoluble components. The solubility problem arising during flash chromatography could be eliminated by the following procedure. Crude product could be dissolved in a polar solvent, such as chloroform and methanol mixture, until the sample was totally dissolved. Then a few grams of silica gel were added into the solution. The slurry so formed was dried by rotary evaporation to yield a damp powder, which could be directly poured on top of the chromatography column dry packed with silica gel.

The successful solvent system for separating TCM₃AAPP from mixed porphyrins and tar is chloroform or DCM as the nonpolar medium with ethyl acetate as the polar medium. Chloroform (or 5% (v/v) ethyl acetate in DCM) will elute TCM₄PP and 2% (v/v) ethyl acetate in chloroform (or 10% (v/v) ethyl

acetate in DCM) will elute TCM₃AAPP. The high level of tar produced did present a purification problem during chromatographic purification of TCM₃AAPP from mixed porphyrins. In the case that a black precipitate instead of a purple precipitate was obtained, it usually took two or more flash chromatographic procedures to get pure TCM₃AAPP, even if the black precipitate was washed with methanol again and again before it was applied on column. The black impurities eluted immediately with the solvent front. The difference between two bands was just barely enough to recognize due to the black color on the column. Such a separated sample needed to be purified again and the recovery usually was low. No solubility problem was encountered in this case, which could be explained by the lower polarity of TCM₃AAPP as compared to TCM₃CPP, because of the lower polarity of the amide substituent than the carboxylic acid substituent on porphyrin, as well as less hydrogen bonding.

HPLC analysis

To determine the best mole ratio of mixed benzaldehydes during TCM₃AAPP synthesis, quantitative analysis of the yields of various porphyrins was investigated with HPLC. Normal phase HPLC analysis on a silica gel column was chosen to do this job since this approach has been successfully used to analyze a TCPP and TAPP mixture by a colleague in our research group, Tristan Jenkins. The tested sample was a mixture of TCM₄PP and TCM₃AAPP. The

solvent system initially chosen was 4% (v/v) methanol in DCM. The resolution was pretty good. However, the second band (TCM₃AAPP) was very broad and had substantial tailing. Increasing the amount of methanol in the solvent system resulted in decreased resolution. Gradient elution was then tested. The analysis started with 4% (v/v) methanol in DCM. Once the first band came out, the amount of methanol in DCM was increased. Although the resolution was adequate, the broadness and tailing problem remained. Considering the solubility of porphyrins with ester and amide substituents and the success on column chromatography, a new solvent system, DCM and ethyl acetate, was tested. The broadness and tailing were reduced, but the result was still not acceptable. According to the reference,⁴³ water-saturated organic solvents could deactivate the silica gel column and solve the tailing problem. Therefore 50% water-saturated DCM and ethyl acetate were prepared (see Chapter II instrumentation section). After a few runs, an optimized solvent system was determined to be a mixture of 2:3 DCM:ethyl acetate. The resolution was good and the peak shape was symmetrical. The crude product was then analyzed under the optimized condition. The retention times of black impurities, TCM₄PP, TCM₃AAPP, trans- and cis- TCM₂AA₂PP were 4, 7.6, 10, 14, 19 minutes, respectively. The raw data are included in Appendix.

It is also worthwhile to note that the silica column needs to be cleaned occasionally with a strong solvent, such as ethyl acetate or acetonitrile. Otherwise

the pump pressure will be increased and the retention times will be different from run to run.

SPECTROSCOPY

NMR spectroscopy:

5,10,15,20-Tetrakis-[4-(carbomethoxy)phenyl]porphyrin (TCM₄PP): ¹H NMR (in CDCl₃) δ -2.81 (s, 2H, NH), 4.1 (s, 12H, OCH₃), 8.3, 8.4 (dd, J = 8Hz, 16H, HAr), 8.8 (s, 8H, β-pyrrole-CH).

5,10,15-Tri-[4-(carbomethoxy)phenyl]-20-(4-carboxyphenyl)porphyrin (TCM₃CPP) : ¹H NMR (in CDCl₃) δ -2.81 (s, 2H, NH), 4.1 (s, 9H, OCH₃), 8.35, 8.53 (dd, J= 8Hz, 4H, HArCOOH), 8.30, 8.45 (dd, J = 8Hz, 12H, HArCOOCH₃), 8.3 (d, 8H, β-pyrrole-CH).

5,10,15-Tri-[4-(carbomethoxy)phenyl]-20-[(4-acetamido)phenyl]porphyrin (TCM₃AAPP): ¹H NMR (in CDCl₃) δ -2.81 (s, 2H, NH), 2.38 (s, 3H, CH₃CO), 4.1 (s, 9H, OCH₃), 7.5 (s, 1H, RCONH-Ar), 7.9, 8.16 (dd, J= 8Hz, 4H, HAr-NHCOCH₃), 8.29, 8.44 (dd, J = 18Hz, 12H, HAr-COOCH₃), 8.81 (s, 6H, β-pyrrole-CH), 8.88 (d, 2H, β-pyrrole-CH).

5,10,15-Tri-(4-carboxyphenyl)-20-(4-aminophenyl)porphyrin(TC₃APP): ¹H NMR (in DMSO-d₆) δ -2.8 (s, 2H, NH), 5.5 (s, 2H, NH₂-Ar), 7.06, 7.90 (dd,

$J = 8\text{ Hz}$, 4H, $\underline{\text{H}}\text{Ar-NH}_2$), 8.34, 8.39 (dd, $J = 6\text{ Hz}$, 12H, $\underline{\text{H}}\text{Ar-COOH}$), 8.8 (d, 6H, β -pyrrole-CH), 8.97 (d, 2H, β -pyrrole-CH).

^1H NMR spectra of TCM_4PP , TCM_3CPP , TCM_3AAPP and TC_3APP are included in the Appendix. All NMR spectra were recorded in CDCl_3 , except for TC_3APP for which DMSO-d_6 was the solvent because this product is insoluble in CDCl_3 . These spectra are consistent with normal porphyrin spectra. The inner pyrrole ring hydrogens bonded to the nitrogens typically resonate at about -2.8 ppm relative to TMS because of ring current effects. For a symmetrical A_4 -porphyrin (eg. TCM_4PP), the hydrogens on a para-substituted benzene ring typically resonate at around 8 ppm, as two sets of pseudo doublets ($\text{AA}'\text{BB}'$ spin system). For unsymmetrical A_3B -porphyrin, this pattern is doubled. Integration of these two groups of peaks shows that their intensity ratio is 3:1, which clearly indicates two different types of substituted benzene rings. In addition, hydrogens at the β -positions of the pyrrole rings typically resonate at 8.8 ppm as a single peak for a symmetrical A_4 -porphyrin. Two peaks with an integrated signal ratio of 3:1 are observed for unsymmetrical A_3B -porphyrin. All this is in accord with anticipated molecular symmetries.

In the ^1H NMR spectrum of the desired porphyrin TC_3APP , the peak positions of the hydrogens on the carboxylic acids and amino substituted benzene rings are consistent with that on TCPP and TAPP , although the peak pattern of

hydrogens on the carboxyphenyl groups is complex instead of well resolved doublet peaks. The absence of peaks at 7.5 and 4.1 ppm, which arise from the hydrogens in amide and methyl ester groups, also clearly indicated that the product we obtained is TC₃APP, rather than the starting material, TCM₃AAPP.

Mass spectrometry

Masses of synthesized TCM₃AAPP and TC₃APP were determined at the Pacific Northwest National Laboratory with ion cyclotron resonance mass spectrometry by Gordon Anderson and James Bruce. All samples were dissolved in very strong acetic acid. These spectra are included in Appendix. The experimental results and calculated values are presented in Tables 2 & 3. The experimental results agree with predicted masses very well.

Mass spectrometry traces obtained by chemical ionization are also included in Appendix. Since the positive charge after ionization is localized essentially in the extended π system of the macrocycle, fragmentation occurs only by the degradation of substituents, which are fixed by the rigid ring system.⁴⁴ M - 58, M - 59, M - 2*59, M - (58 + 59), M - (59 + 76), M - (58 + 76) ion peaks were observed for TCM₃AAPP. These corresponded to the masses of TCM₃AAPP losing an amide, an ester, two ester, an amide and an ester, an amide and a phenyl, an ester and a phenyl group, respectively. M - 16, M - 45, M - (45 + 16), M - 2*45, M - (45 + 76) ion peaks were observed for TC₃APP. They

corresponded to the masses of TC₃APP losing an amino, a carboxylic acid, an amino and a carboxylic acid, two carboxylic acid, a carboxylic acid and a phenyl group, respectively.

Table 2. Masses of TC₃APPH⁺ (C₄₇H₃₂N₅O₆⁺)

	MW.	(M+1)%	(M+2)%
Expt.	762.2302	52	14
Cal.*	762.2354	55	15

Table 3. Masses of TCM₃AAPPH⁺ (C₅₂H₄₀O₇N₅⁺)

	MW.	(M+1)%	(M+2)%
Expt.	846.2979	40	13
Cal.*	846.2930	59	18

* These values were calculated by using following atomic masses and formula.⁴⁵

$${}^1\text{H} = 1.00783, {}^{12}\text{C} = 12.0000, {}^{14}\text{N} = 14.0067, {}^{16}\text{O} = 15.9994$$

$$\%(M+1) = 1.1 * \text{Number of C atoms} + 0.36 * \text{Number of N atoms}$$

$$\%(M+2) = (1.1 * \text{Number of C atoms})^2 / 200 + 0.2 * \text{Number of O atoms}$$

Ultraviolet/Visible spectroscopy

UV-visible absorption spectra of TCM₄PP, TCM₃CPP, TCM₃AAPP and TC₃APP are presented in the Appendix. All spectra were taken in DCM, except

for TC₃APP, which was obtained in DMSO since it is insoluble in DCM. These are consistent with the normal free base porphyrin spectra. All spectra have an intense Soret band around 420 nm, which represents the S₀ to S₂ transition, and four Q bands (Q_{y(1,0)}, Q_{y(0,0)}, Q_{x(1,0)}, Q_{x(0,0)}), which represent different vibrational levels of the S₀ to S₁ transition. The UV-visible absorption spectra of TCM₄PP, TCM₃CPP and TCM₃AAPP in DCM are almost identical (Table 4). The spectrum of TC₃APP has characters of both TAPP and TCPP, although the spectrum of TC₃APP is more like that of TCPP (Table 5). The spectrum of TC₃APP has four Q bands instead of three Q bands as in TAPP. However, the anomalous character of the spectrum of TAPP, three broad Q bands instead of four Q bands, is also shown in the spectrum of TC₃APP in the form of Q_{y(0,0)} and Q_{x(1,0)} bands which are closer to each other than they are in TCPP. Also, all Q bands of TC₃APP are red-shifted as compared with those of TCPP, but are blue-shifted as compared with those of TAPP.

Table 4. Absorption wavelength (nm) of TCM₄PP, TCM₃CPP and TCM₃AAPP in DCM.

	Soret	Q _{y(1,0)}	Q _{y(0,0)}	Q _{x(1,0)}	Q _{x(0,0)}
TCM ₄ PP	419	514	550	591	646
TCM ₃ AAPP	419	515	551	592	646
TCM ₃ CPP	418	513	550	589	646

Table 5. Absorption wavelength (nm) of TC₃APP, TCPP and TAPP in DMSO.

	Soret	Q _{y(1,0)}	Q _{y(0,0)}	Q _{x(1,0)}	Q _{x(0,0)}
TCPP	420	514	550	590	644
TC ₃ APP	420	518	560	592	653
TAPP	439	528	582		670

Spectrophotometric acid titrations of TCPP and TC₃APP were carried out in DMSO with methanesulfonic acid (MSA). Figure 7 shows the spectra of successive acid-titration additions to TCPP to form TCPPH₂²⁺. The titration with MSA gives only single sets of good isosbestic points, up to complete protonation, with no indication of intermediate monocation formation. The Soret band of protonated TCPP is shifted from 420 nm to 447 nm and two Q bands show up at 656 nm and 605 nm, which agree very well with that of protonated porphyrins, characterized as a red-shifted Soret band and two Q bands due to the increased symmetry of molecule from D_{2h} to D_{4h}.

Spectra of successive acid-titration additions to TC₃APP are given in Figure 8 parts a, b and c. Protonation occurs in two separated stages, though the first protonation step is not completely finished when the second step starts,

which probably results from two close pKa values of the analytes. The initial product, assigned to two proton additions ($0 \rightarrow 2+$) at the central nitrogens, shows a somewhat increased and slightly blue-shifted ($420 \rightarrow 419$ nm) Soret band, disappearance of the original broadened four-banded spectrum, and two new bands, a broad absorption at 512 nm and a flat far-red band at 712 nm, extending almost to 800 nm, which is a typical so-called hyperporphyrin spectrum.^{46, 47} The second step ($2+ \rightarrow 3+$) at higher concentration of MSA protonates the single peripheral amine, giving a “normal” porphyrin-acid spectrum, with a sharp Soret peak at 446 nm and a red band at 658 nm with a shoulder around 602 nm. Except that a blue-shifted Soret band instead of red-shifted was observed during first protonation step, these spectra are consistent with some literature results for a monoamino substituted tetraphenylporphyrin.^{43,44} The theoretical interpretation is that charge-transfer excited states, involving charge movement either into or out of the macrocycle, are responsible for the features of these spectra. Regular porphyrin spectra arise from the four-orbital model: HOMOs $a_{2u}(\pi)$, $a_{1u}(\pi) \rightarrow$ LUMOs $e_g(\pi^*)$. The orbitals responsible for the hyper porphyrin spectra are filled π orbitals on the amino nitrogen atoms which permit transmissions to the porphyrin LUMOs. The possibility that such charge-transfer transitions play a role is indicated by the resonance structures as shown in Figure 9. Structure A is the expected protonated dication structure for TC_3APPH^{2+} . Structure B is a

resonance form in which one of the central positive charges of the dication migrates out to the aminophenyl group. This corresponds to a charge transfer from the peripheral amino nitrogen to the ring.

Spectrophotometric base titrations of TCPP and TC₃APP were carried out in DMSO with sodium methoxide (NaOMe). Spectra of successive base-titration additions of TCPP and TC₃APP are given in Figures 10 & 11. They are almost identical for TCPP and TC₃APP. The deprotonation occurs in two separate steps. The first step is assigned as the deprotonation of all carboxylic acid groups because the carboxylic acid usually is a stronger acid than pyrrole. Since the symmetry of the porphyrin molecule is not changed during this step, only an increased Soret band, but no isosbestic, was observed in the titration with the low concentrations of NaOMe. Continued titration with more concentrated NaOMe gave a set of good isosbestic points. The Soret band is red-shifted from 420 nm to 438 nm, and two Q bands appear at 582 nm and 626 nm, which are consistent with that of deprotonated porphyrins with D_{4h} symmetry. However, a very flat peak around 775 nm was also observed. This may result from porphyrin aggregation since the peak around 300 nm, which is caused from light scattering, was increased during the titration and continued titration decreased the Soret band. The solution was observed to become cloudy, also an indication of aggregation.

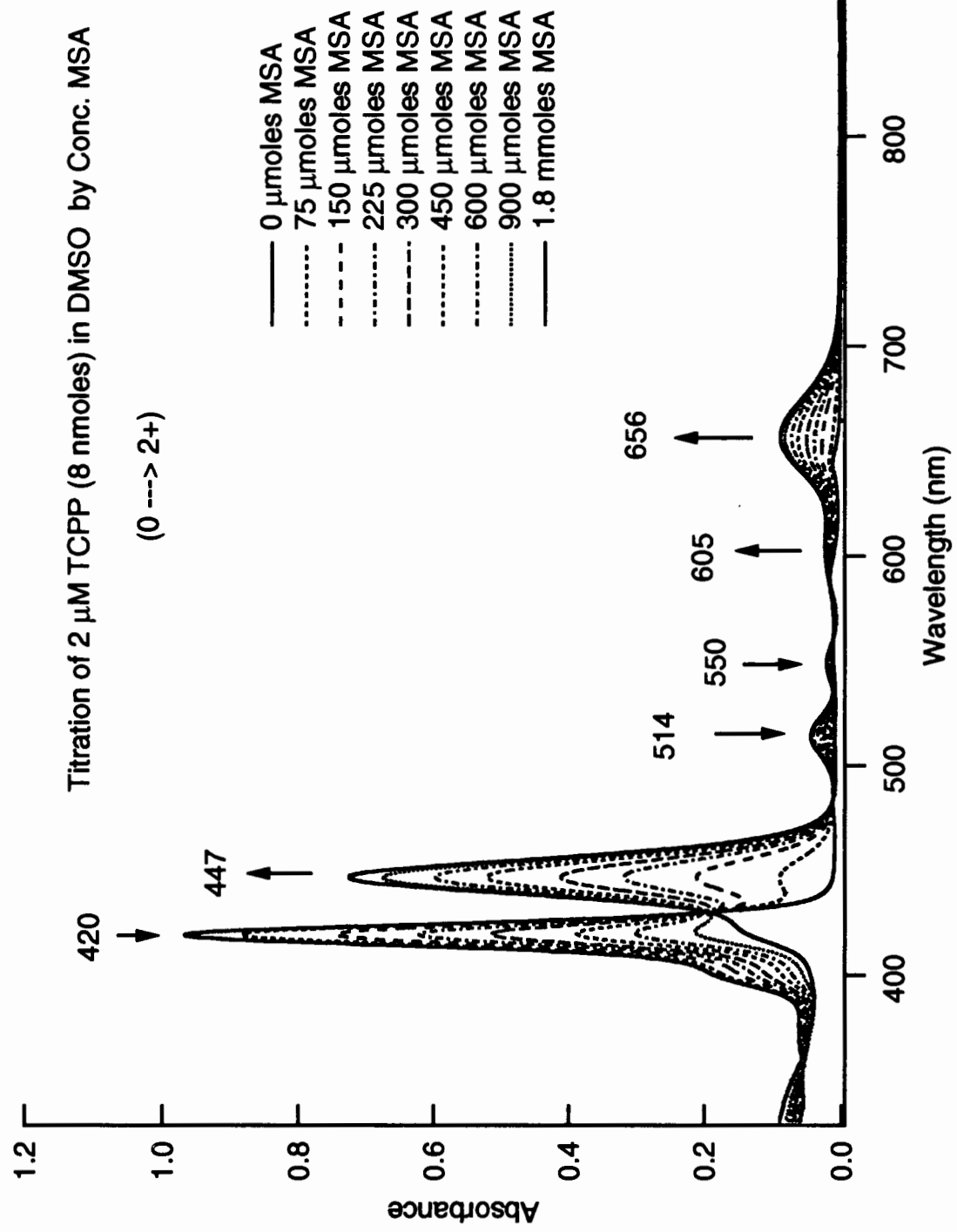


Figure 7. Absorption spectra of successive acid-titration additions of TCPP

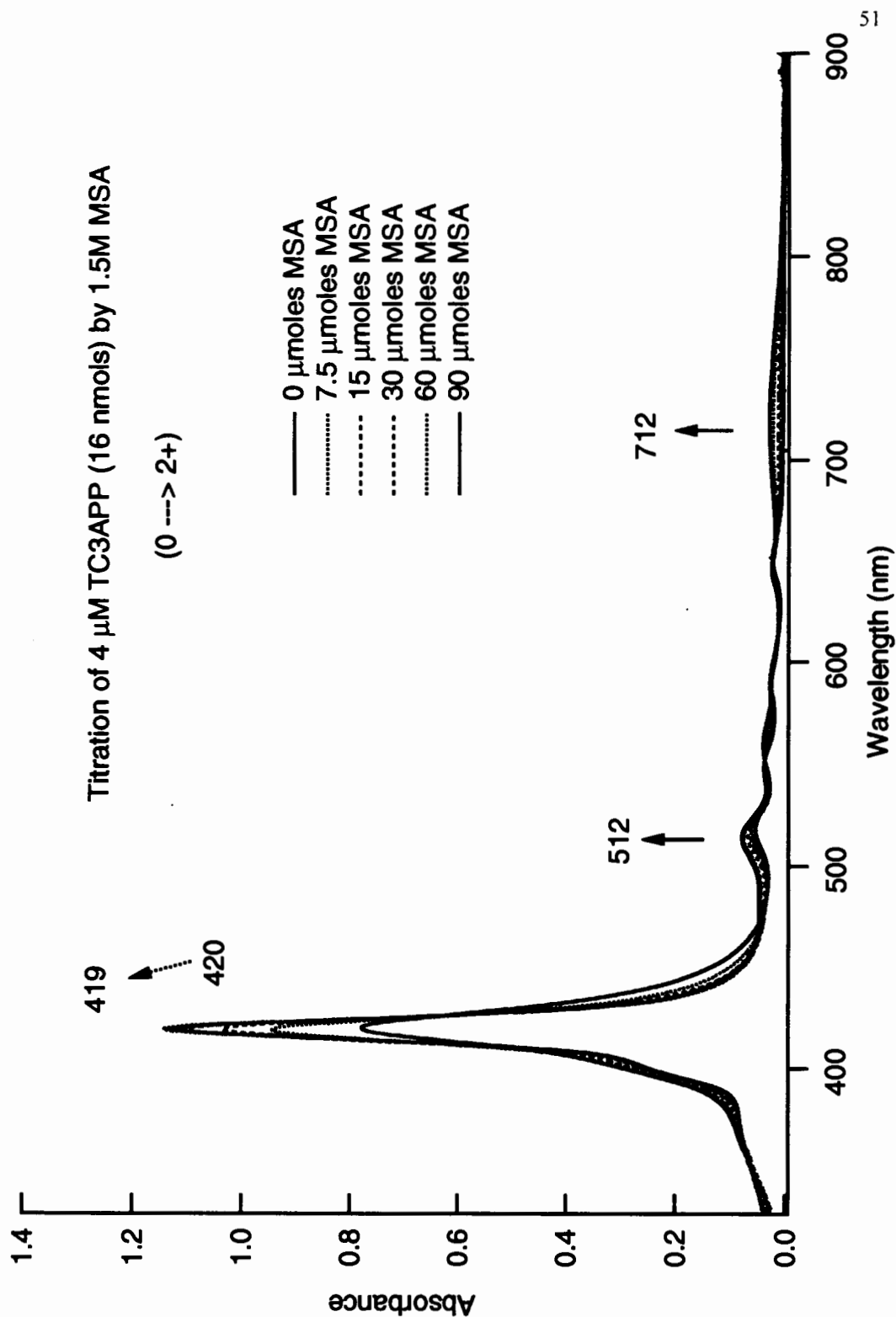


Figure 8a. Absorption spectra of successive acid-titration additions of TC₃APP

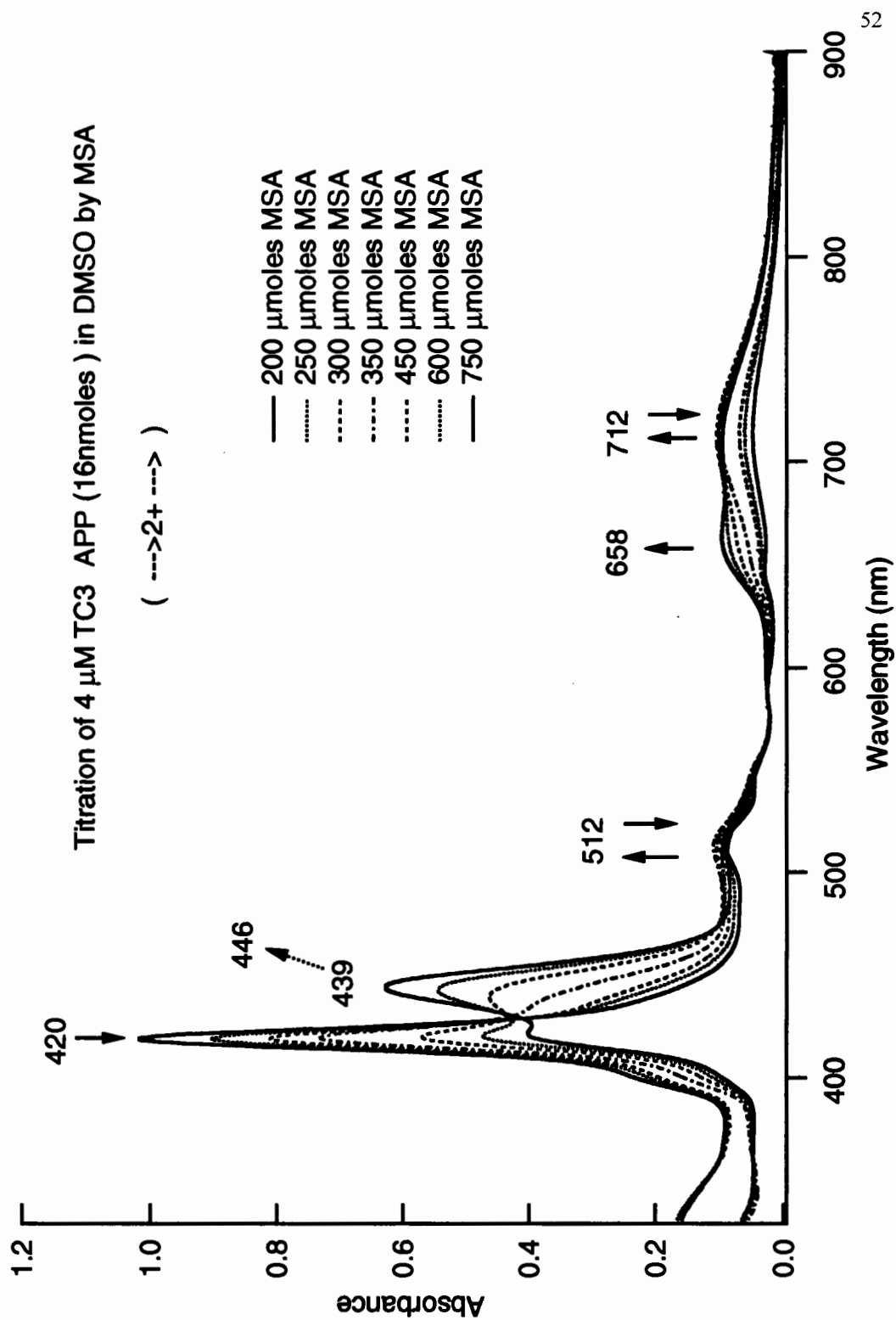


Figure 8b. Absorption spectra of successive acid-titration additions of TC₃APP

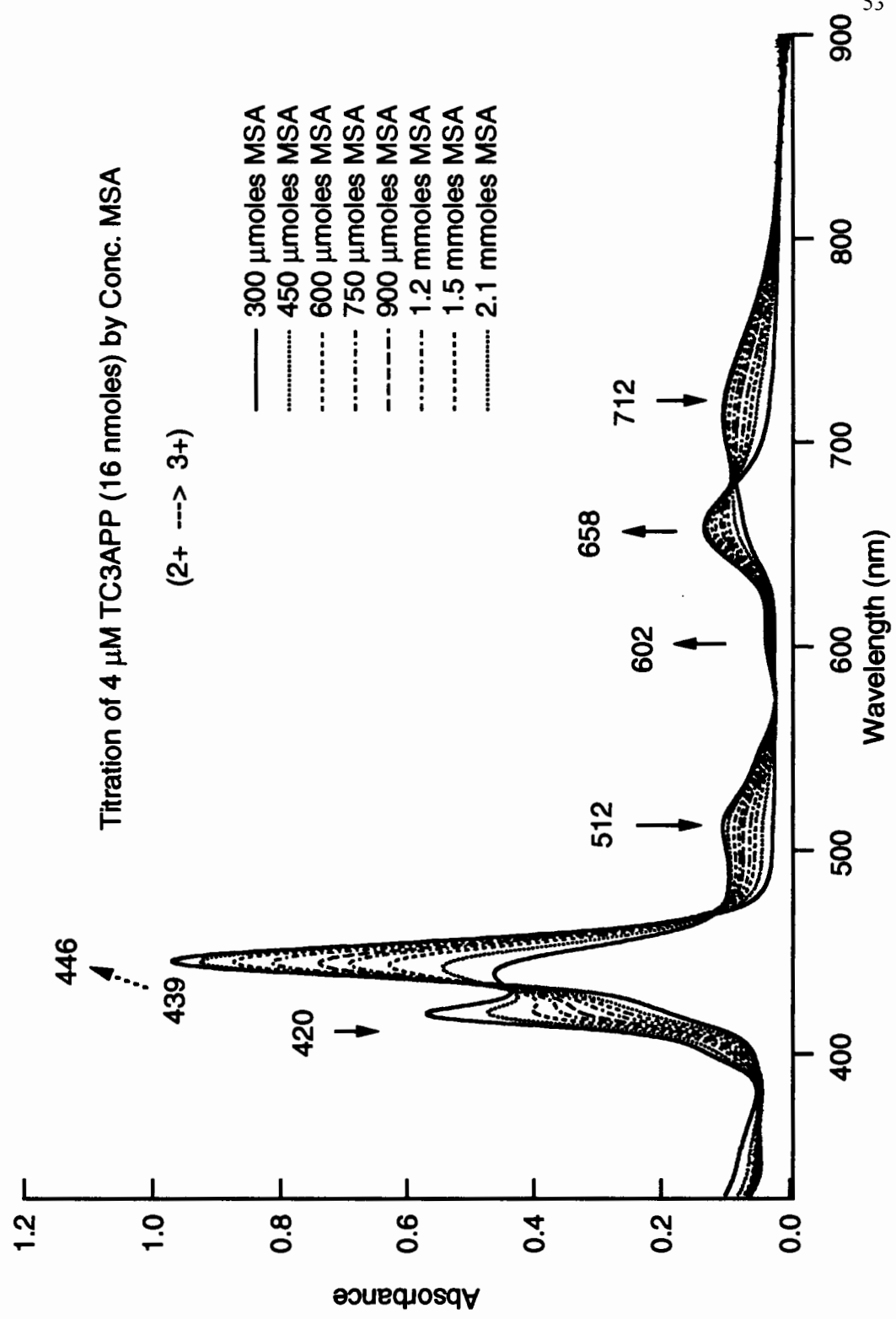


Figure 8c. Absorption spectra of successive acid-titration additions of TC₃APP

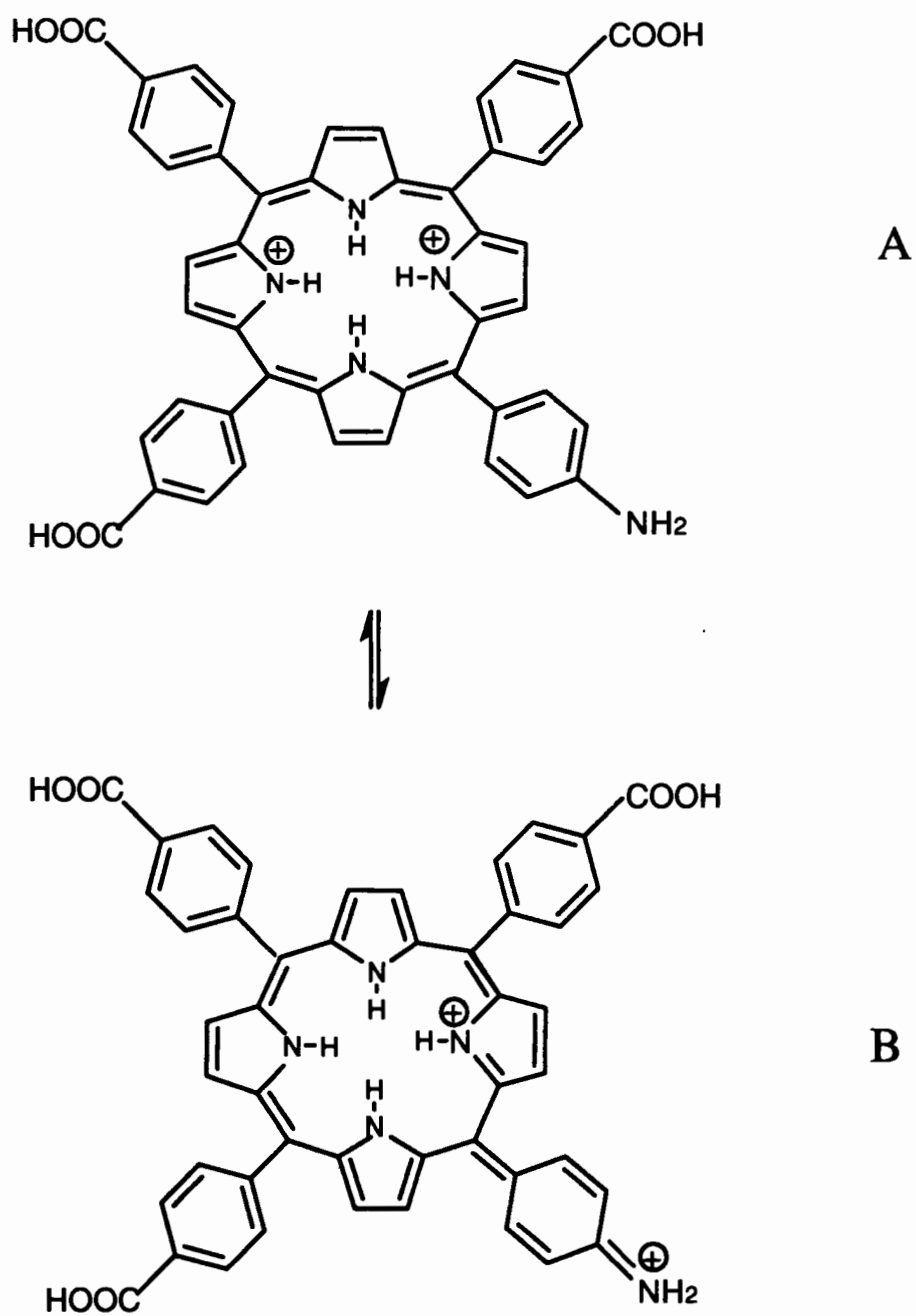


Figure 9. Resonance forms for the dication of TC₃APP

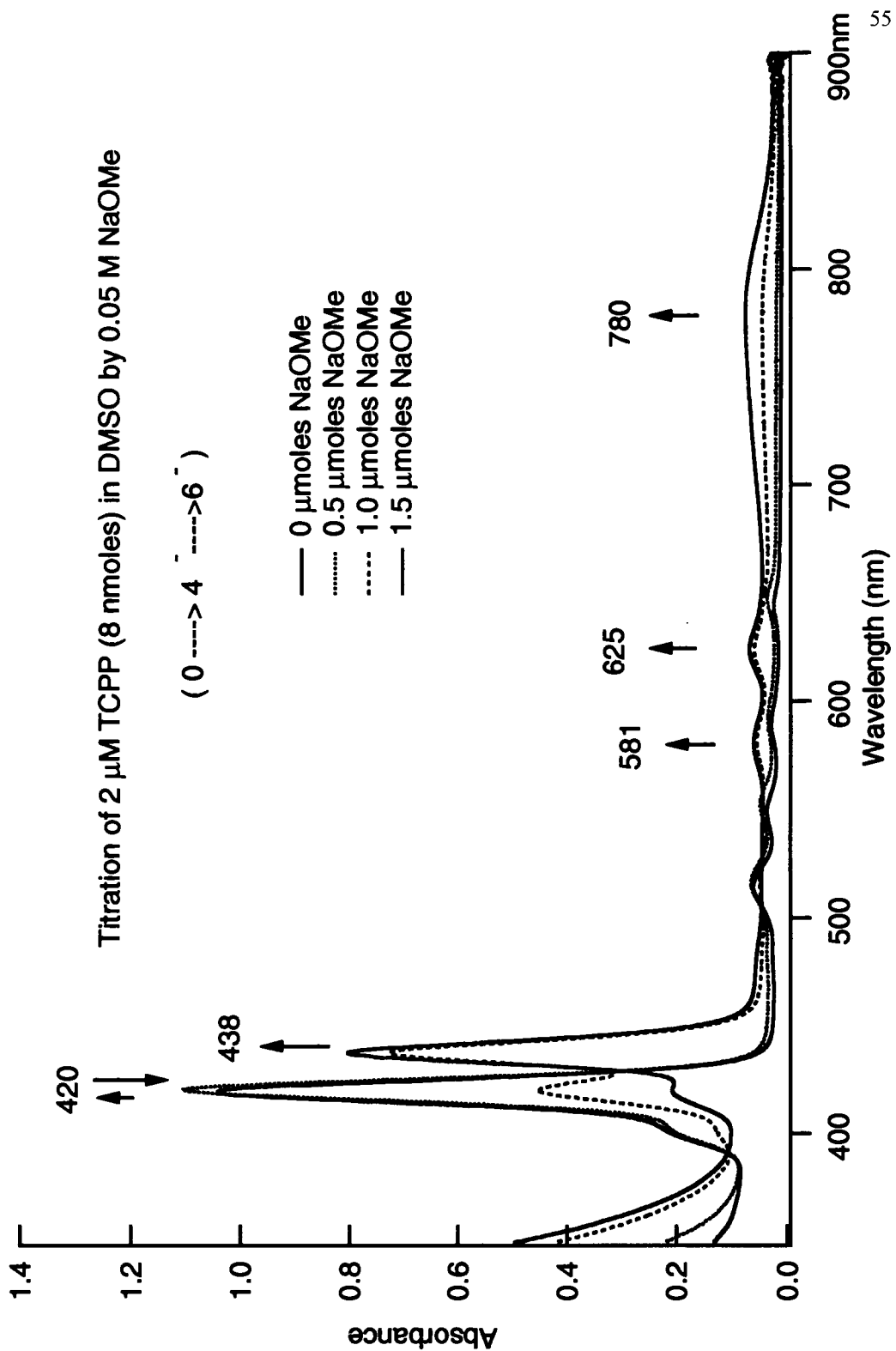


Figure 10. Absorption spectra of successive base-titration additions of TCPP

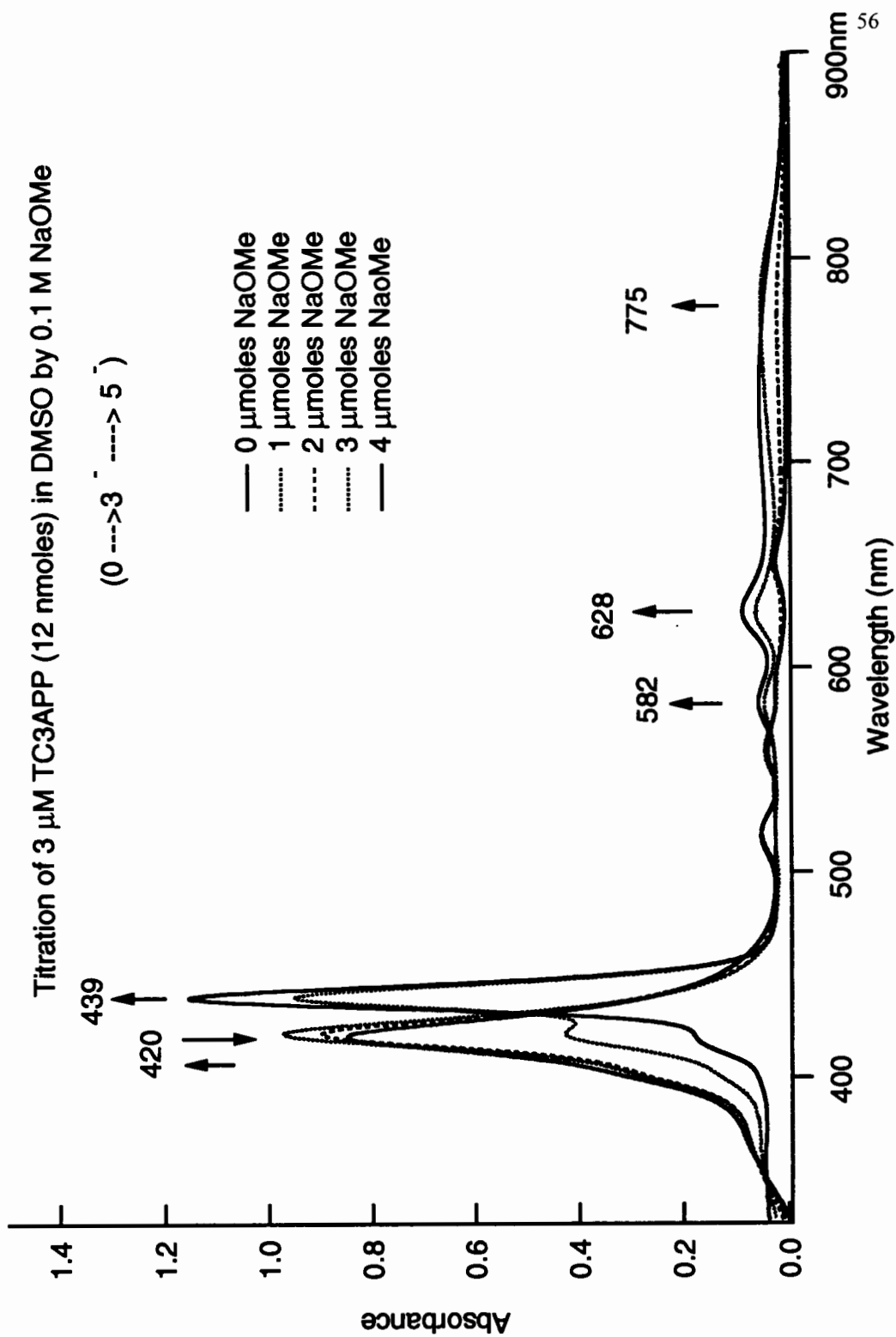


Figure 11. Absorption spectra of successive base-titration additions of TC₃APP

Fluorescence spectroscopy

Fluorescence spectra allow us to determine the relative electronic energy levels of ground and excited states. This information is important to evaluate the photosensitizer whether it has appropriate photochemical properties.

Emission and excitation spectra of TCM₄PP, TCM₃CPP, TCM₃AAPP and TC₃APP are presented in Appendix. All spectra were taken in DCM, except for TC₃APP which was recorded in DMSO. The excitation spectra are almost identical to the absorption spectra, except that the last Q band was not observed in excitation spectra because the spectrum was cut off at about 640 nm to avoid scattered excitation light from entering the detector.

Remarkably, the emission spectra of TCM₄PP, TCM₃CPP and TCM₃AAPP are identical. The first maximum (the Q_(0,0) transition) appears within the range 649-651 nm and the second (the Q_(0,1) transition) within the range 714-716 nm. Furthermore, the emission spectrum of TC₃APP is more like that of TCPP, but not TAPP. Two peaks were observed at 654 and 716 nm, like TCPP, instead of one peak, like TAPP. However, the emissions are somewhat red-shifted for TC₃APP compared with that for TCPP, which may be the contribution of aminophenyl substituent. Therefore, the difference on one of the four substituents has very little effect on the excited state characteristics of the molecule.

Excitation and emission spectra of protonated and deprotonated TCPP and TC₃APP are also presented in Appendix. All emission spectra are excited at most intense Soret band. For comparison, the emission spectra were also taken while samples were excited at an isosbestic point since they will have same absorbance at that particular wavelength.

Figure 12 shows the emission spectra of TCPP and TCPP(2+) excited at 435 nm, which is an isosbestic point for TCPP and TCPP(2+). TCPP emission spectrum shows two emission peaks at 649 and 713 nm and TCPP(2+) shows only one emission peak at 699 nm. The quantum efficiency is almost the same, judging by the integrated intensities.

Figure 13 shows the emission spectra of TC₃APP and TC₃APP(2+) excited at 420 nm because there is no obvious isosbestic point for TC₃APP and TC₃APP(2+) but both have an absorption peak at 420 nm. Compared to TC₃APP, two peaks were observed in the emission spectrum of TC₃APP(2+), except that they were more intense and somewhat blue-shifted. We were doubtful that the emission was from TC₃APP(2+). Therefore, the sample was excited at 512 and at 712 nm, at which wavelengths the TC₃APP(2+) is supposed to have absorption but TC₃APP and TCPP(3+) do not. However, the same emission was obtained while sample was excited at 512 nm, yet no emission was observed in the wavelength range 720 to 900 nm while sample was excited at 712 nm, even when the solution was 100 times more concentrated. This may suggest that the new

excited state generated by absorption at 712 nm has a very different geometry compared to the ground state and the emission from there is forbidden (*e.g.* planar instead of twisted phenyl substituents, because positive charge was shifted out of the macrocycle and phenyl rings adopt a quinonoid structure).

The emission spectra of TC₃APP(2+) and TC₃APP(3+) excited at 435 nm, an isosbestic point, are presented in Figure 14. The emission spectrum of TC₃APP(3+) has the characteristics of normal protonated porphyrin, with only one emission at 700 nm.

The emission spectra of deprotonated TCPP and TC₃APP excited at an isosbestic point, 429 nm, are presented in Figures 15 & 16. Compared with neutral porphyrins, the emissions from these deprotonated porphyrins are blue-shifted, but the Q_(0,0) transition is much stronger than Q_(0, 1) transition. This is observed in that the Q_(0, 1) peak shows up only as a shoulder of the Q_(0,0) peak in both cases.

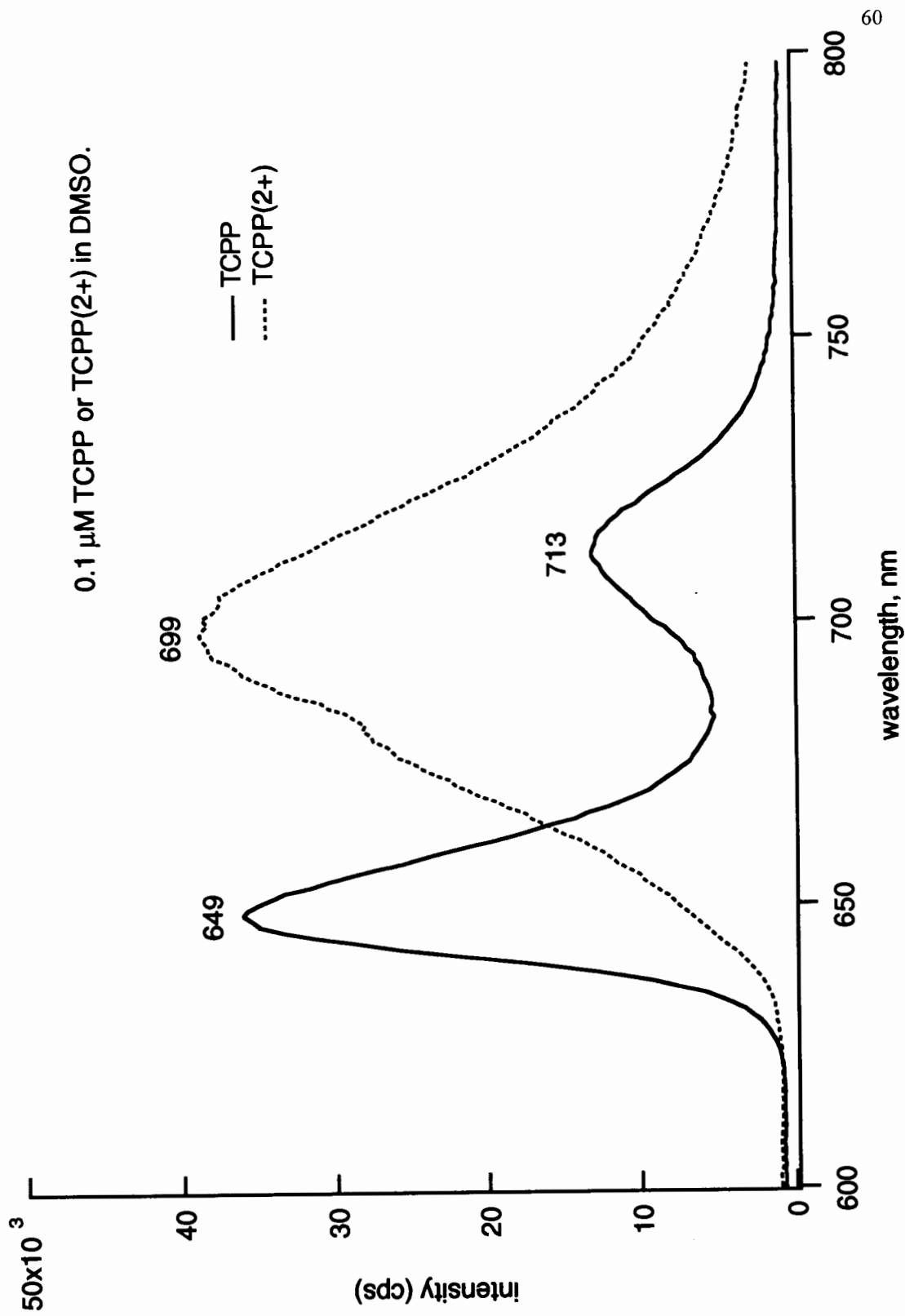


Figure 12. Emission spectra of TCPP and TCPP(2+) excited at 435 nm

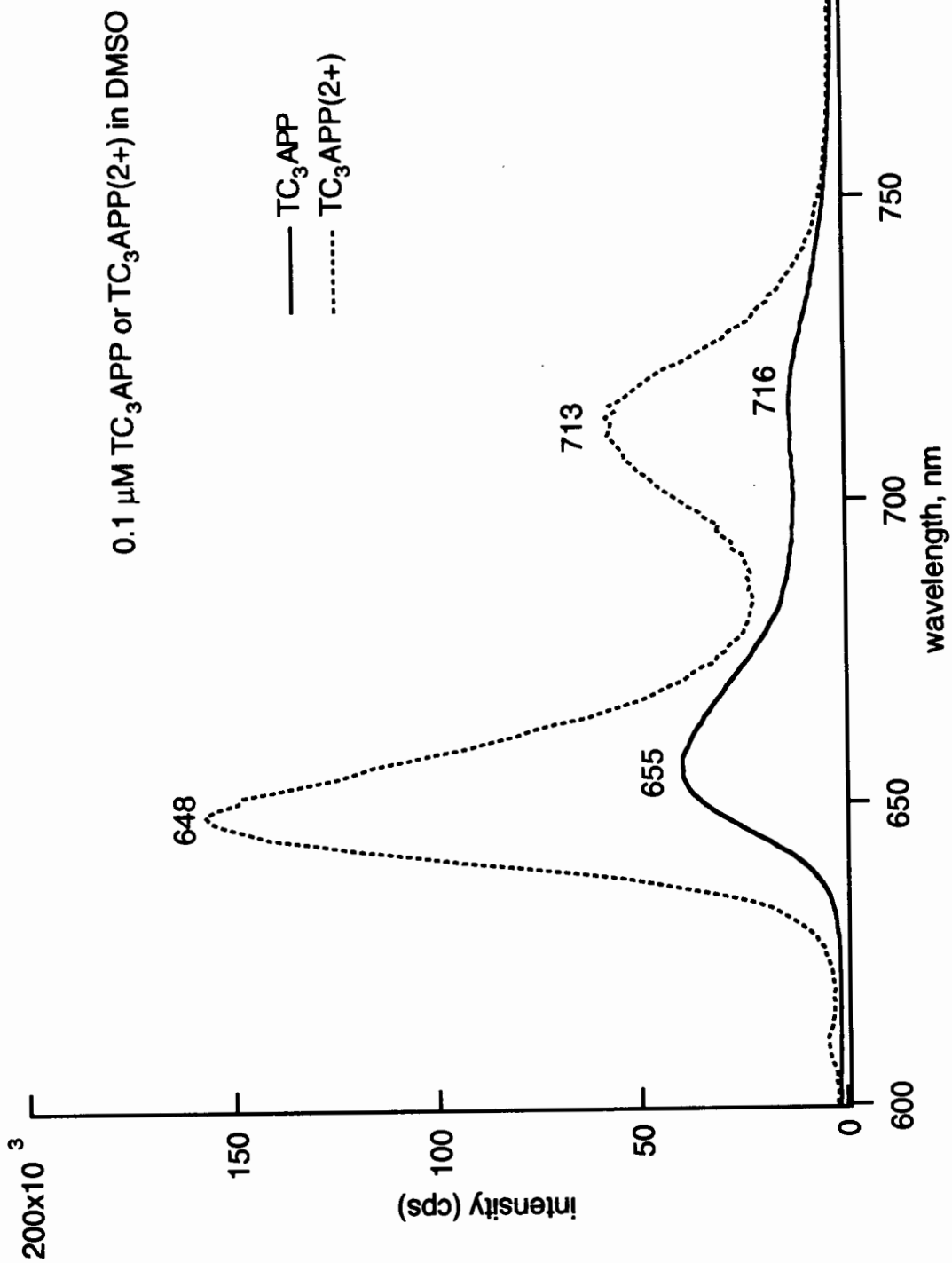


Figure 13. Emission spectra of TC_3APP and $\text{TC}_3\text{APP}(2+)$ excited at 420 nm

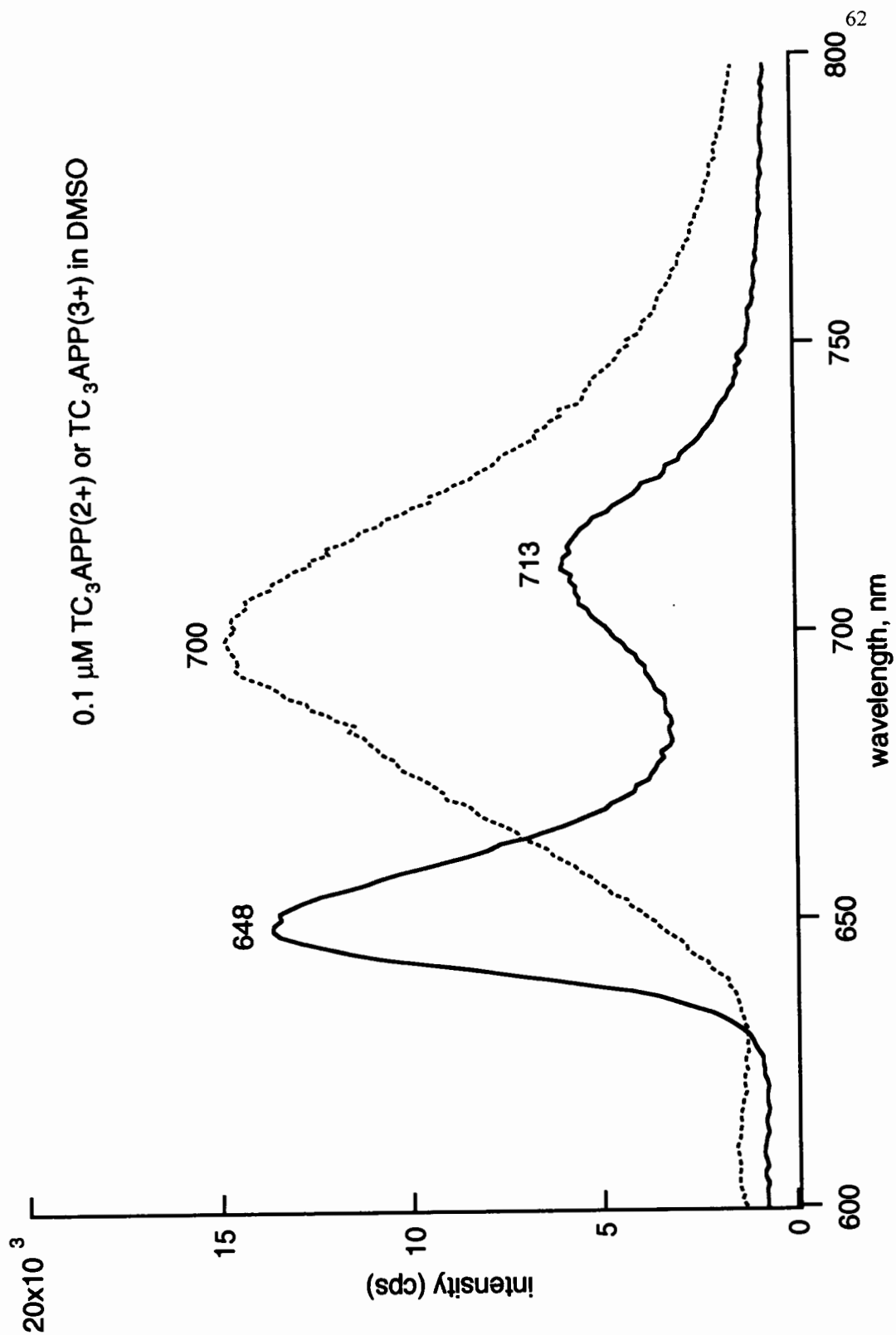


Figure 14. Emission spectra of $\text{TC}_3\text{APP}(2+)$ and $\text{TC}_3\text{APP}(3+)$ excited at 435 nm

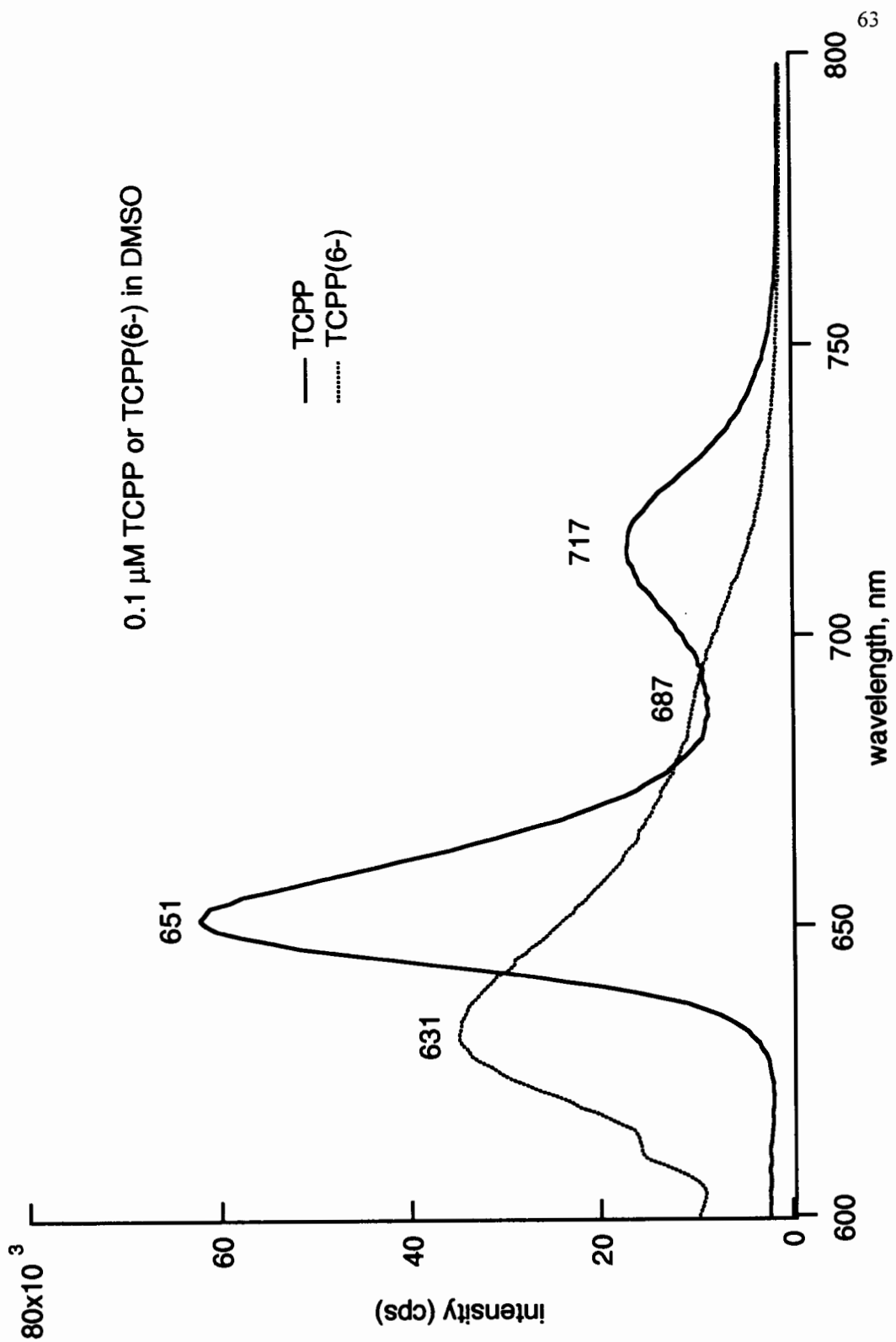


Figure 15. Emission spectra of TCPP and TCPP(6-) excited at 429 nm

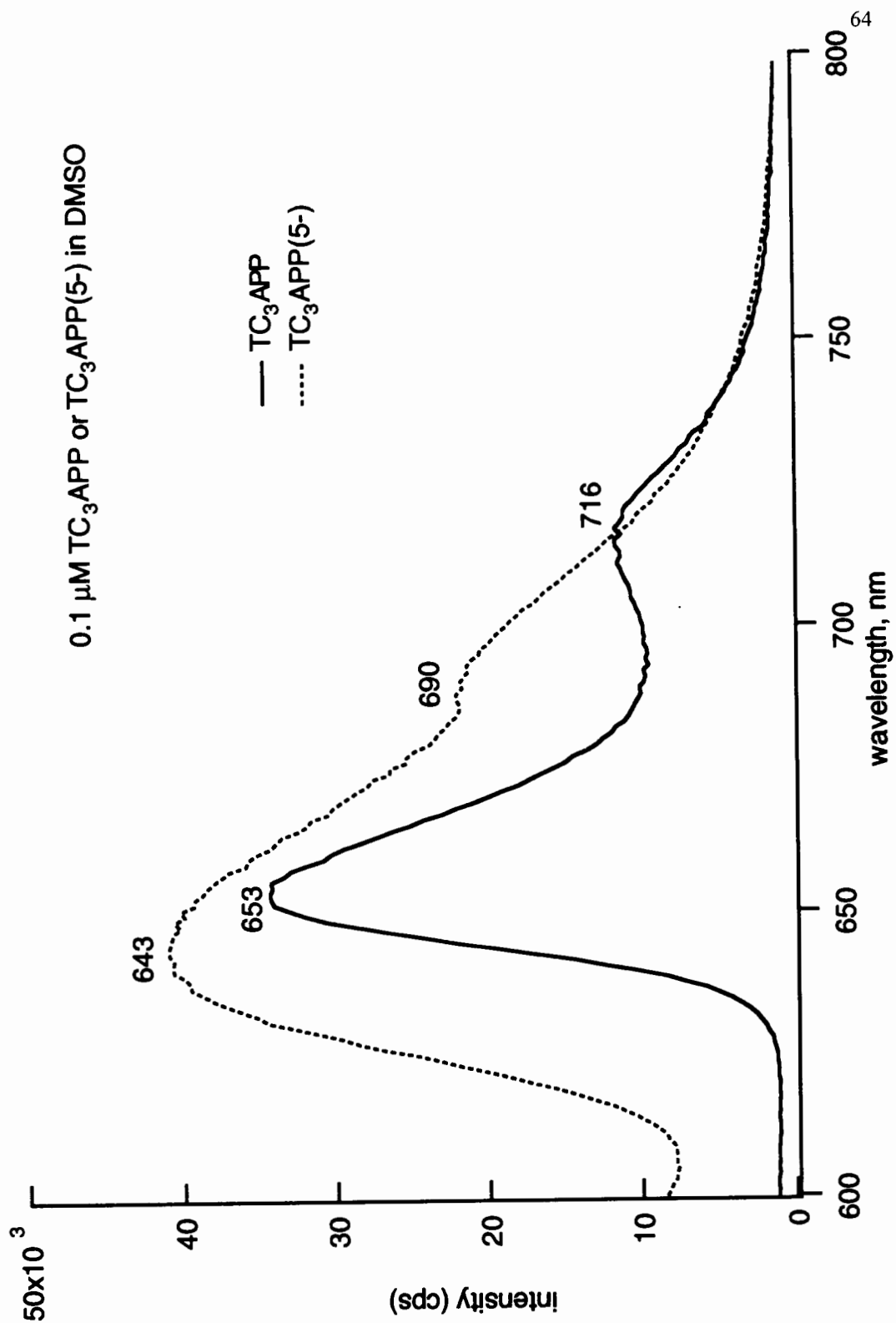


Figure 16. Emission spectra of TC_3APP and $\text{TC}_3\text{APP}(5-)$ excited at 429 nm

Fluorescence lifetime

The fluorescence lifetime of a substance usually represents the average amount of time the molecule remains in the excited state prior to its return to the ground state.⁴⁸ These data can reveal the rate of energy transfer and are very useful for evaluation of the synthesized porphyrins as a photosensitizer. As a photosensitizer, the longer fluorescence lifetime, the better, since the chance of excited state decay by fluorescence emission will be less, and the long-lived excited state would be beneficial for forward electron injection to semiconductor.

The fluorescence intensity $F(t)$, which is proportional to the excited state population, usually decays exponentially.⁴⁴ For a single fluorophore, one can write:

$$F(t) = F_0 e^{-t/\tau}$$

Frequently, the decays are not adequately described by a single exponential. In these instances the observed decay is generally fitted to a sum of exponentials:

$$F(t) = \sum_i a_i e^{-t/\tau_i}$$

where a_i is a preexponential factor representing the fractional contribution to the time-resolved decay of the component with a lifetime τ_i . The least-squares method is usually used for estimation of the impulse response function $F(t)$ from the measured decay curve $R(t)$. The basis of the least-squares method is the calculation of the expected value of the $R(t)$, given assumed value of a_i and τ_i . The

calculated values are compared with the observed values. The a_i and τ_i values are varied until the best fit is obtained. A minimum value of χ^2 indicates the best fit. χ^2 values larger than 2 indicate a poor fit and χ^2 values less than 1.2 indicate a good fit.⁴⁸

The fluorescence lifetimes of symmetrical porphyrins (TAPP and TCPP) and unsymmetrical porphyrins (TC₃APP and TCM₃AAPP) in DMSO at 20 °C have been measured by phase modulation method on a SPEX Fluorolog Tau-2 instrument at the University of Texas in the laboratories of Professor Stephen Webber. The results are shown in Table 6.

It was found that TAPP has a relaxation time of 5.59 ns from single exponential decay. Although the χ^2 value is very low for the triple exponential fit curve, the negative a_3 and zero τ_3 number seem to be unreasonable. The best fit exponential decay curve for TCPP seems to be the triple exponential according to the χ^2 value. However, there is no major component because every one have almost the same weighting factor (39.5%, 32.9%, 27.7%). Thus the double exponential fit curve may give the reasonable result, which is 10.61 ns (57.7%) for TCPP. The reason that the experimental results for TCPP are not very good is because that the sample we sent might have been compromised by the DMSO attacking the vial cap. It was found that the liner of the vial cap was swollen and destroyed by the solvent DMSO and dropped down into the solution partially

when the solution vial was being opened. The solution was not clear and there was a huge wide emission peak observed, located around 500 nm, which would be unusual for this sample.

The similar χ^2 values of double and triple exponential fit curves for TC₃APP or single and double exponential fit curves for TCM₃AAPP indicate that the increased complexity of the assumed decay law did not improve the fit much. Therefore, we conclude that the lifetime of TC₃APP is 10.42 ns (86%) from double exponential decay and the lifetime of TCM₃AAPP is 10.93 ns (100%) from single exponential decay. These results are generally consistent with normal porphyrins, whose lifetimes are usually around 10 ns.^{49,50} However, the χ^2 values are unusually large for all samples. A different method may be used to calculate the χ^2 values or these large χ^2 values may suggest that decays of fluorescence are nonexponential, which are expected and frequently observed for fluorophores which are quenched by energy transfer or which undergo solvent relaxation.⁴⁸ An energy transfer mechanism seems to be impossible for a porphyrin monomer unless aggregation occurs. However, the concentration seems to be too low for aggregation. Solvent relaxation usually occurs within picoseconds, and so does not seem to be a factor in our case. Thus, more information will be necessary to make such conclusion and we are looking forward to hear the results of some experiments from another source (SPEX Instruments).

Table 6. Fluorescence lifetimes of TAPP, TCPP, TC₃APP and TCM₃AAPP

Samples	single exp. fit	double exp. fit	triple exp. fit
TAPP	a₁=1.0 τ₁=5.59* χ ² =95	a ₁ =0.725 τ ₁ =5.59 a ₂ =0.275 τ ₂ =5.6 χ ² =107 <τ>=5.59	a ₁ =0.758 τ ₁ =6.338 a ₂ =0.257 τ ₂ =3.523 a ₃ = -0.016 τ ₃ =0.00 χ ² =7.4 <τ>=5.72
TCPP**		a₁=0.577 τ₁=10.61 a ₂ =0.423 τ ₂ =1.72 χ ² =20.1 <τ>=6.85	a ₁ =0.395 τ ₁ =13.08 a ₂ =0.329 τ ₂ =5.09 a ₃ =0.277 τ ₃ =1.06 χ ² =4.4 <τ>=7.13
TC ₃ APP		a₁=0.860 τ₁=10.42 a ₂ =0.140 τ ₂ =0.479 χ ² =94.5 <τ>=9.03	a ₁ =0.709 τ ₁ =11.35 a ₂ =0.173 τ ₂ =6.608 a ₃ =0.118 τ ₃ =0.000 χ ² =91.9 <τ>=9.19
TCM ₃ AAPP	a₁=1.0 τ₁=10.93 χ ² =55.3	a ₁ =0.127 τ ₁ =20.78 a ₂ =0.873 τ ₂ =10.39 χ ² =48.2 <τ>=11.71	

* Boldface indicates the values considered most reliable.

**sample was compromised

CONCLUSION

TCM₃AAPP can be synthesized by a mixed aldehyde condensation with pyrrole in propionic acid. The best mole ratio of methyl 4-formylbenzoate to 4-acetamidobenzaldehyde is 3:1. The desired porphyrin can be separated chromatographically from a mixture of six porphyrins on a silica gel column. The successful solvent system is a mixture of chloroform or DCM with ethyl acetate for chromatographic separation. Chloroform (or 5% (v/v) ethyl acetate in DCM) will elute TCM₄PP and 2% (v/v) ethyl acetate in chloroform (or 10% (v/v) ethyl acetate in DCM) will elute TCM₃AAPP. The desired functionalized porphyrin TC₃APP can be achieved further by cleaving off protecting groups with concentrated HCl in TFMSA at 80-90 °C at reflux for 48 hours. The synthesized porphyrins TCM₃AAPP and TC₃APP have been successfully identified by NMR and mass spectra. The characteristics of TC₃APP from UV-visible and fluorescence spectra indicate characters of both TCPP and TAPP, but more like TCPP, as expected. The UV-visible absorption spectrum of TC₃APP shows a Soret band and four Q bands like TCPP, except that two middle Q bands are very close, like TAPP. The UV-visible absorption spectrum of TC₃APP(2+) has the characters of a typical hyperporphyrin spectrum, indicating the influence of the amino group. The fluorescence emission spectrum of TC₃APP is similar to that of

TCPP except that it is somewhat red-shifted. The fluorescence lifetime of TC₃APP is about 10.4 ns, which is consistent with a normal tetraphenylporphyrin. All these results shows that TC₃APP may be a good photosensitizer for our proposed solid state solar cell.

The TCPP-TAPP dyad also can be synthesized, although there are still some difficulties. The best method of synthesis of TCM₃CPP is from a mixed aldehyde condensation with pyrrole in propionic acid. The successful solvent system for purifying TCM₃CPP on a silica gel column was a mixture of chlorinated hydrocarbon (either chloroform or DCM) and methanol. One may start with chloroform (or 2.5% (v/v) MeOH in DCM), which will elute TCM₄PP, then increase the solvent polarity by using 3% (v/v) methanol in chloroform (or 6% (v/v) methanol in DCM). The second band eluted is the desired TCM₃CPP. During the subsequent coupling reaction, chloroform should not be used as reaction solvent because chloroform usually contains ethanol as a stabilizer, which will react with acid chloride of TCM₃CPP. More caution should be paid in order to have a better yield because acid chloride was very sensitive to moisture. Gel filtration may be a good method to purify the dyad.

REFERENCES

1. Wöhrle, D.; Meissner, D., "Organic Solar Cells", *Adv. Mater.* **1991**, 3, 129-138.
2. Grätzel, M; "Low-cost Solar cells"; *Natural Science* **1993**,228-236.
3. Nazeeruddin, M. K.; Kay, A.; Rodicio, I.; Humphry, B. R.; Mueller, E.; Liska, P.; Vlachopoulos, N.; Grätzel, M.; *J. Am. Chem. Soc.* **1993**,115,6382.
4. Kamat, P. V.; "Photochemical Solar Cells". *Inter-American Photochemical Society Newsletter*, **1996**, Vol.19(1),14-23.
5. Kay A.; Grätzel, M.; "Low Cost Photovoltaic Modules Based on Dye Sensitized Nanocrystalline Titanium Dioxide and Carbon Powder". *Solar Energy Materials and Solar Cells*, **1996**, 44, 99-117.
6. Kamat, P. V.; *Langmuir* **1990**, 6, 512.
7. Kamat, P. V.; Das, S.; Thomas, K. G.; George, M. V.; *Chem. Phys. Lett.* **1991**, 178, 75.
8. Eichberger, R.; Willig, F. *Chem. Phys. Lett.* **1990**,141,159.
9. Kietzmann, R.; Willig, F.; Weller, H.; Vogel, R.; Nath, D. N.; Eichberger, R.; Liska, P.; Lethnert, J. *Mol. Cryst. Liq. Cryst.* **1991**, 194, 169.
10. Vinodgopal, K.; Hua, H.; Dahlgren, R. L.; Lappin, A. G.; Patterson, L. K.; Kamat, P. V. *J. Phys. Chem.* **1995**, 99, 10883.

11. Fessenden, R. W.; Kamat, P. V. *J. Phys. Chem.* **1995**, *99*, 12902.
12. Argazzi, R.; Bignozzi, C. A.; Heimer, T. A.; Castellano, F. N.; Meyer, G. J. *Inorg. Chem.* **1994**, *33*, 5741.
13. Lu, H.; Prieskorn, J. N.; Hupp, J. T. *J. Am. Chem. Soc.* **1993**, *115*, 4927.
14. O'Regan, B.; Moser, J.; Anderson, M.; Grätzel, M. *J. Phys. Chem.* **1990**, *94*, 8720.
15. Bedja, I.; Hotchandani, S.; Kamat, P. V. *J. Phys. Appl. Phys.* **1994**, *75*, 5444.
16. Hotchandani, S.; Kamat, P. V.; *Chem. Phys. Lett.* **1992**, *191*, 320.
17. Hotchandani, S.; Das, S.; Thomas, K. G.; George, M. V.; Kamat, P. V.; *Res. Chem. Intermed.* **1994**, *20*, 927.
18. Lui, D.; Kamat, P. V.; *J. Electrochem. Soc.* **1995**, *142*, 835.
19. Yu, G.; Gao, J.; Hummelen, J. C.; Wudl, F.; Heeger, A. J.; "Polymer Photovoltaic Cells: Enhanced Efficiencies via a Network of Internal Donor-Acceptor Heterojunctions", *Science*. **1995**, *270*, 1789-1791,
20. Sariciftci, N.; Braun, D.; Zhang, C.; Srdanov, V. I.; Heeger, A. J.; Stucky, G.; Wudl, F., "Semiconducting Polymer-Buckminsterfullerene Heterojunctions: Diodes, Photodiodes, and Photovoltaic Cells", *Appl. Phys. Lett.* **1993**, *62*, 585-587.
21. Halls, J. J. M.; Walsh, C. A.; Grenham, N. C.; Marseglis, E. A.; Friend, R. H.; Moratti, S. C. Holmes, A. B. "Efficient Photodiodes from Interpenetrating polymer Networks", *Nature* **1995**, *376*, 498-500.

22. O'Regan, B.; Schwartz, D.T., "Efficient Dye-Sensitized Charge Separation in a Wide-Band-Gap p-n Heterojunction", *J. Appl. Phys.* **1996**, 80, 4749-4754.
23. MacDiarmid, A. G.; Epstein, A. J., "The Polyanilines: Potential Technology Based on New Chemistry and New Properties", *Science and Applications of Conducting Polymers*; IOP publishing, **1990**, pp 117-127.
24. Skotheim, T. A. *Electroresponsive Molecular and Polymeric Systems*; Skotheim, T. A., Ed.; Marcel Dekker: New York, **1991**, Vol. 2
25. Salaneck, W.R.; Clark, D. T.; Samuelsen, E. J. *Science and Application of Conducting Polymers*; Salaneck, W. R.; Clark, D. T.; Samuelsen, E. J.; Ed.; IOP Publishing: Bristol, **1991**.
26. Nazeeruddin, M. K.; Kay, A.; Rodicio, I.; Baker, R. H.; Meller, E.; Liska, P.; Vlachopoulos, N.; Grätzel, M. "Conversion of Light to Electricity by cis-X₂Bis(2,2'-bipyridyl-4,4'-dicarboxylate)ruthenium(II) Charge-Transfer Sensitizers (X= Cl⁻, Br⁻, CN⁻ and SCN⁻) on Nanocrystalline TiO₂ Electrodes", *J. Am. Chem. Soc.* **1993**, 115, 6382-6390.
27. Kay, A.; Grätzel, M. "Artificial Photosynthesis. 1. Photosensitization of TiO₂ Solar Cells with Chlorophyll Derivatives and Related Natural Porphyrins", *J. Phys. Chem.* **1993**, 97, 6272-6277.
28. Pechy, P.; Rotzinger, F. P.; Nazeeruddin, M. K.; Khaja, M.; Kohle, O.; Zakeeruddin, S. M.; Humphry-Baker, R.; Grätzel, M. "Preparation of

Phosphonated Polypyridyl Ligands to Anchor Transition Metal

Complexes on Oxide Surfaces”, *J. Chem. Soc., Chem. Comm.* **1995**, 65-66 & 1093

29. Bonhote, P.; Moser, J. E.; Vlachopoulos, N.; Walder, L.; Zakeeruddin, S. M.; Baker, R. H.; Pechy, P.; Grätzel, M. “Photoinduced Electron Transfer and Redox-type Photochromism of a TiO₂-anchored Molecular Diad”, *Chem. Commun.*, **1996**, 1163-1164.
30. Tunesi, S.; Anderson, M. A. *Langmuir* **1992**, 8, 487-495.
31. Wamser, C. C., unpublished results.
32. Ransdell, R. A.; Wamser, C. C. “Solvent and Substituent Effects on the Redox Properties of Free-Base Tetraphenylporphyrins in DMSO and Aqueous DMSO”, *J. Phys. Chem.* **1992**, 96, 10572-10575.
33. Wamser, C. C.; Bard, R. R.; Senthilathipan, V.; Anderson, V. C.; Yayas, J. A.; Lonsdale, H. K.; Rayfield, G. W.; Friesen, D. T.; Lorenz, D. A.; Stangle, G. C.; Van, Eikeren, P.; Baer, D. R.; Ransdell, R. A.; Golbeck, J. H.; Babcock, W. C.; Sandberg, J. J.; Clark, S.E. “Synthesis and Photoactivity of Chemically Asymmetric Polymeric Porphyrin Films Made by Interfacial Polymerization”, *J. Am. Chem. Soc.* **1989**, 111, 8485-8491.
34. Wamser, C. C.; Senthilathipan, V.; Li, W., “Asymmetric Photopotentials from Thin Polymeric Porphyrin Films” *SPIE Proc.* **1991**, 1436, 114-124.

35. Adler, A. D.; Longo, F.; Finarelli, J.; Goldmacher, J.; Acour, J.; Korsakoff, L. "A Simplified Synthesis for meso-Tetraphenylporphyrin", *J. Org-chem.* **1966**, 33, 476.
36. Lindsey, J. S.; Schreiman, I.C.; Hsu, H. C.; Kearney, P. C.; Marguerettaz, A. M. "Rothmund and Alder-Longo Reactions Revisited: Synthesis of Tetraphenylporphyrins under Equilibrium Conditions", *J. Org. Chem.* **1987**, 52, 827-836.
37. Lindsey, J. S.; Prathapan, S.; Johnson, T. E.; Wagner, R. W. "Porphyrin Building Blocks for Modular Construction of Bioorganic Model Systems", *Tetrahedron* **1994**, Vol. 50, No. 30, 8941-8968.
38. McMurry, J. E.; Wong, G. B. "An Improved Method for The Cleavage of Methyl Esters", *Synthetic Communications* **1972**, 2(6), 389-394.
39. Braden, D. A. *MS. Thesis*, Portland State University, **1995**.
40. Adler, A. D.; Longo, F. R.; Shergalis, W. *J. Am. Chem. Soc.* **1964**, 86, 3145
41. Lindsey, J. S.; Wagner, R. W. "Investigation of the Synthesis of Ortho-substituted Tetraphenylporphyrins", *J.Org. Chem.* **1989**, 54, 828-836.
42. Lindsey, J. S.; MarCrum, K. A.; Tyhonas, J. S.; Chuang, Y. Y. "Investigation of a Synthesis of Meso-porphyrins Employing High Concentration Conditions and an Electron Transport Chain for Aerobic Oxidation", *J.Org. Chem.* **1994**, 59, 579- 587.

43. Bidlingmeyer, B. A. "*Practical HPLC Methodology and Applications*", John Wiley & Sons, INC.: New York, **1992**.
44. Dolphin, D. "*The Porphyrins*", Academic Press: New York, San Francisco, London, **1978**.
45. Silverstein, R. M.; Bassler, G. C.; Morrill, T. C. "*Spectrometric Identification of Organic Compounds*", John Wiley & Sons, INC.: New York, **1991**.
46. Ojadi, E. C. A.; Linschitz, H.; Gouterman, M.; Walter, R. I.; Lindsey, J. S.; Wagner, R. W.; Droupadi, P. R.; Wang, W. *J. Phys. Chem.* **1993**, *97*, 13192-13197.
47. Walter, R. I.; Ojadi, E. C. A.; Linschitz, H. *J. Phys. Chem.* **1993**, *97*, 13308-13312.
48. Lakowicz, R. J. "*Principles of Fluorescence Spectroscopy*", Plenum Press: New York and London, **1983**.
49. Akins, D. L.; Özcelik, S.; Zhu, H.; Guo, C. *J. Phys. Chem.* **1996**, *100*, 14390 - 14396
50. Maiti, N.; Ravikanth, M.; Mazumdar, S.; Periasamy, N. *J. Phys. Chem.* **1995**, *99*, 17159.

APPENDIX

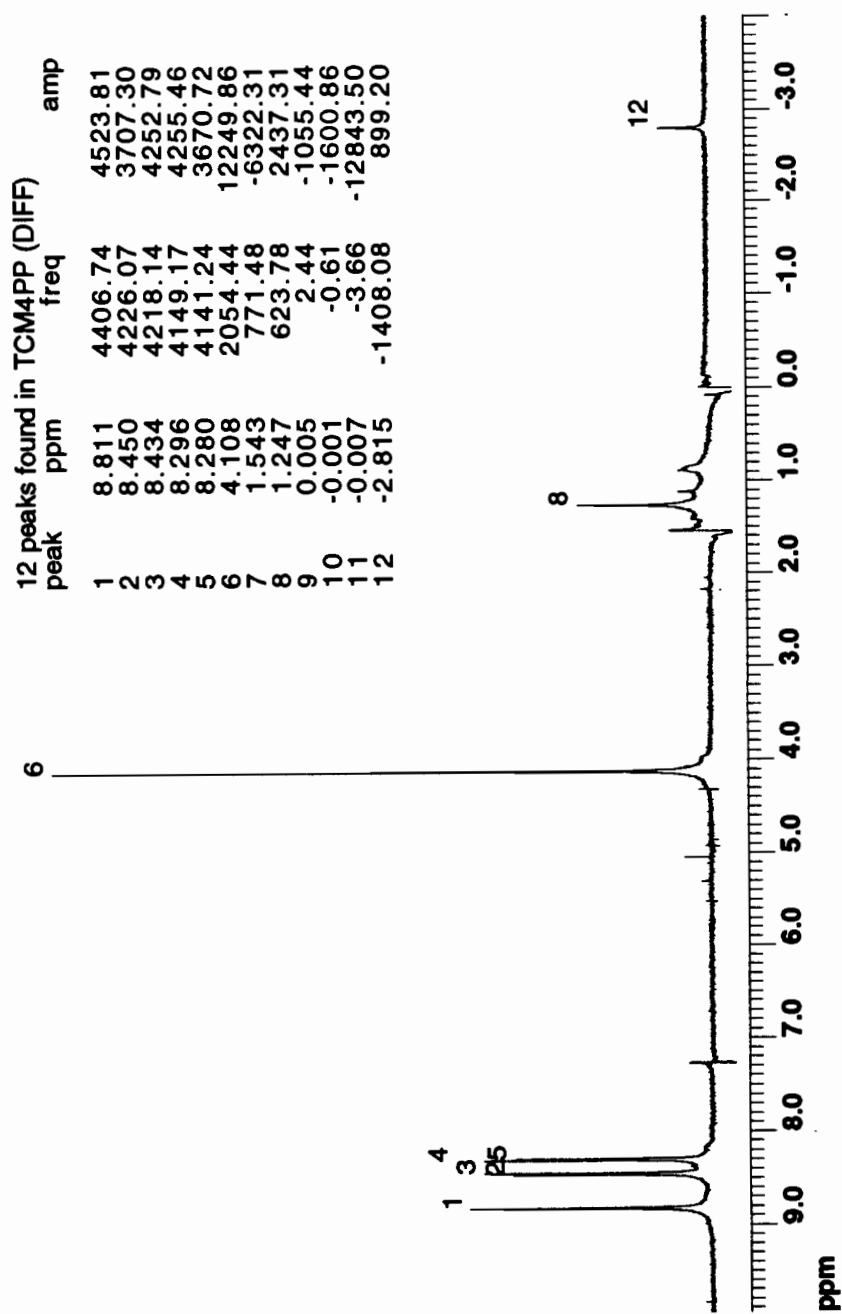


Figure 17. 500 MHz ^1H NMR spectrum of TCM₄PP

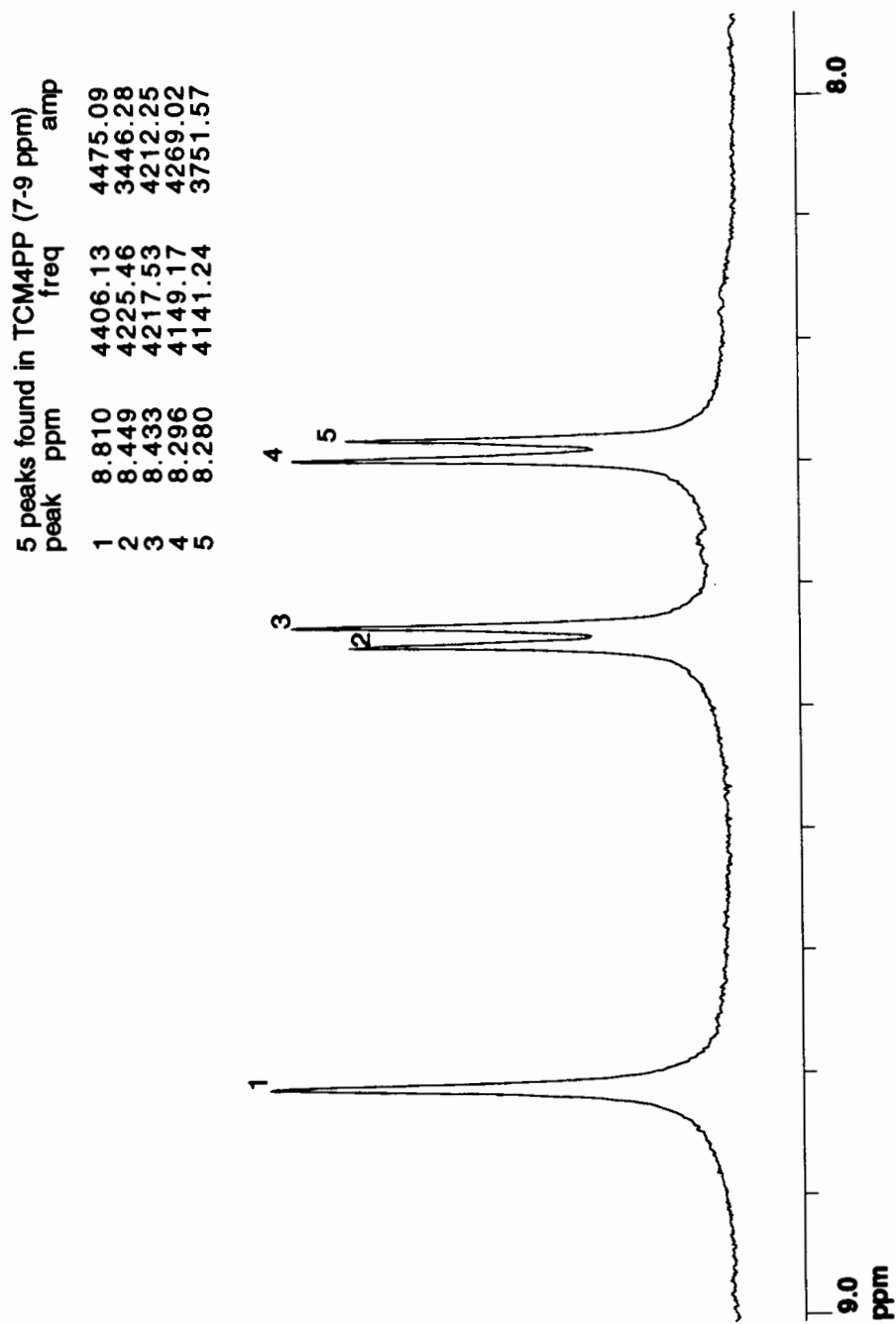


Figure 18. 500 MHz ^1H NMR spectrum (7-9 ppm) of TCM₄PP

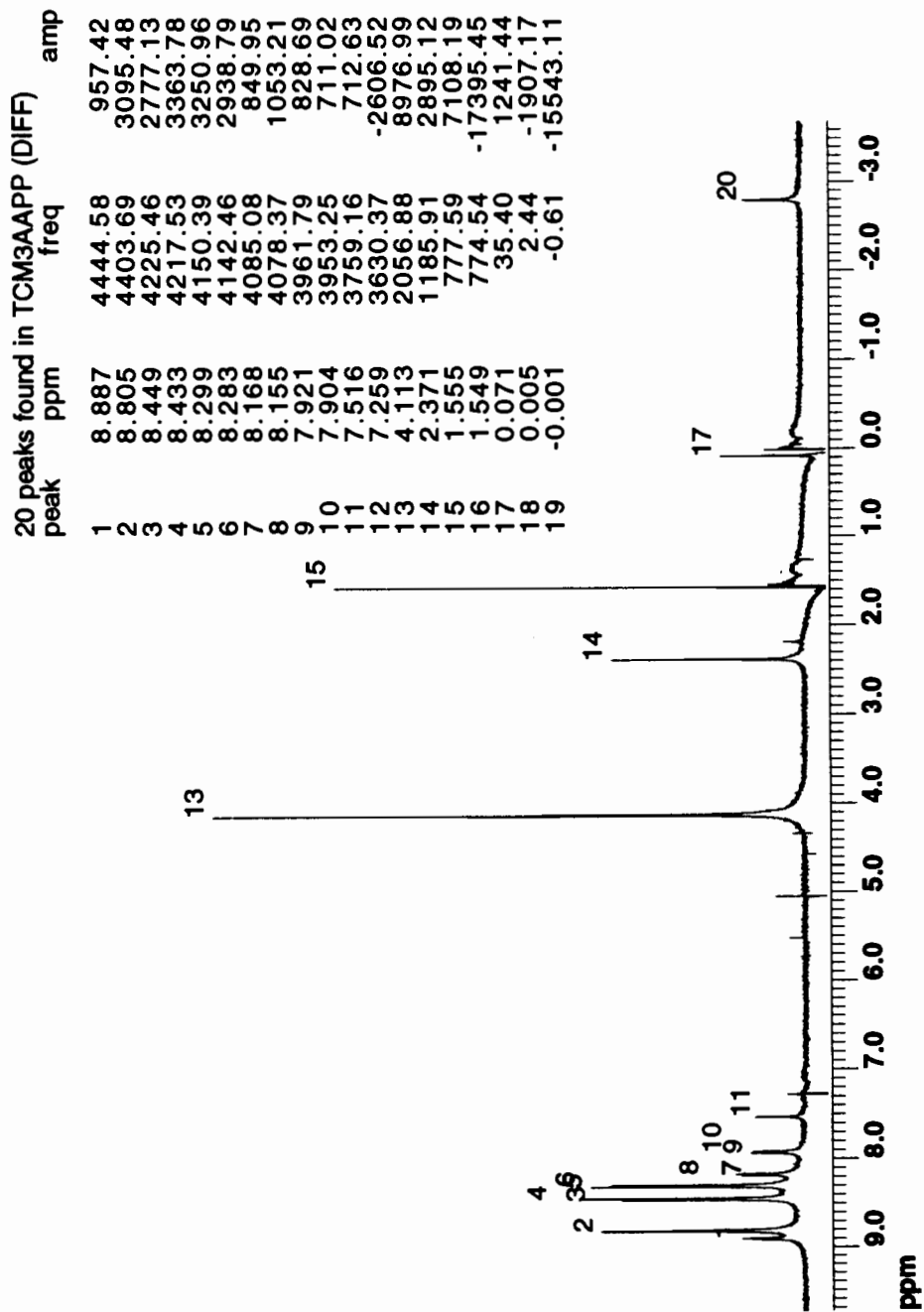


Figure 19. 500 MHz ^1H NMR spectrum of TCM_3AAPP

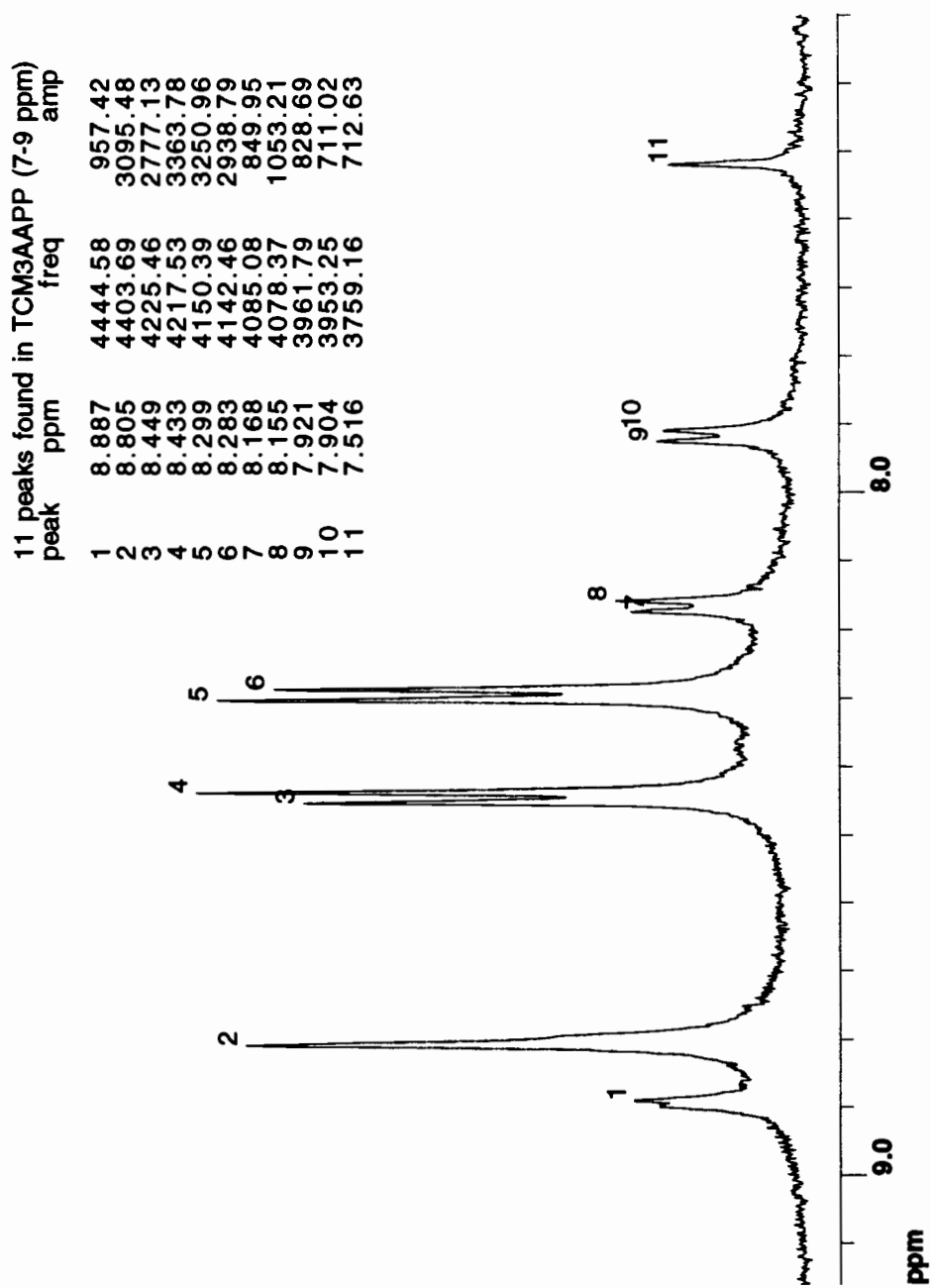


Figure 20. 500 MHz ¹H NMR spectrum (7-9 ppm) of TCM₃AAPP

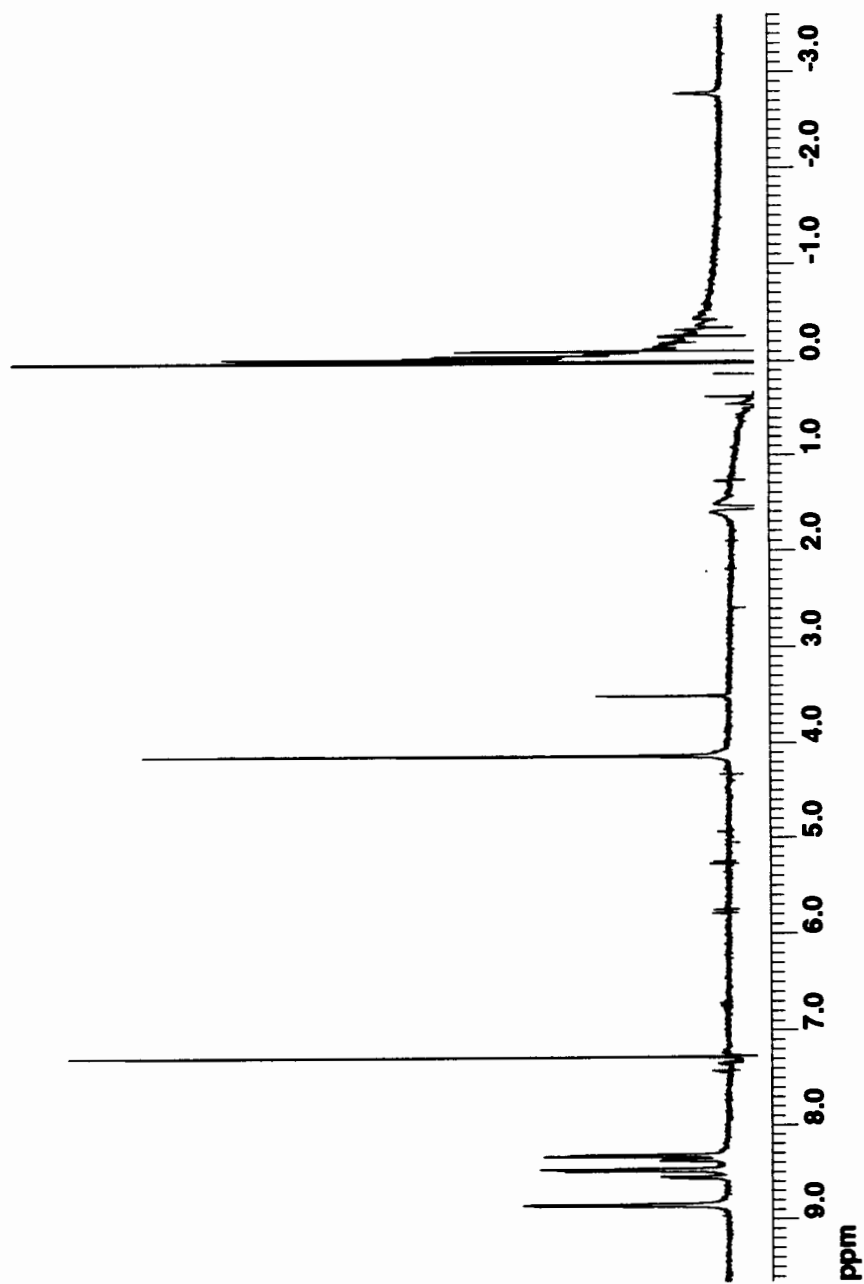


Figure 21. 500 MHz ^1H NMR spectrum of TCM₃CPP

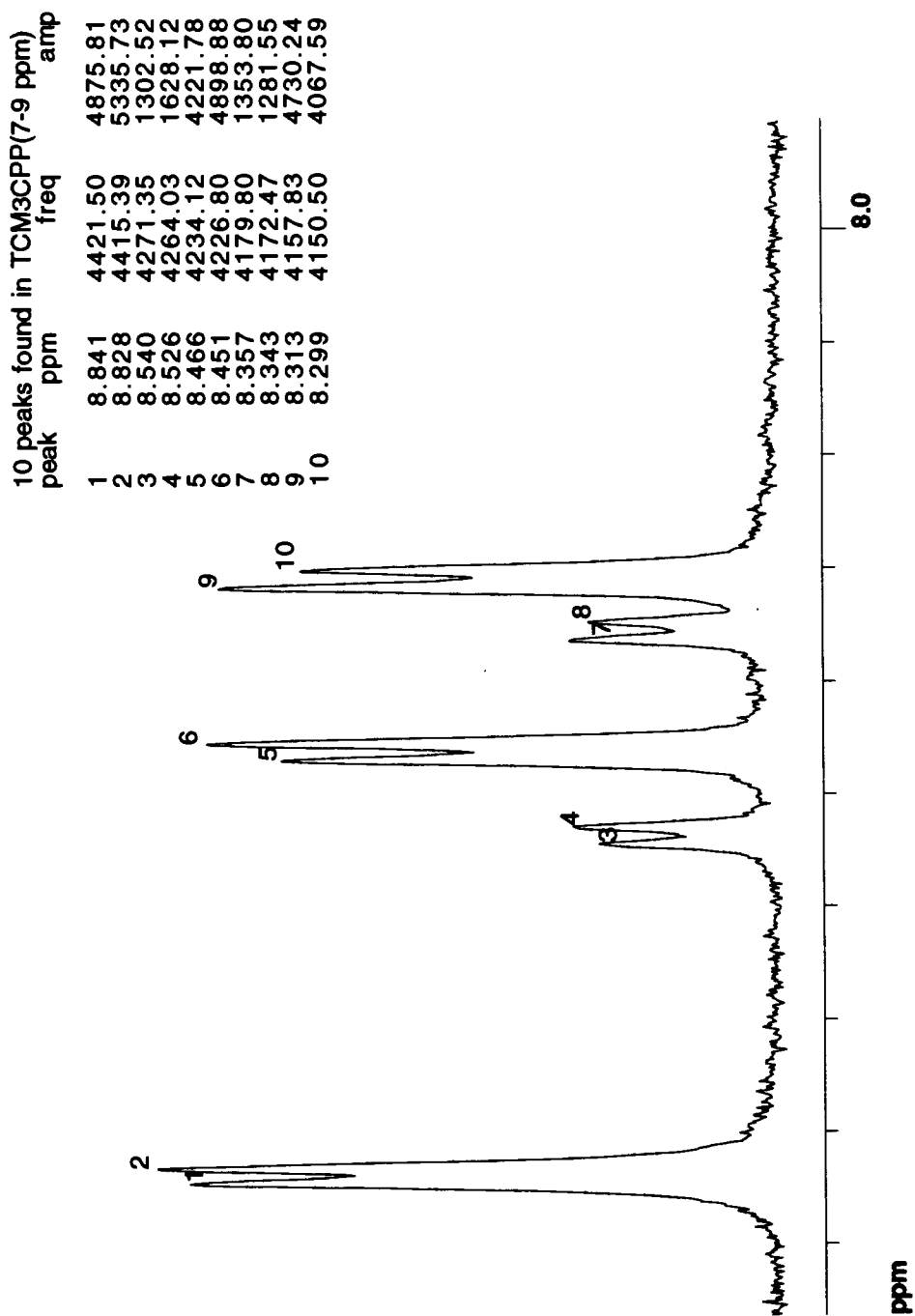


Figure 22. 500 MHz ¹H NMR spectrum (7-9 ppm) of TCM₃CPP

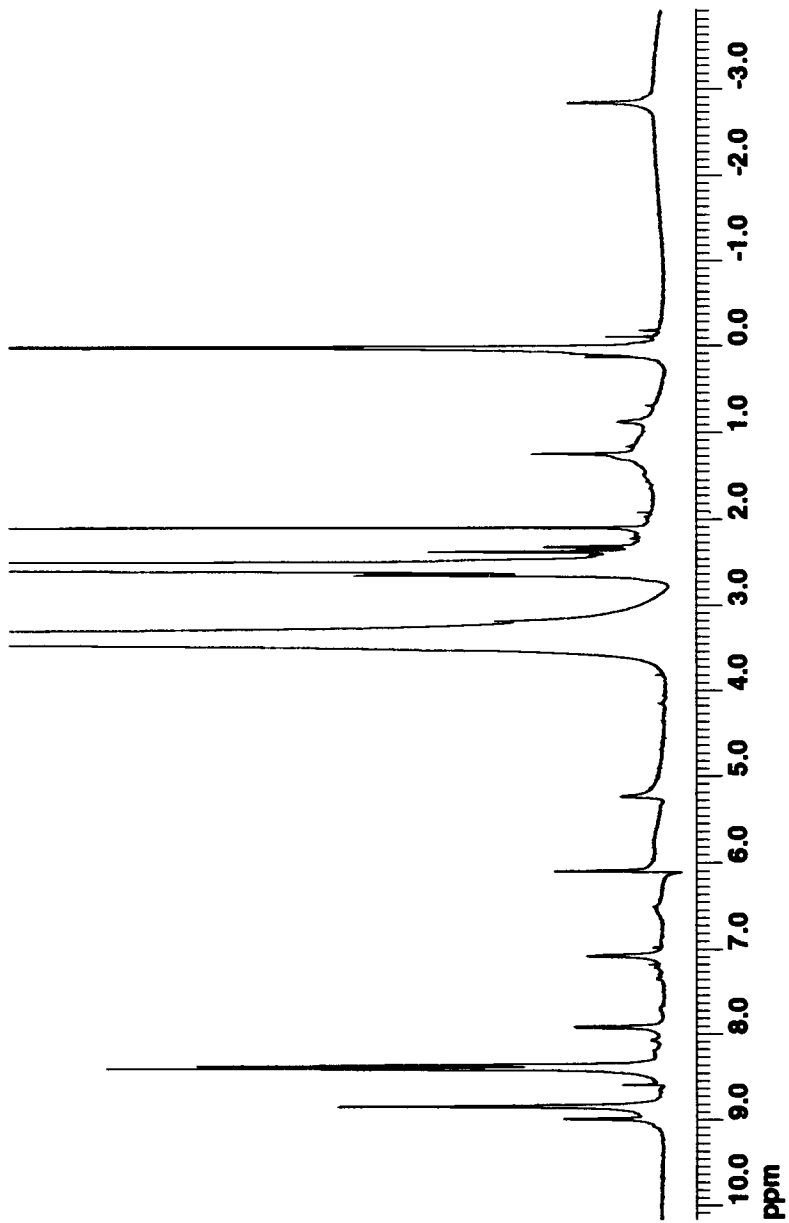


Figure 23. 500 MHz ^1H NMR spectrum of TC₃APP

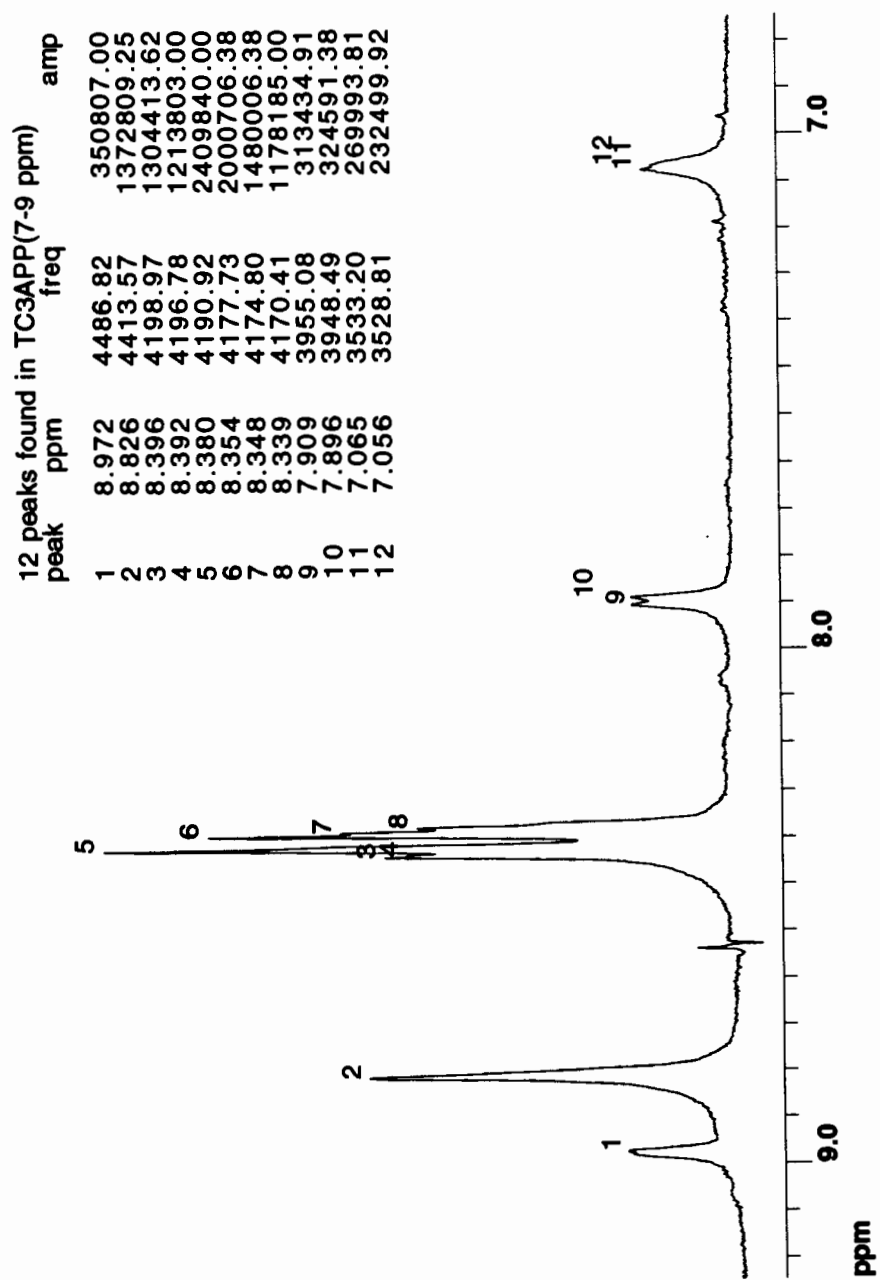


Figure 24. 500 MHz ^1H NMR spectrum (7-9 ppm) of TC₃APP

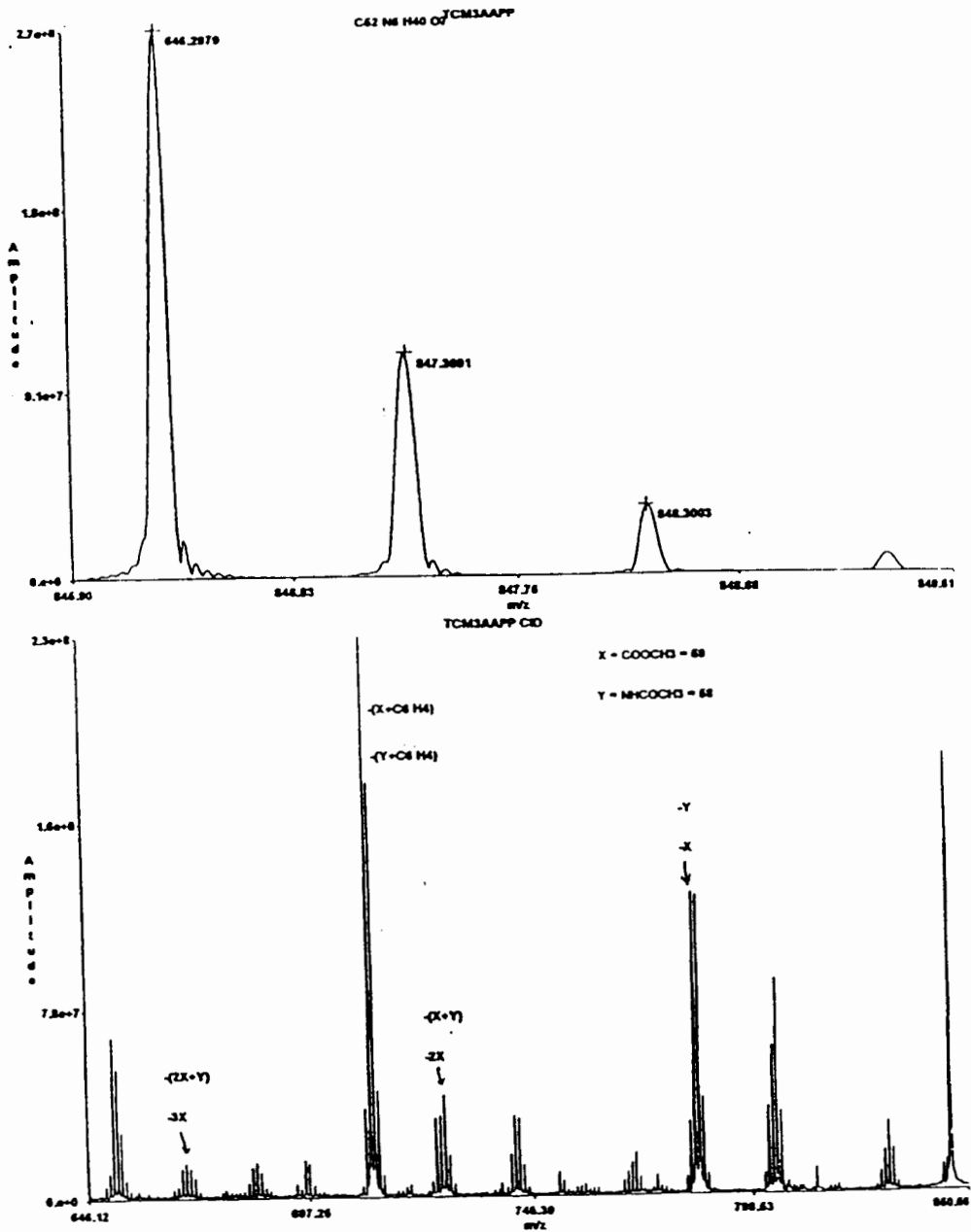


Figure 25. Mass spectra of TCM₃AAPP

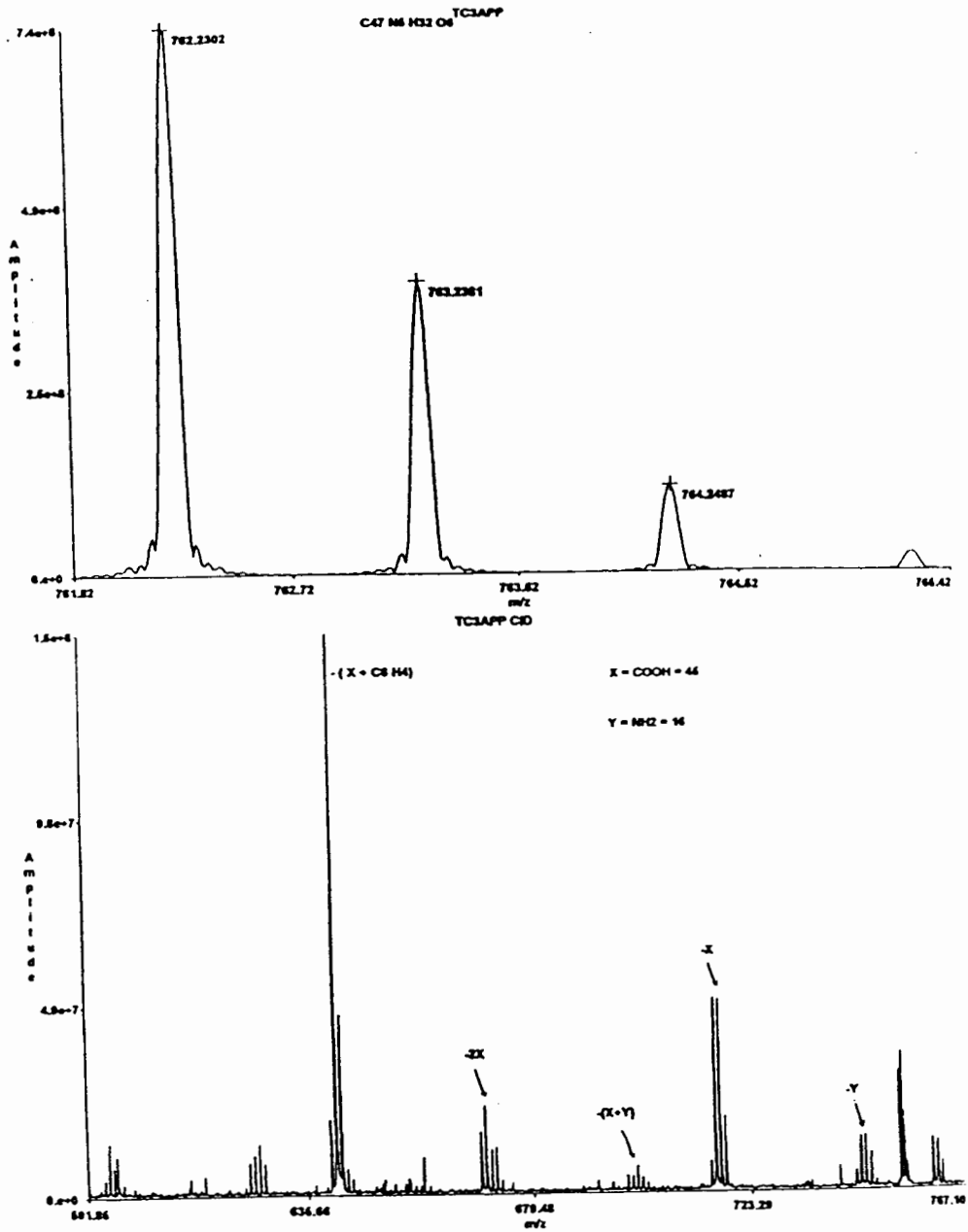


Figure 26. Mass spectra of TC₃APP

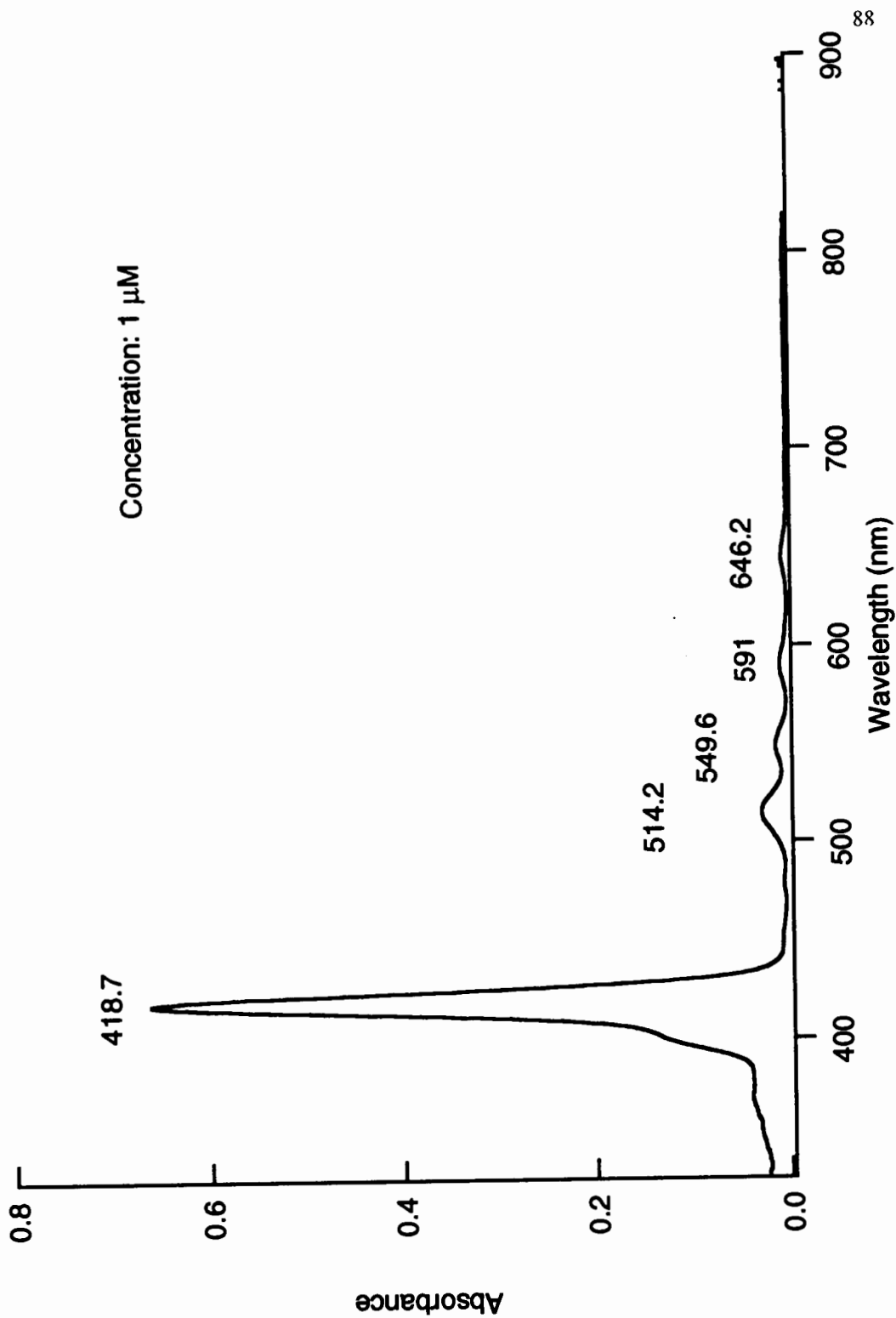


Figure 27. Absorption spectrum of TCM_4PP in DCM

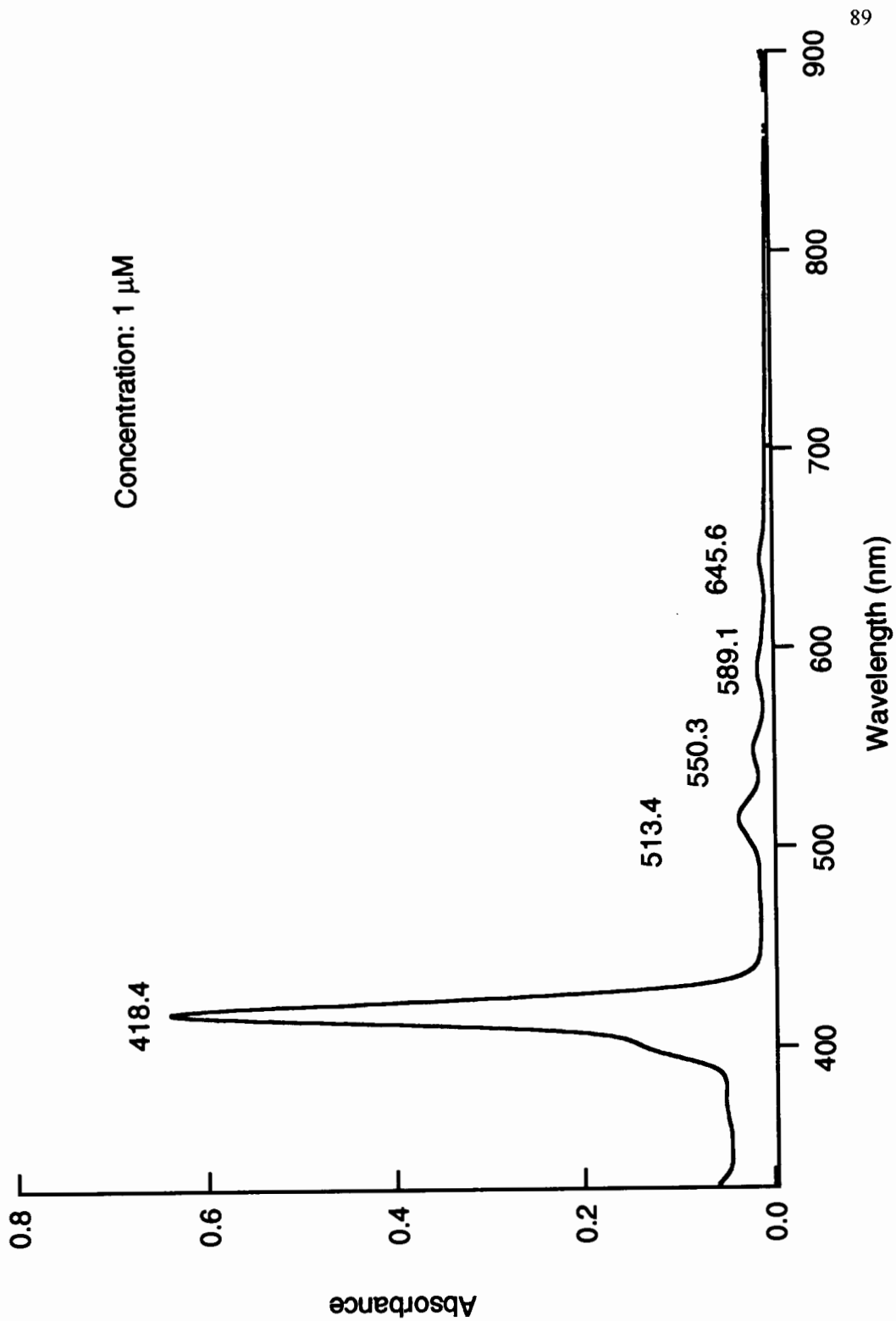


Figure 28. Absorption spectrum of TCM_3CPP in DCM

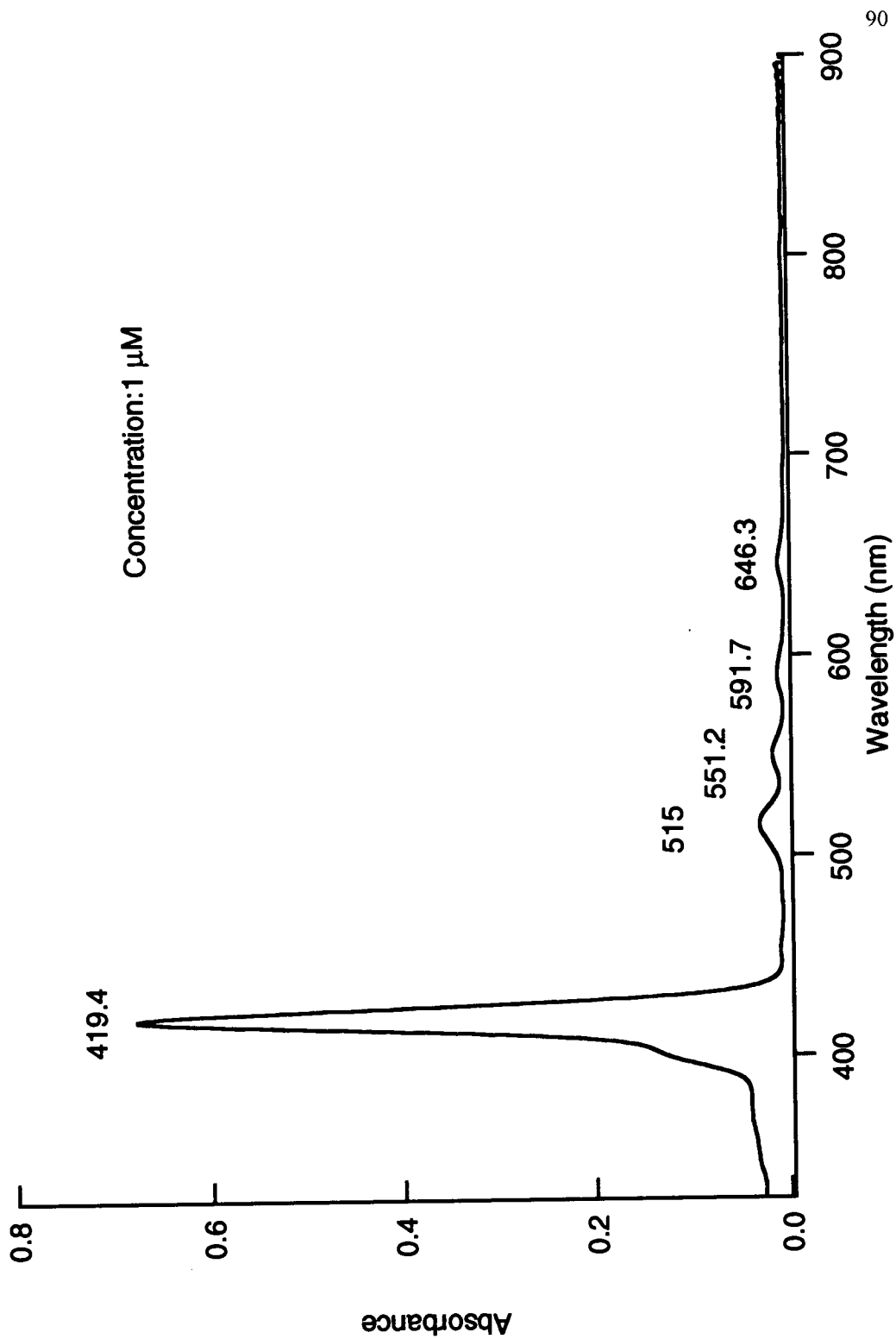


Figure 29. Absorption spectrum of TCM_3AAPP in DCM

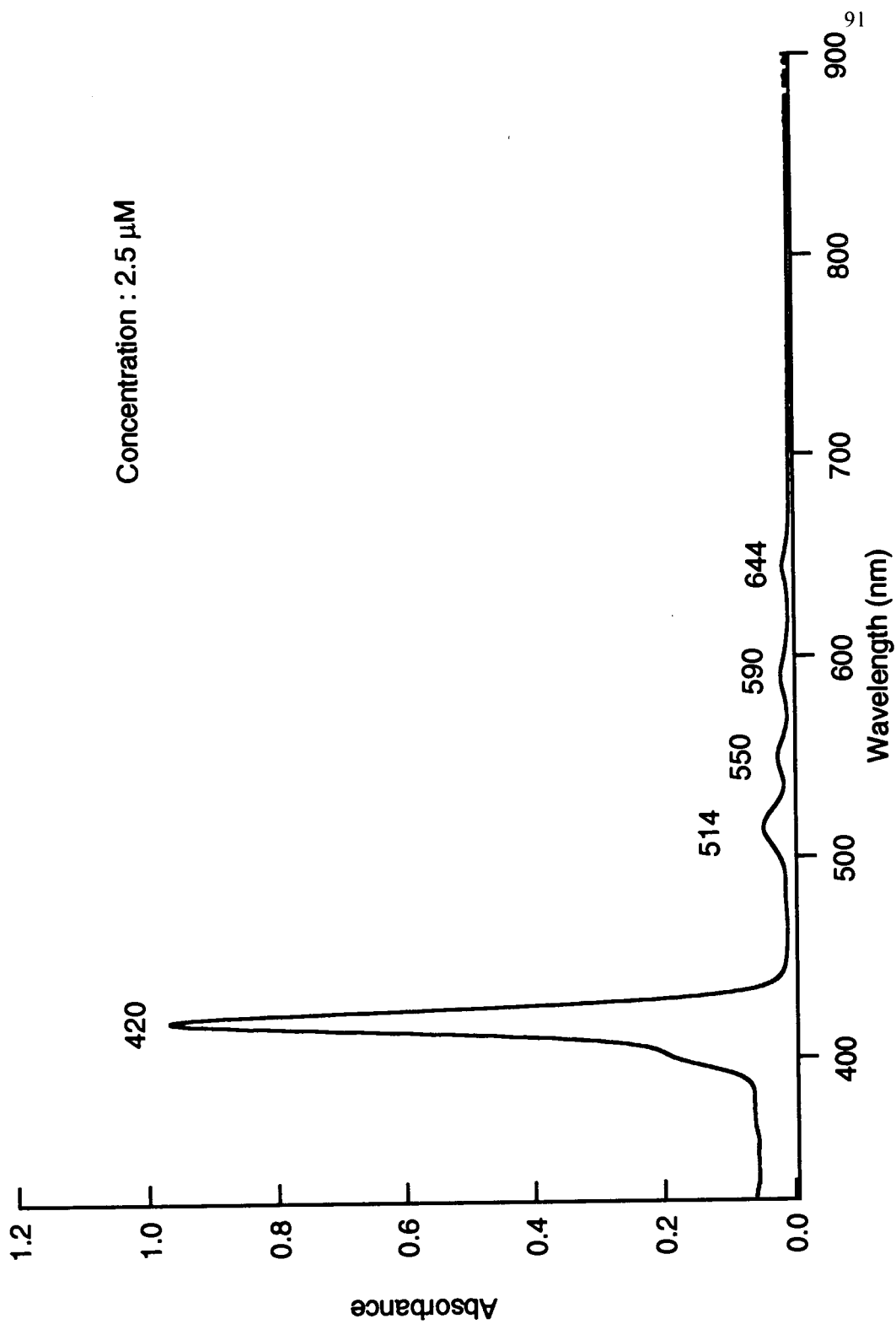


Figure 30. Absorption spectrum of TCPP in DMSO

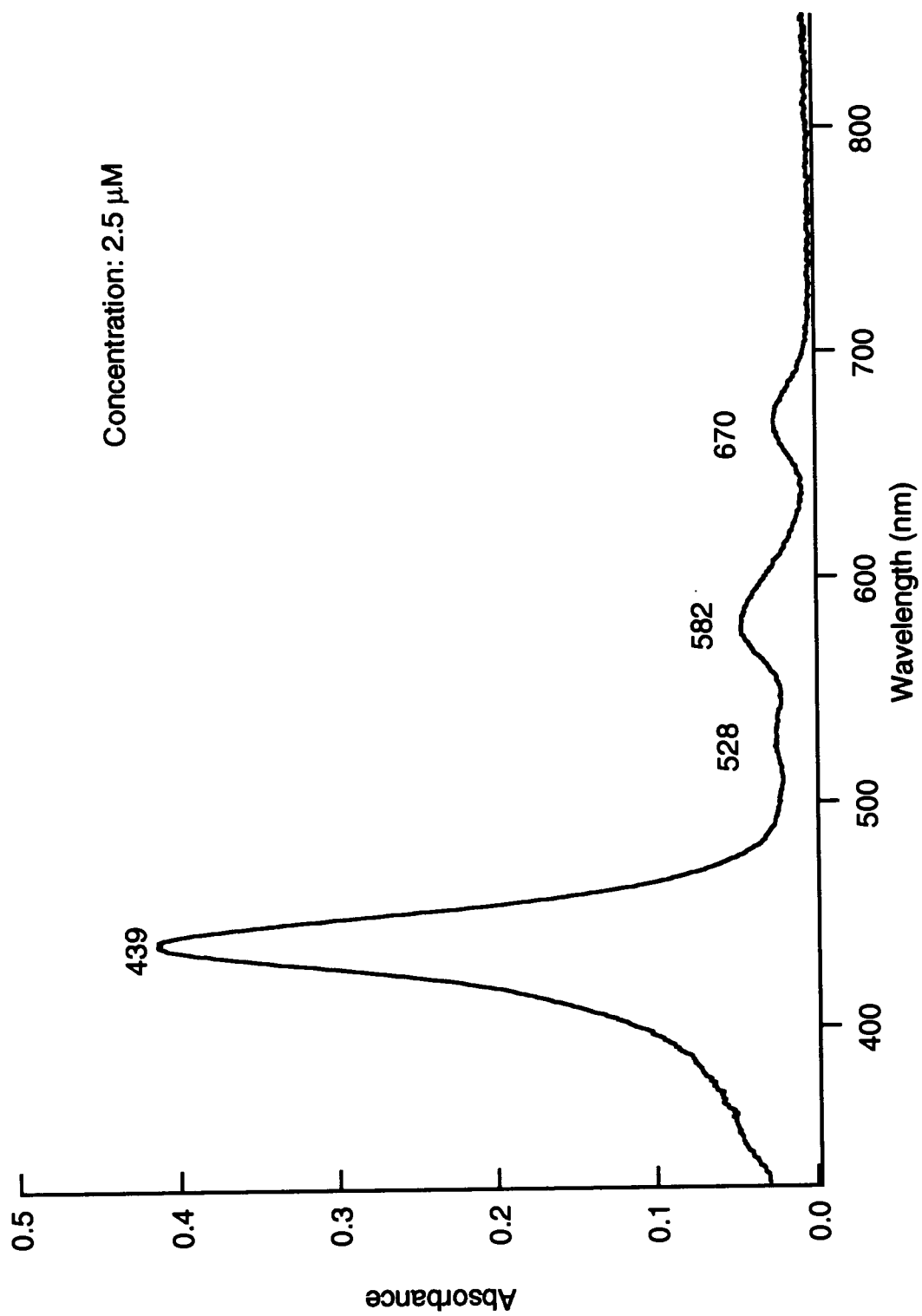


Figure 31. Absorption spectrum of TAPP in DMSO

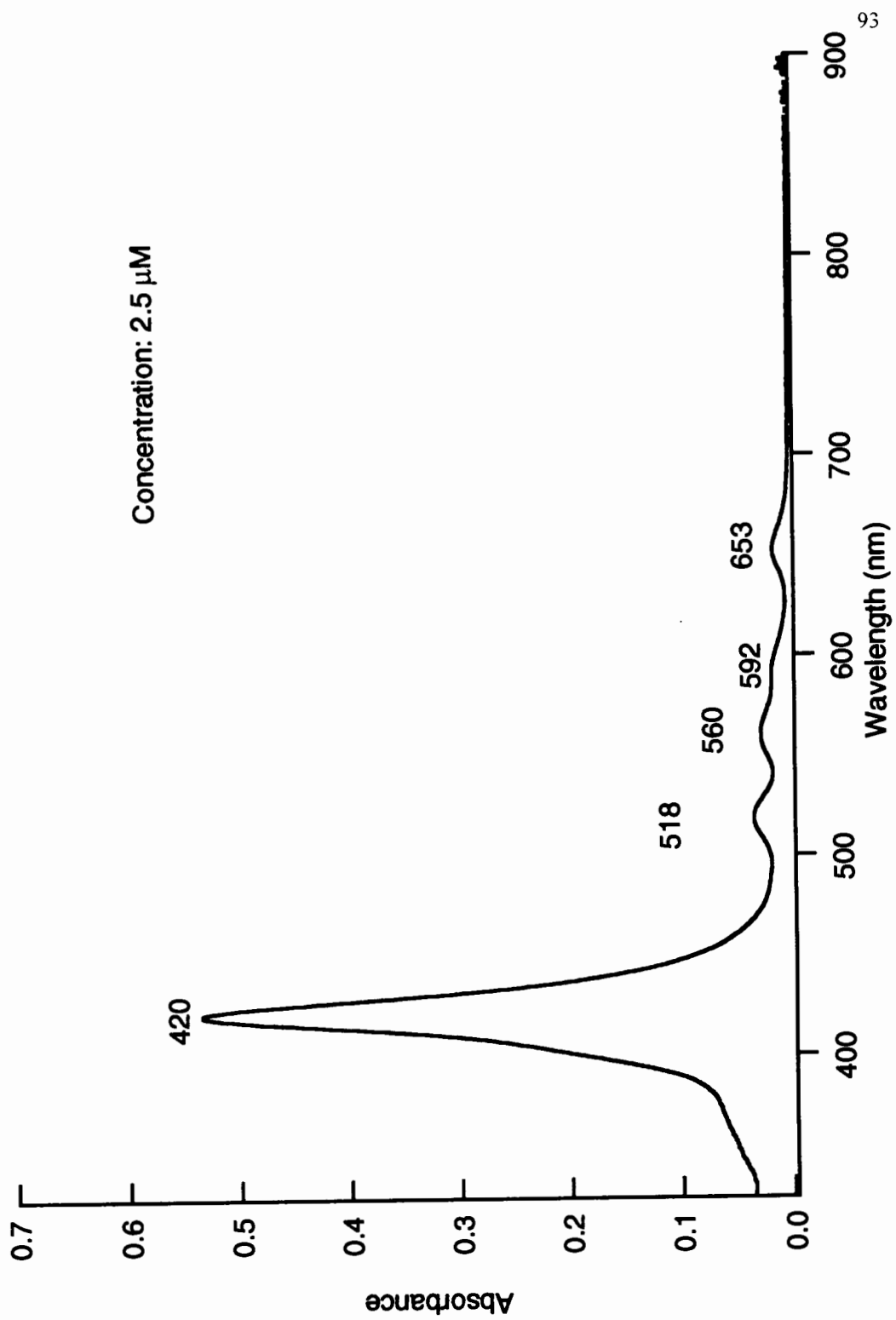


Figure 32. Absorption spectrum of TC₃APP in DMSO

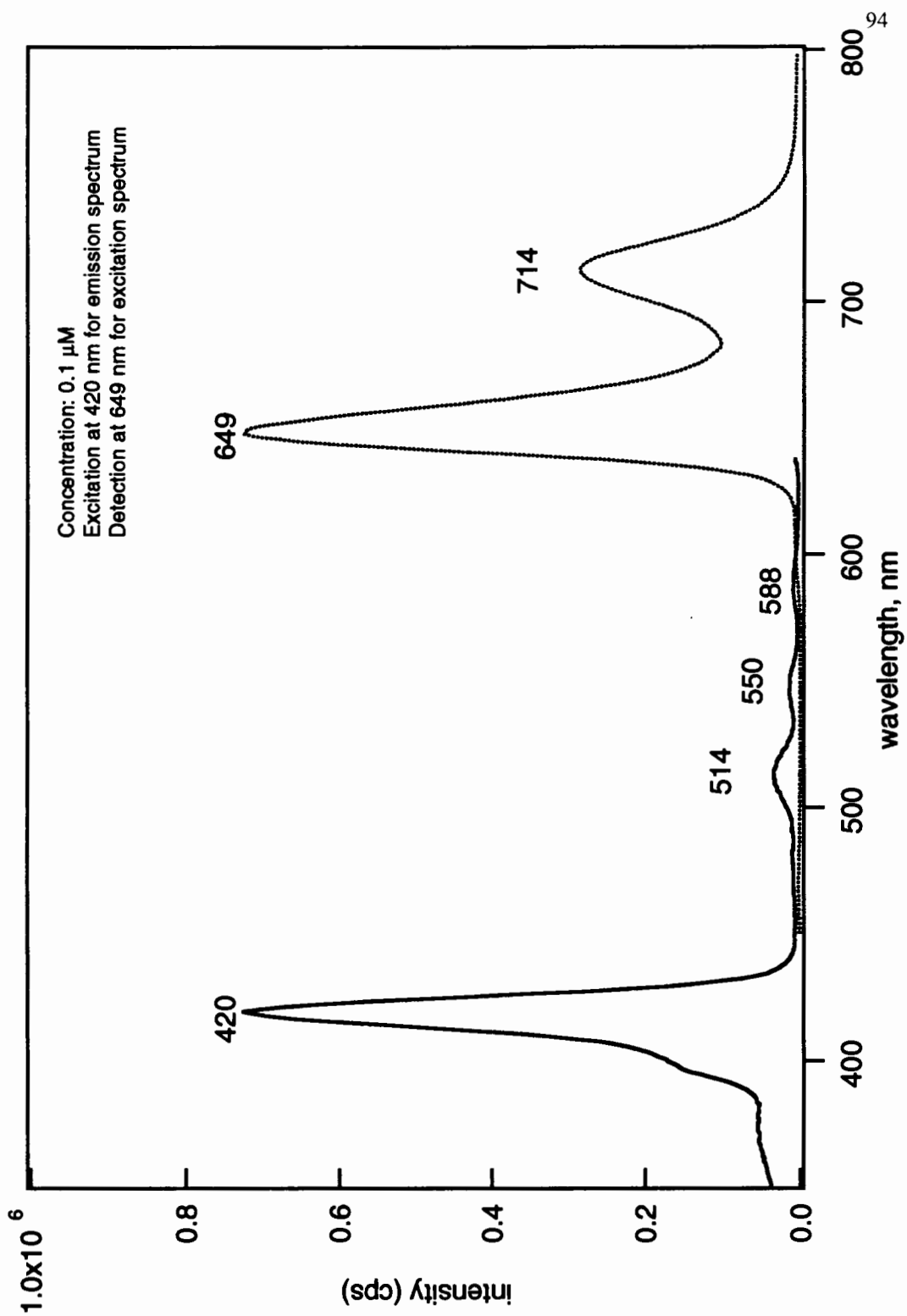


Figure 33. Excitation and emission spectra of TCM₄PP in DCM

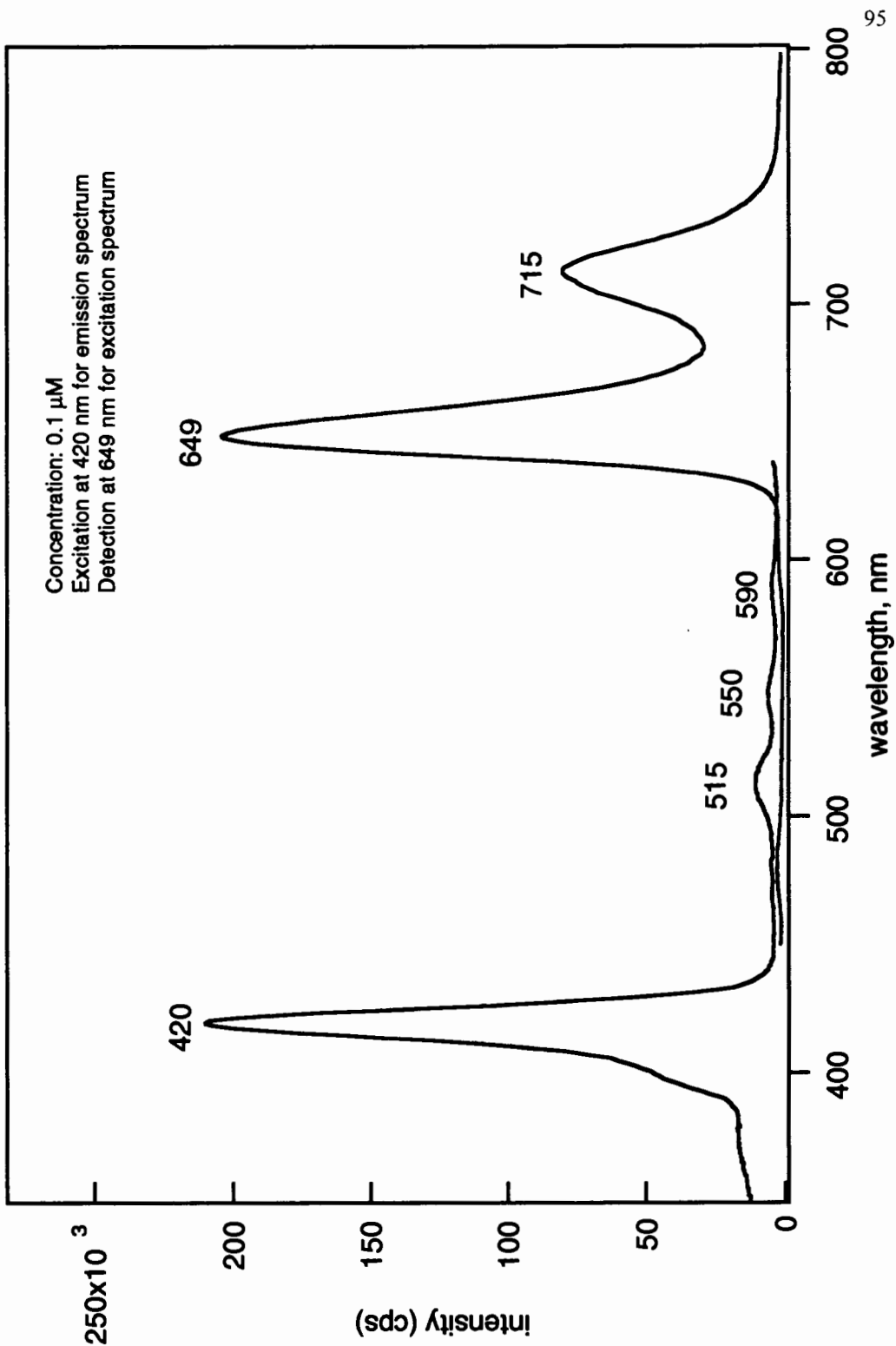


Figure 34. Excitation and emission spectra of TCM_3CPP in DCM

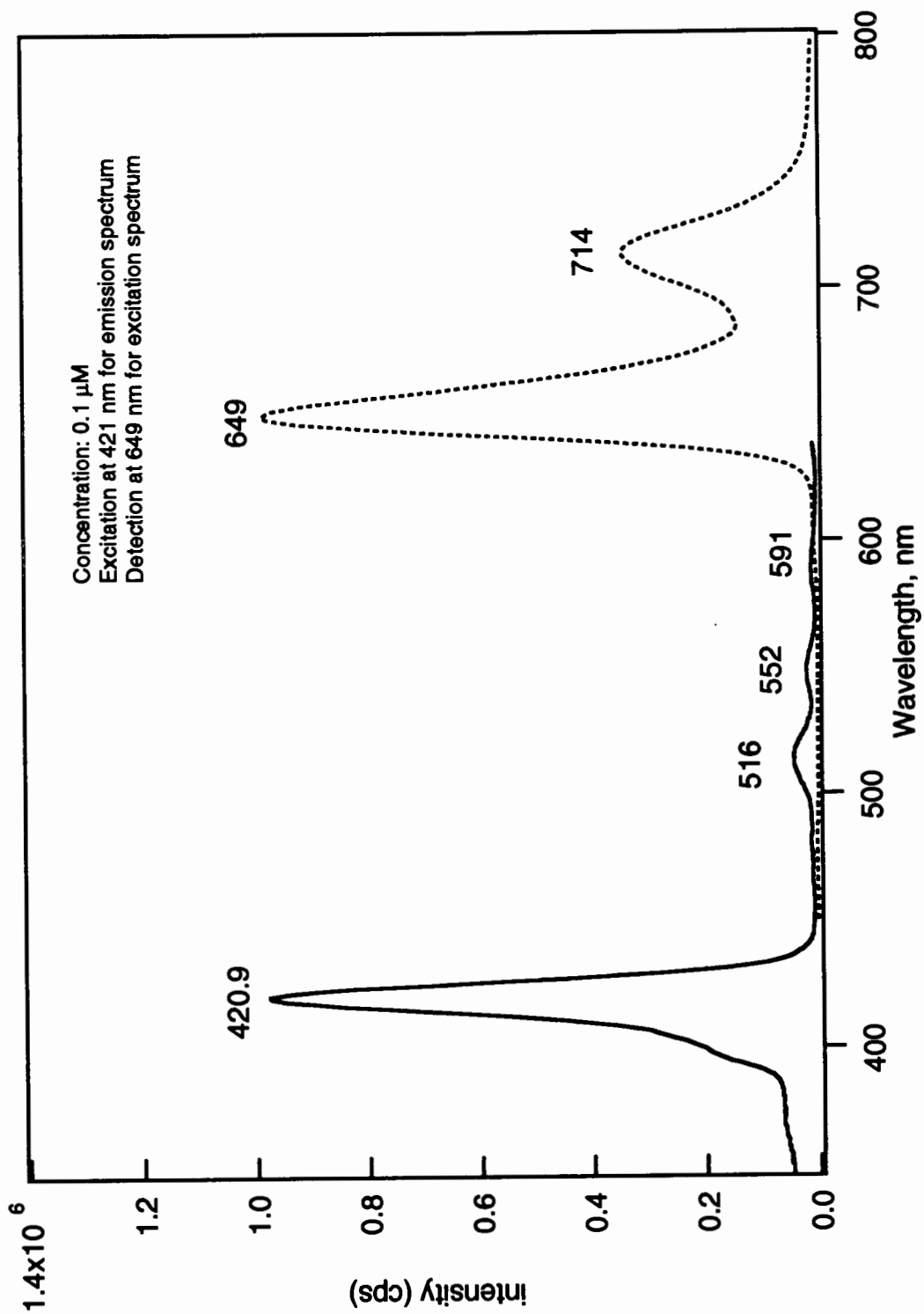


Figure 35. Excitation and emission spectra of TCM₃AAPP in DCM

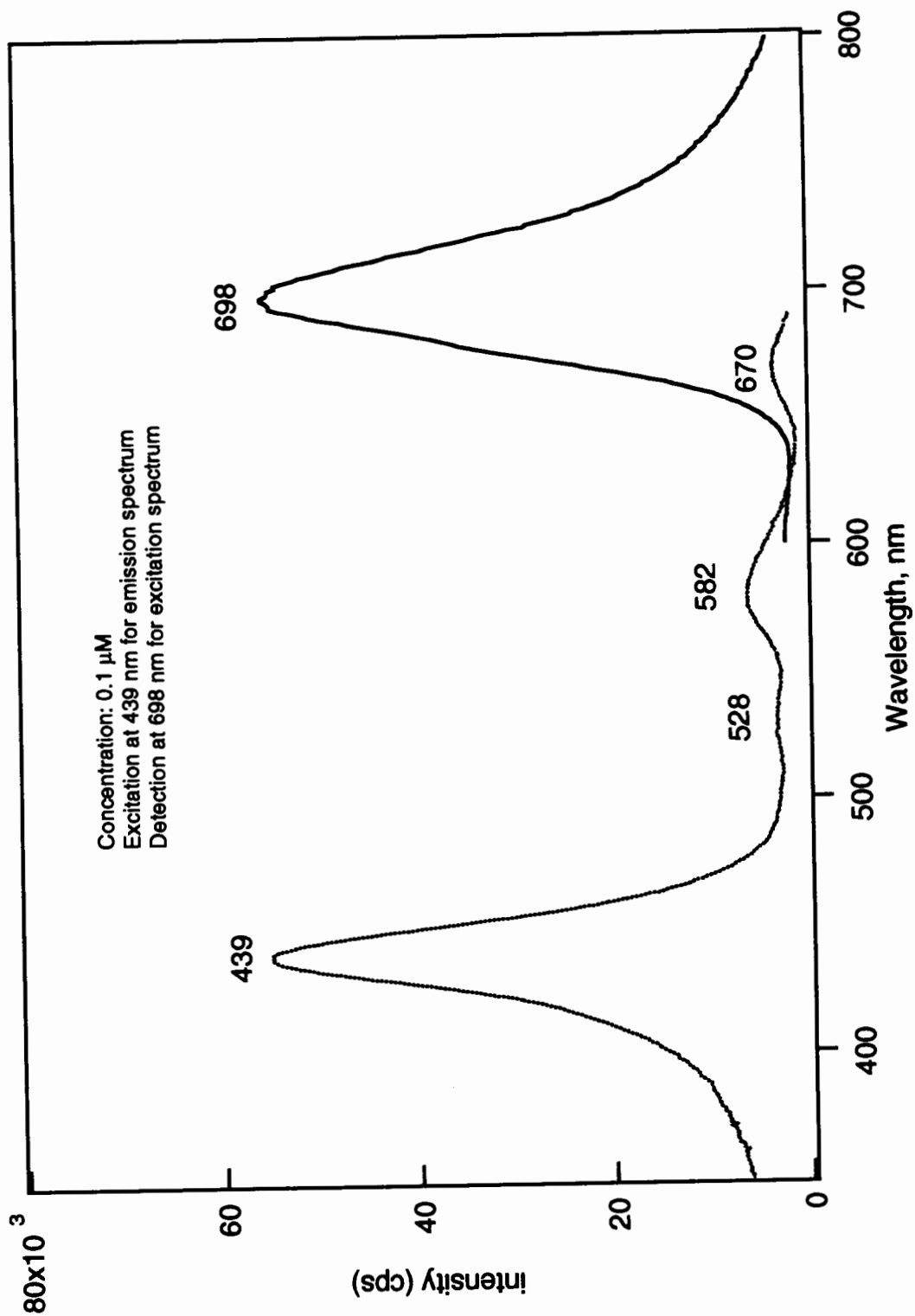


Figure 36. Excitation and emission spectra of TAPP in DMSO

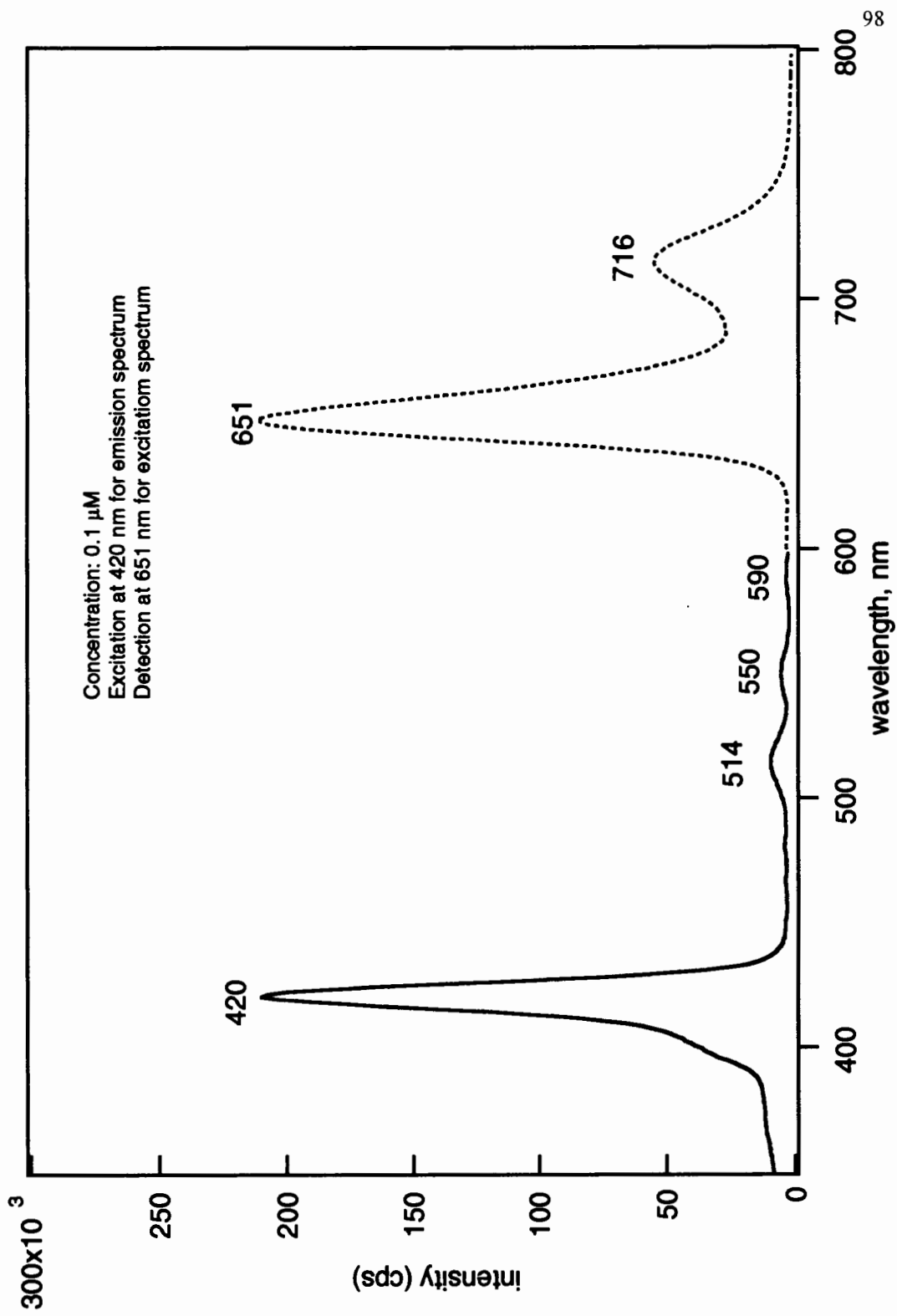


Figure 37. Excitation and emission spectra of TCPP in DMSO

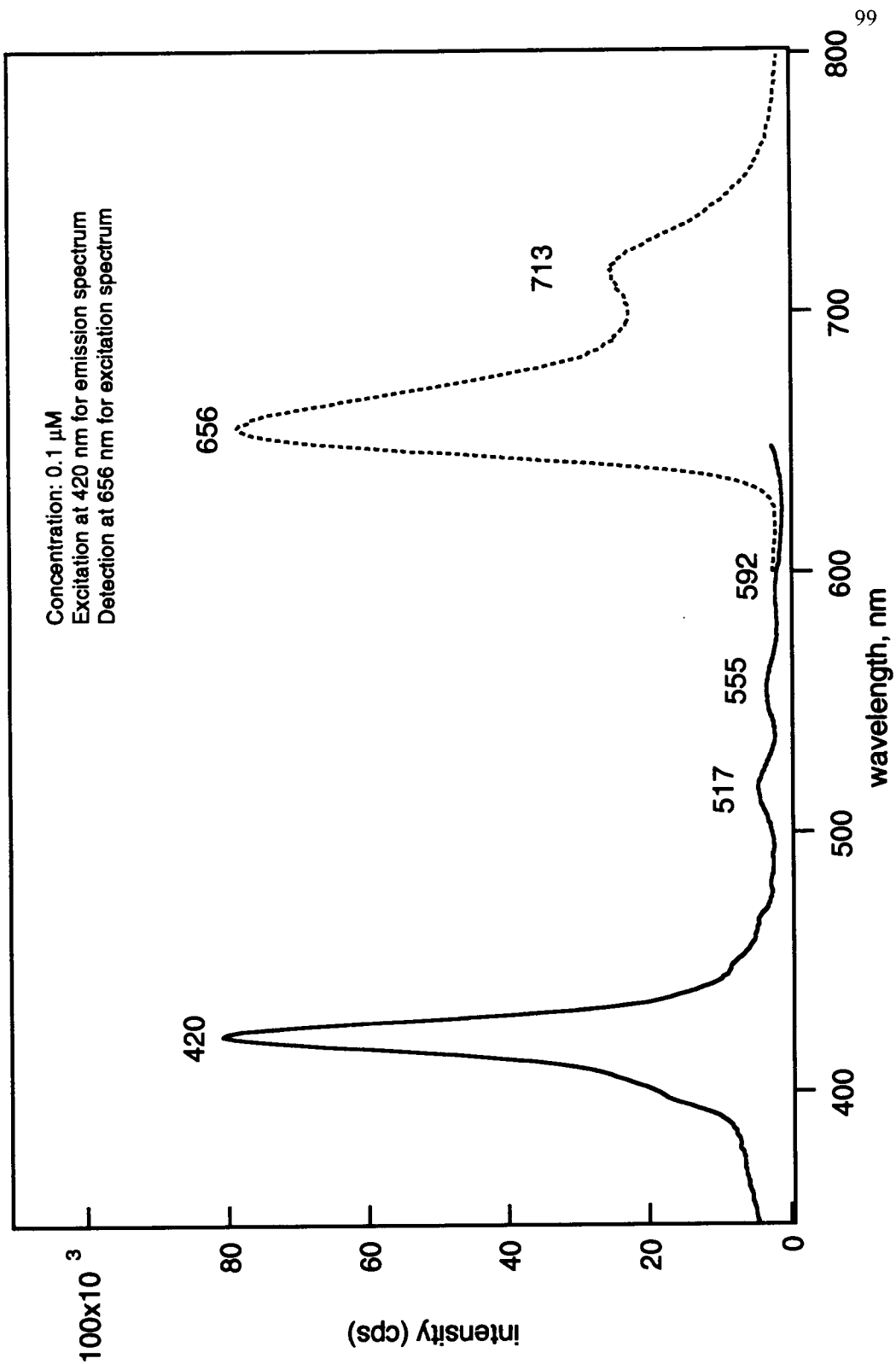


Figure 38. Excitation and emission spectra of TC₃APP in DMSO

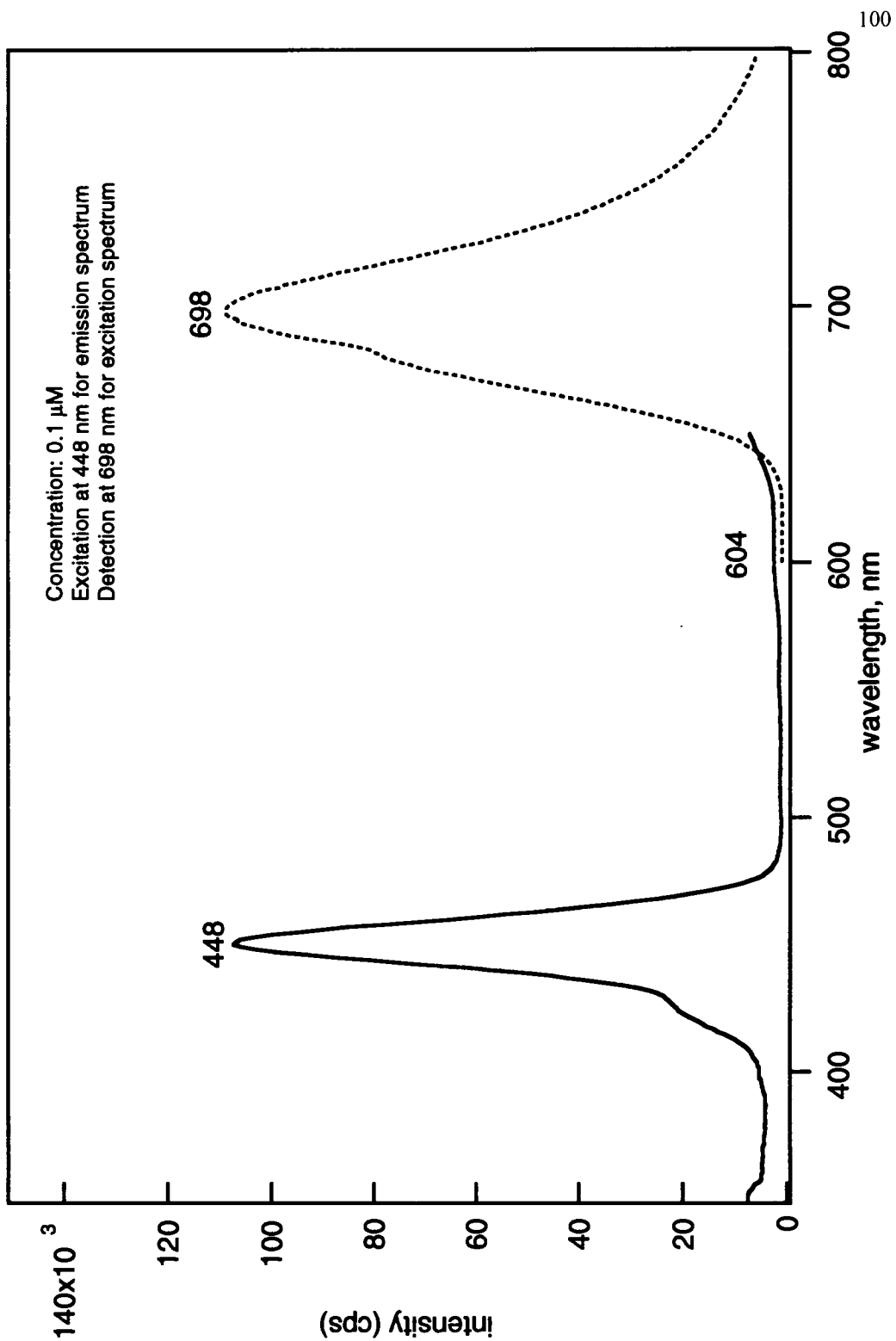


Figure 39. Excitation and emission spectra of TCPP(2+) in DMSO

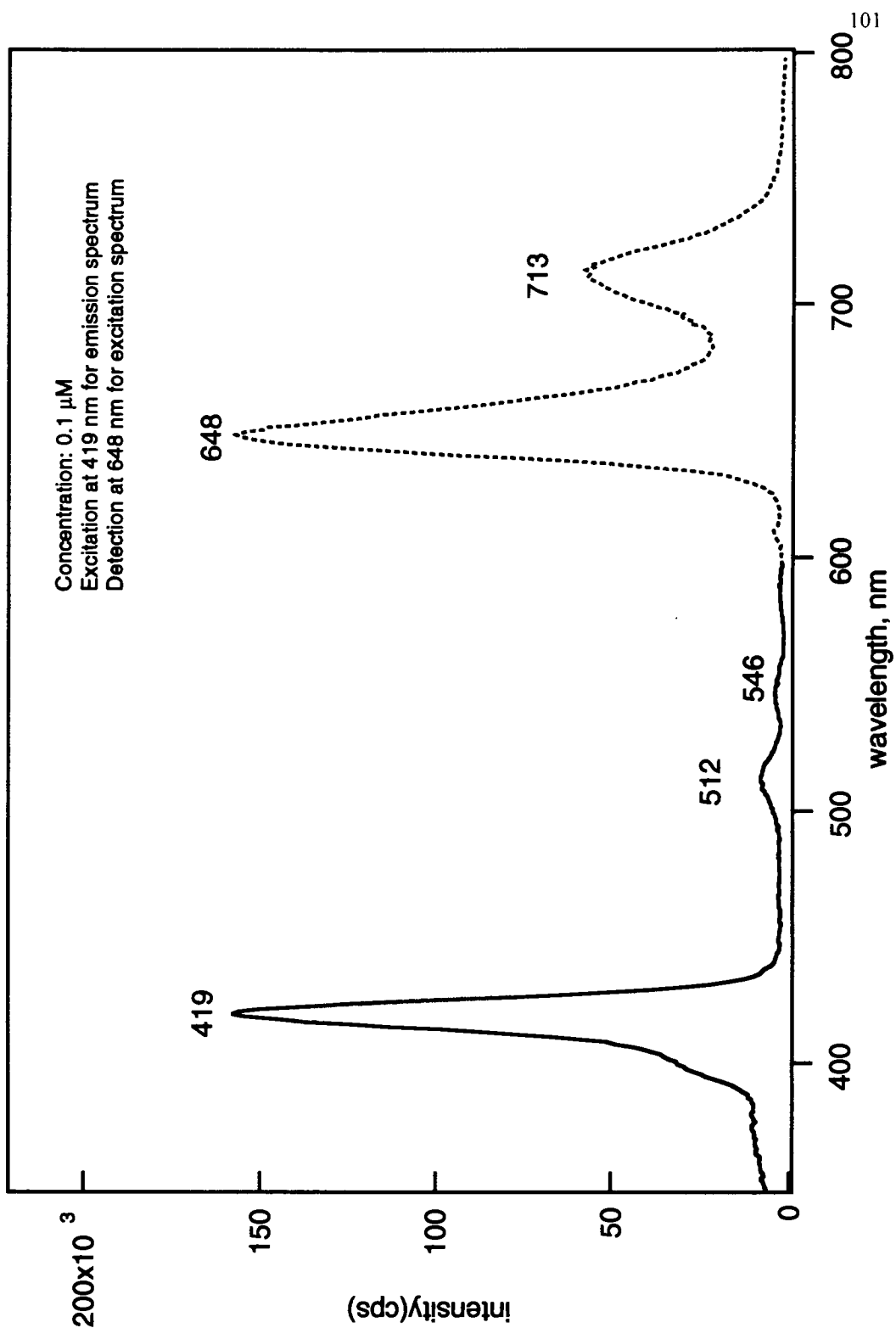


Figure 40. Excitation and emission spectra of TC₃APP(2+) in DMSO

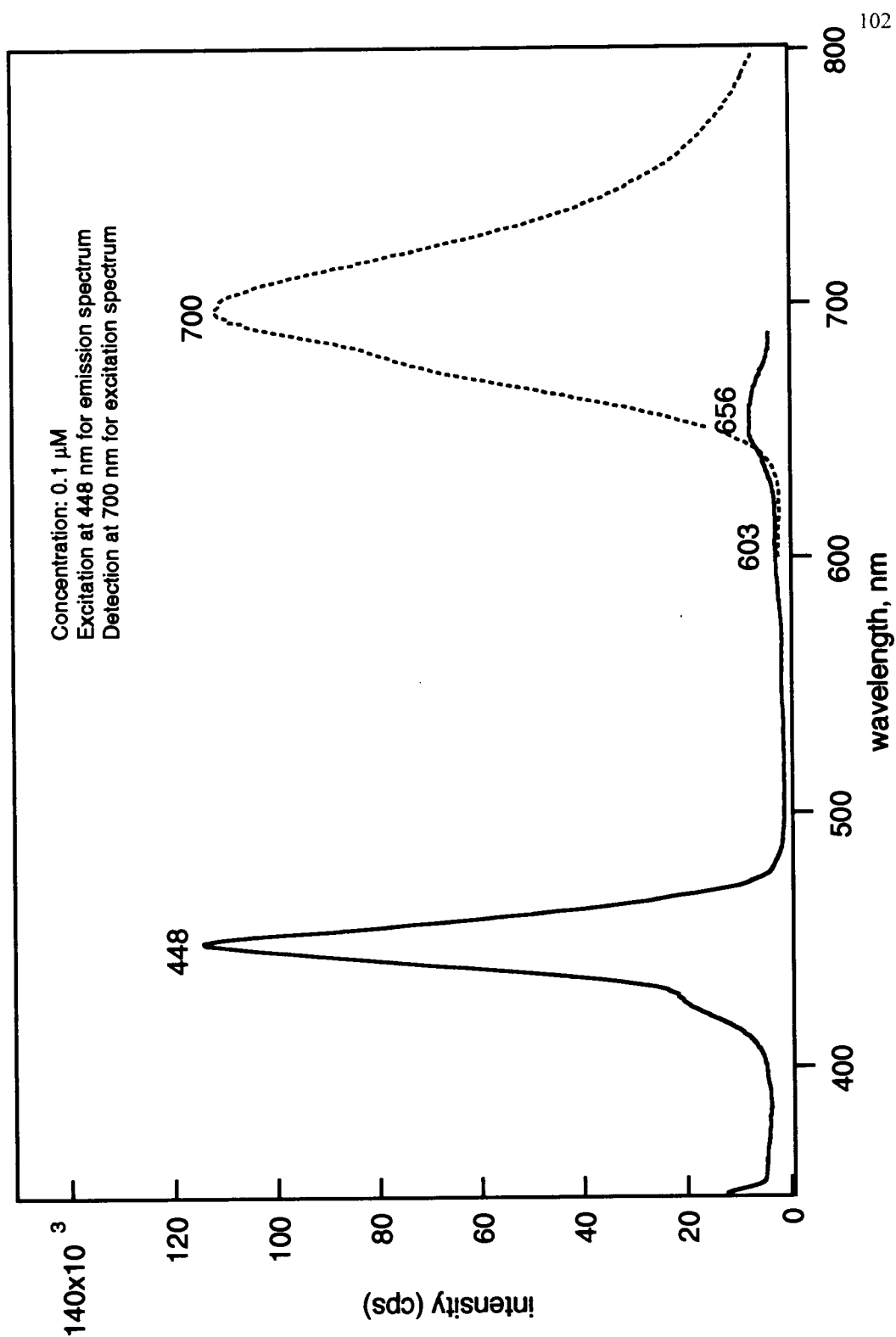


Figure 41. Excitation and emission spectra of TC₃APP(3+) in DMSO

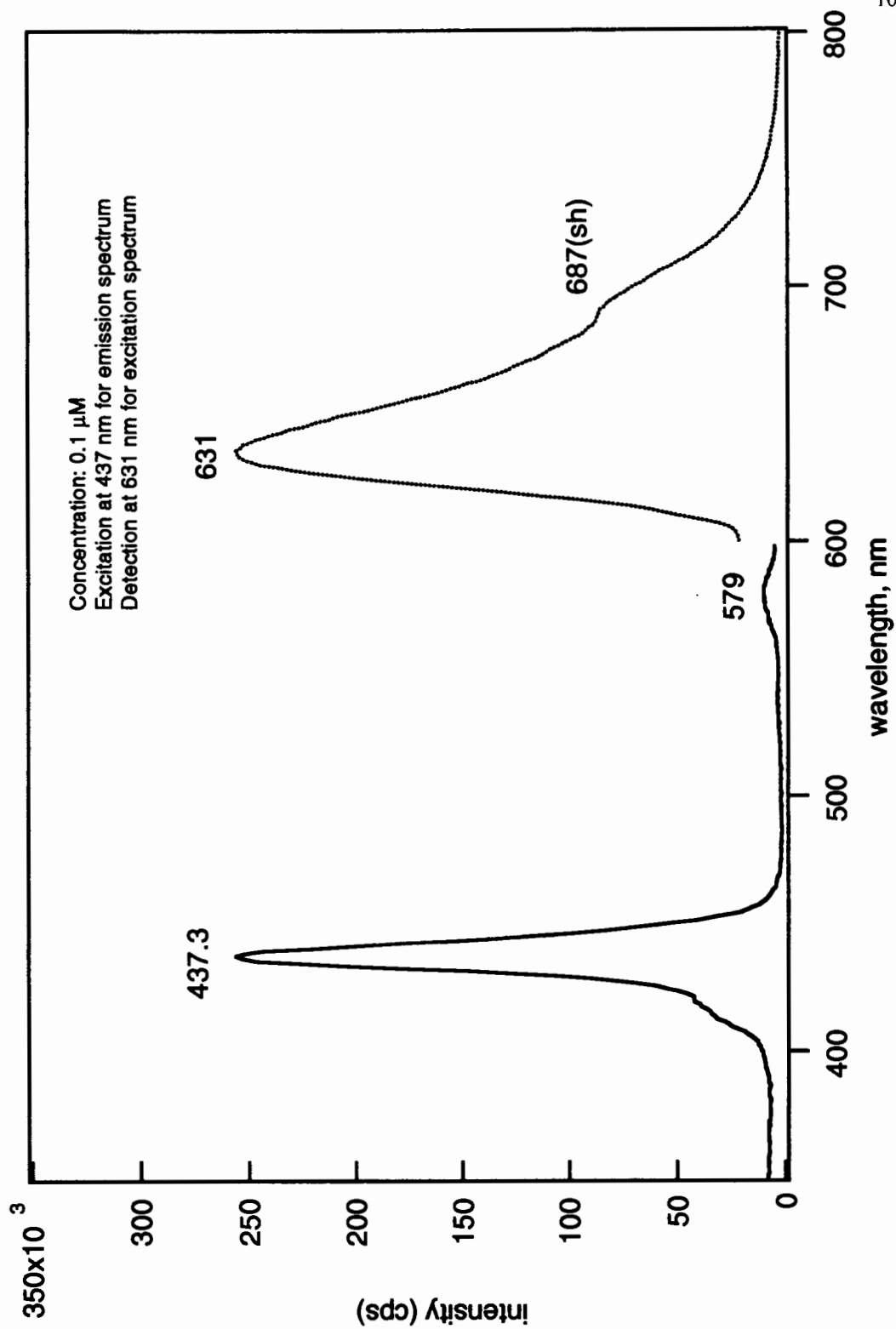


Figure 42. Excitation and emission spectra of TCPP(6-) in DMSO

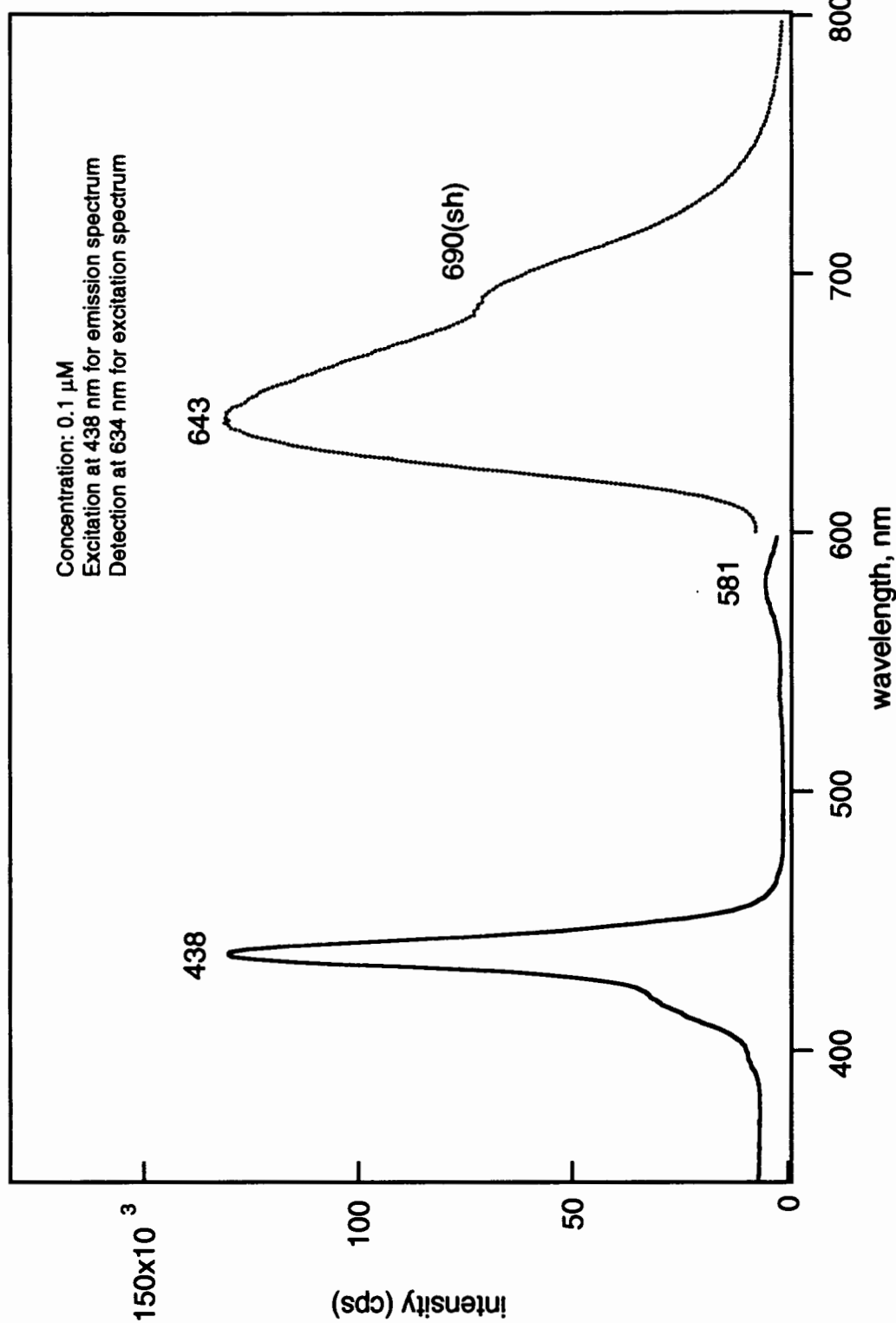


Figure 43. Excitation and emission spectra of TC₃APP(5-) in DMSO

Date: Mon, Mar 10, 1997 2:47 PM

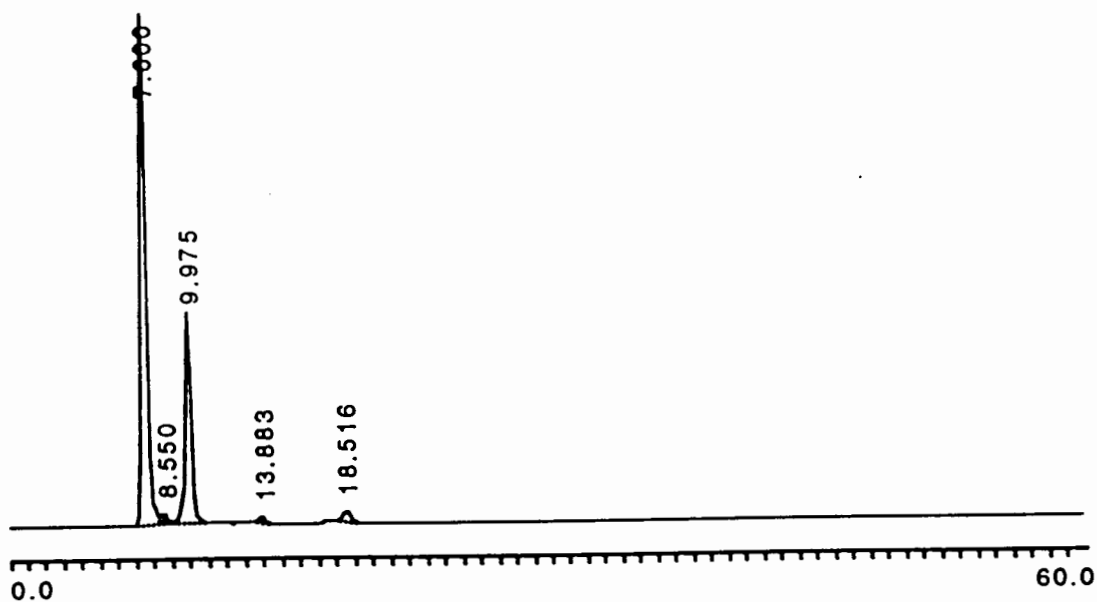
Data: Test-60%-10MAR97-004

Sample: Start at P= 0.48kPSI finish at P= 0.55KPS
 Column: 25cm Si 80-125-C5
 mobile phase: 40%DCM and 60%EtAC, solvents are water saturated
 injection: 10ul Reaction mixture (5:1)

Method: Test-60%

Sampling Int: 0.5 Seconds

Data:



Analysis: Channel A

Peak No.	Time	Type	Height(μ V)	Area(μ V-sec)	Area%
1	7.600	N1	128730	1982877	66.703
	8.333	N2	1978	19985	0.672
2	8.550	N3	2491	33435	1.124
	9.266	N1	711	6903	0.232
3	9.975	N2	52813	853715	28.718
4	13.883	N	1145	20149	0.677
5	18.516	N	2500	55596	1.870
Total Area				2972660	99.996

Figure 44. HPLC report of analysis of crude product (5:1)

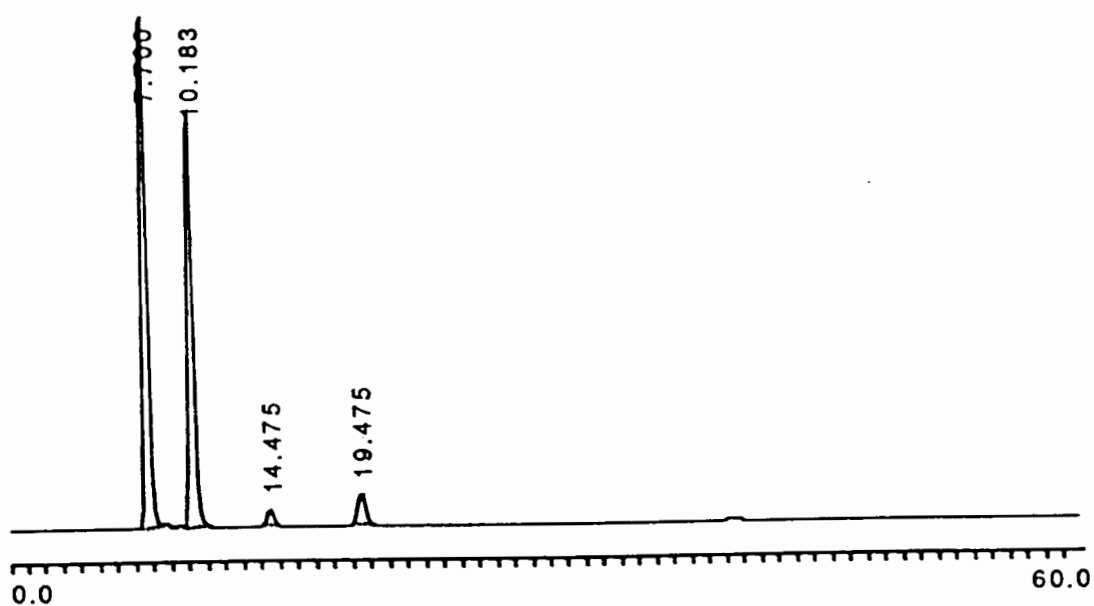
Date: Mon, Mar 10, 1997 11:39 AM

Data: Test-60%-10MAR97-002

Sample: Start at P= 0.48kPSI finish at P= 0.55KPS
 Column: 25cm Si 80-125-C5
 mobile phase: 40%DCM and 60%EtAC, solvents are water saturated
 injection: 10ul Reaction mixture (3:1)

Method: Test-60%
 Sampling Int: 0.5 Seconds

Data:



Analysis: Channel A

Peak No.	Time	Type	Height(μ V)	Area(μ V-sec)	Area%
1	7.700	N	128017	1844115	50.919
2	10.183	N	104689	1527475	42.176
3	14.475	N	3839	66619	1.839
4	19.475	N	7835	183443	5.065
Total Area				3621652	99.999

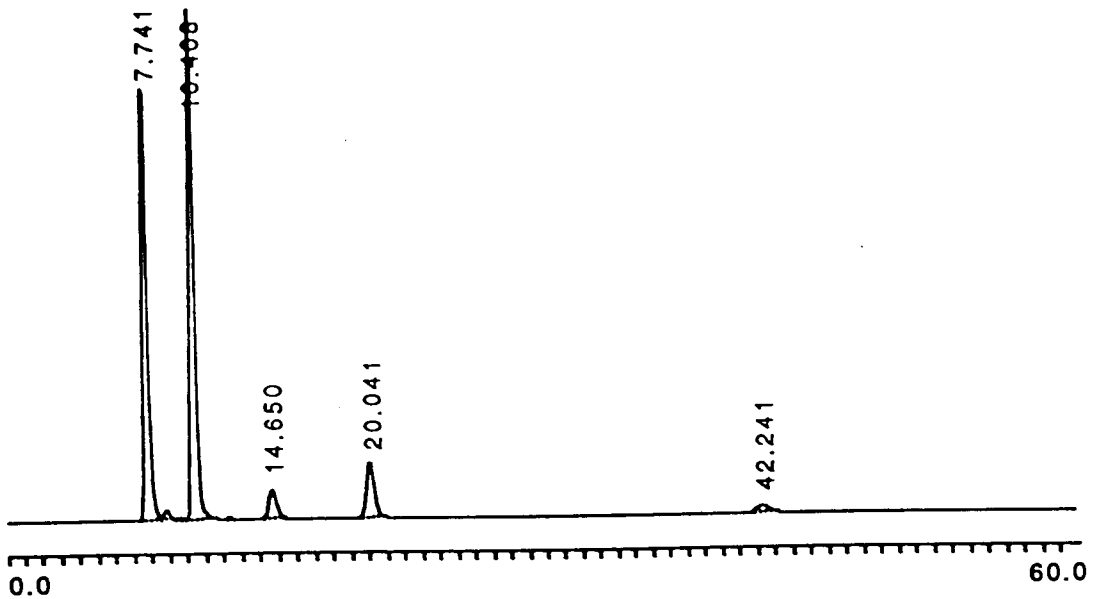
Figure 45. HPLC report of analysis of crude product (3:1)

Date: Mon, Mar 10, 1997 10:35 AM
 Data: Test-60%-10MAR97-001

Sample: Start at P= 0.44kPSI finish at P= 0.48KPS
 Column: 25cm Si 80-125-C5
 mobile phase: 40%DCM and 60%EtAC, solvents are water saturated
 injection: 10ul Reaction mixture (2:1)

Method: Test-60%
 Sampling Int: 0.5 Seconds

Data:



Analysis: Channel A

Peak No.	Time	Type	Height(μV)	Area(μV-sec)	Area%
1	7.741	N1	108363	1302505	37.110
	8.816	N2	2330	38098	1.085
	9.558	N	303	3016	0.085
2	10.408	N	128276	1607268	45.793
	12.316	N	159	1750	0.049
3	14.650	N	7835	167735	4.779
4	20.041	N	13864	329272	9.381
5	42.241	N	1430	60170	1.714
Total Area				3509814	99.996

Figure 46. HPLC report of analysis of crude product (2:1)